MEASURED AND PREDICTED ROTOR-PAD TRANSFER FUNCTIONS FOR A ROCKER-PIVOT TILTING-PAD JOURNAL BEARING

Presented By: **Jason Wilkes**

PhD: Final Examination

Turbomachinery Laboratory
Mechanical Engineering Department
Texas A&M University
College Station, Texas

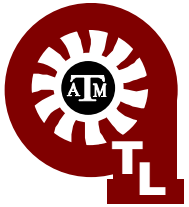

Dedication:

- To Monica – who has worked tirelessly at home while I put in my time at the lab.

Overview:

- Introduction
  - Previous Work
- Objective of the Research
- Theoretical Model
  - Geometry, Kinematics, and Pad Dynamics
  - Rotor-Pad Transfer function
  - Bearing Impedances
- Hardware
  - Test Rig Description
  - Bearing Description/Instrumentation
- Results
  - Pad and Pivot Stiffness
  - Bearing Clearance and Static Measurements
  - Measured vs. Predicted Rotor-Pad Transfer functions
  - Measured vs. Predicted Bearing Impedances
- Summary and Outlook

Introduction: Bearings

- Primary Functions of a bearing
  - Permit relative rotation
  - Transmit reaction forces
- Types of bearings
  - Rolling element
  - Mechanical contact (sliding bearings)
  - Magnetic levitation
  - Fluid-film bearings
- Reaction force models
  - Stiffness (k_{ij}) and damping (c_{ij}) (KC) model

$$-\begin{Bmatrix} f_{bx} \\ f_{by} \end{Bmatrix} = \begin{bmatrix} k_{xx} & k_{xy} \\ k_{yx} & k_{yy} \end{bmatrix} \begin{Bmatrix} x \\ y \end{Bmatrix} + \begin{bmatrix} c_{xx} & c_{xy} \\ c_{yx} & c_{yy} \end{bmatrix} \begin{Bmatrix} \dot{x} \\ \dot{y} \end{Bmatrix}$$

  - Stiffness, damping, and virtual-mass (m_{ij}) (KCM) model

$$-\begin{Bmatrix} f_{bx} \\ f_{by} \end{Bmatrix} = \begin{bmatrix} k_{xx} & k_{xy} \\ k_{yx} & k_{yy} \end{bmatrix} \begin{Bmatrix} x \\ y \end{Bmatrix} + \begin{bmatrix} c_{xx} & c_{xy} \\ c_{yx} & c_{yy} \end{bmatrix} \begin{Bmatrix} \dot{x} \\ \dot{y} \end{Bmatrix} + \begin{bmatrix} m_{xx} & m_{xy} \\ m_{yx} & m_{yy} \end{bmatrix} \begin{Bmatrix} \ddot{x} \\ \ddot{y} \end{Bmatrix}$$

Direct Stiffness

Cross-Coupled Stiffness

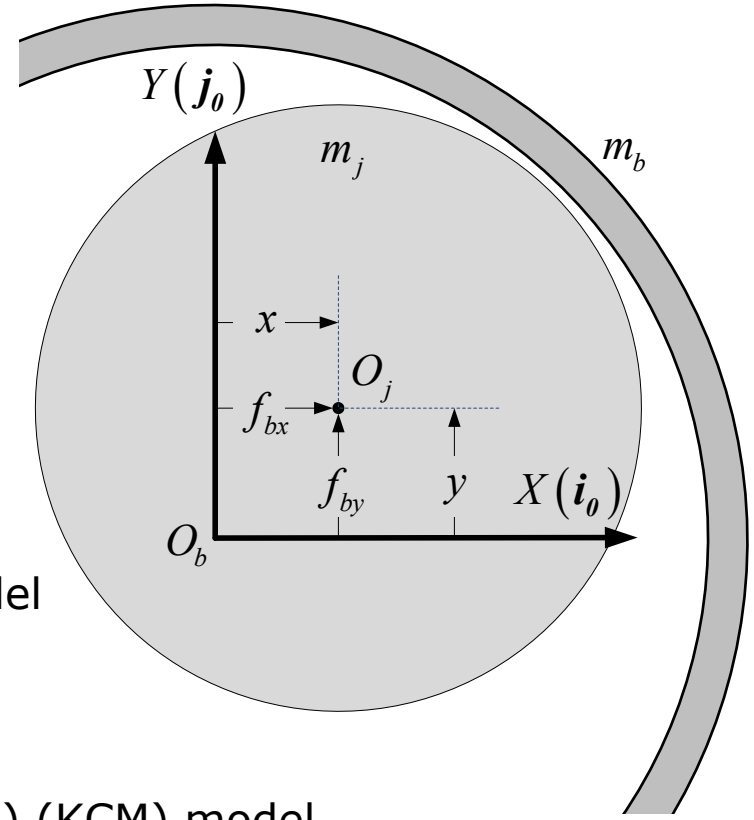

Introduction: Tilting Pad Journal Bearings (TPJB)

- Composed of multiple *pads*, or *shoes*, that are free to tilt
- This feature results in a reaction force that is directed through each pad's pivot.
- Inherently stable (reduced/eliminated destabilizing k_{xy})

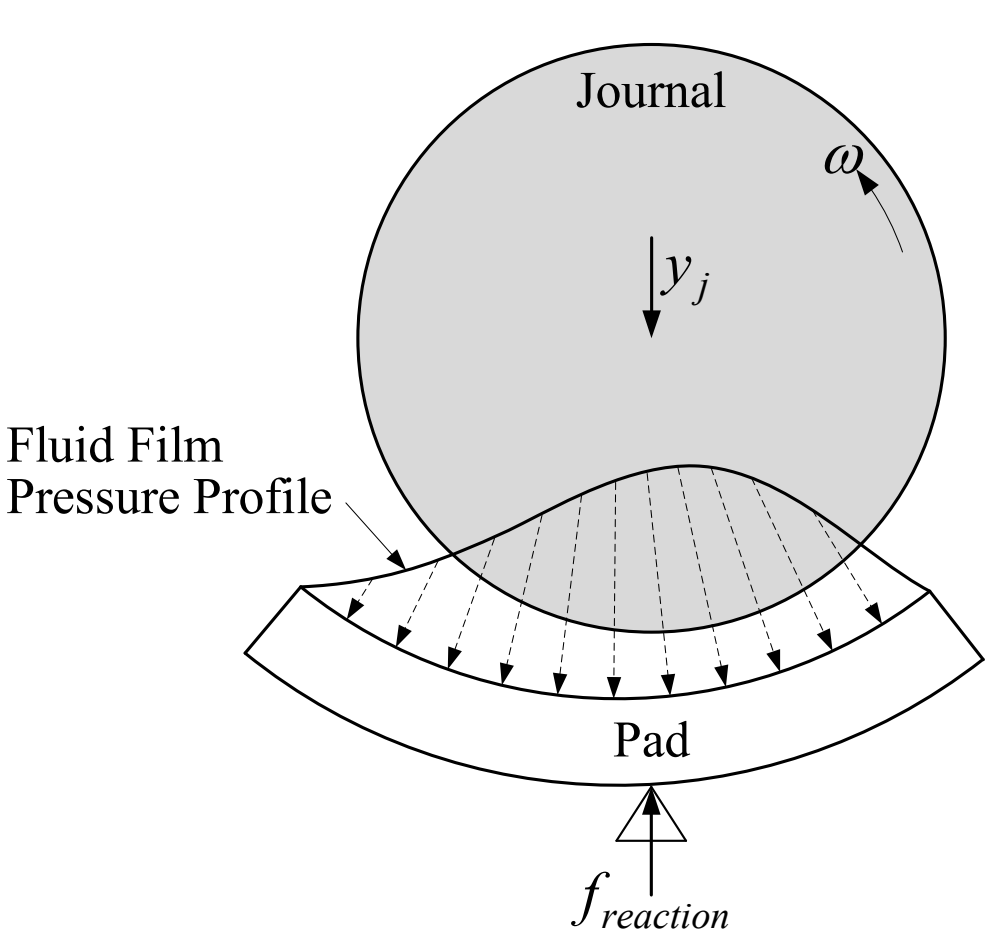

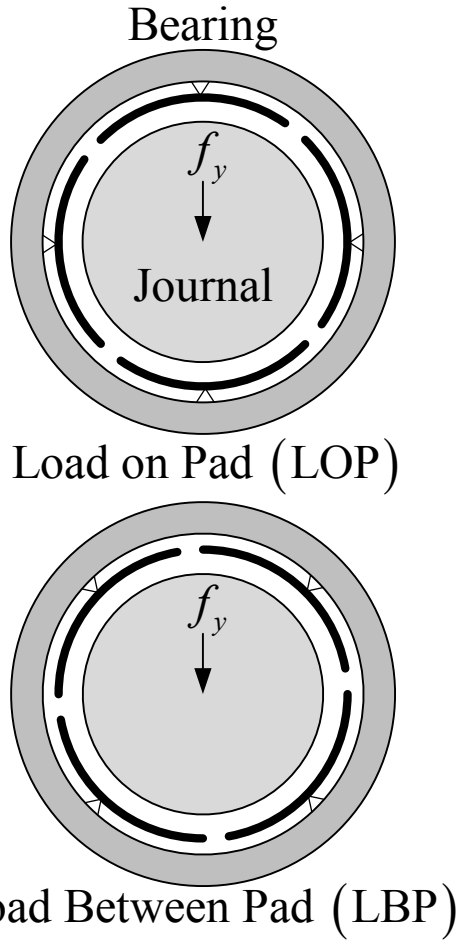

Introduction: TPJB Terminology

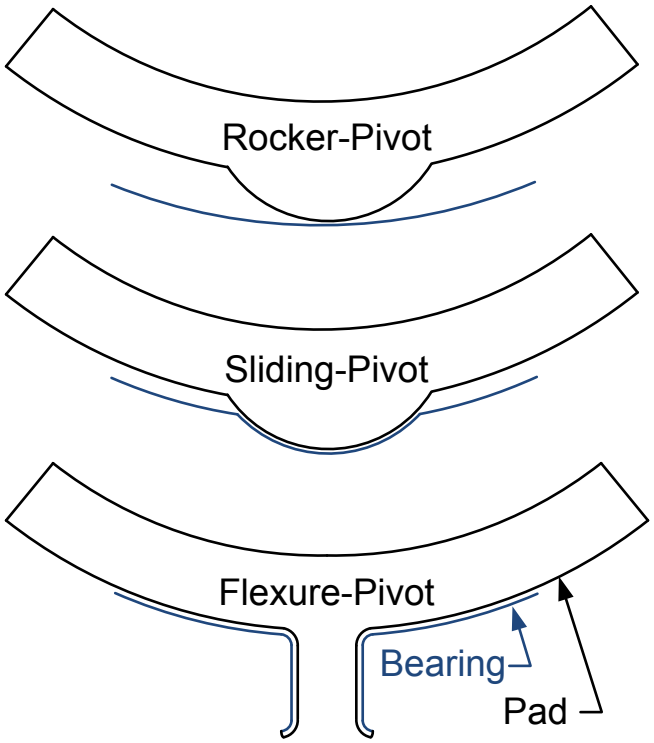

Pivot configurations

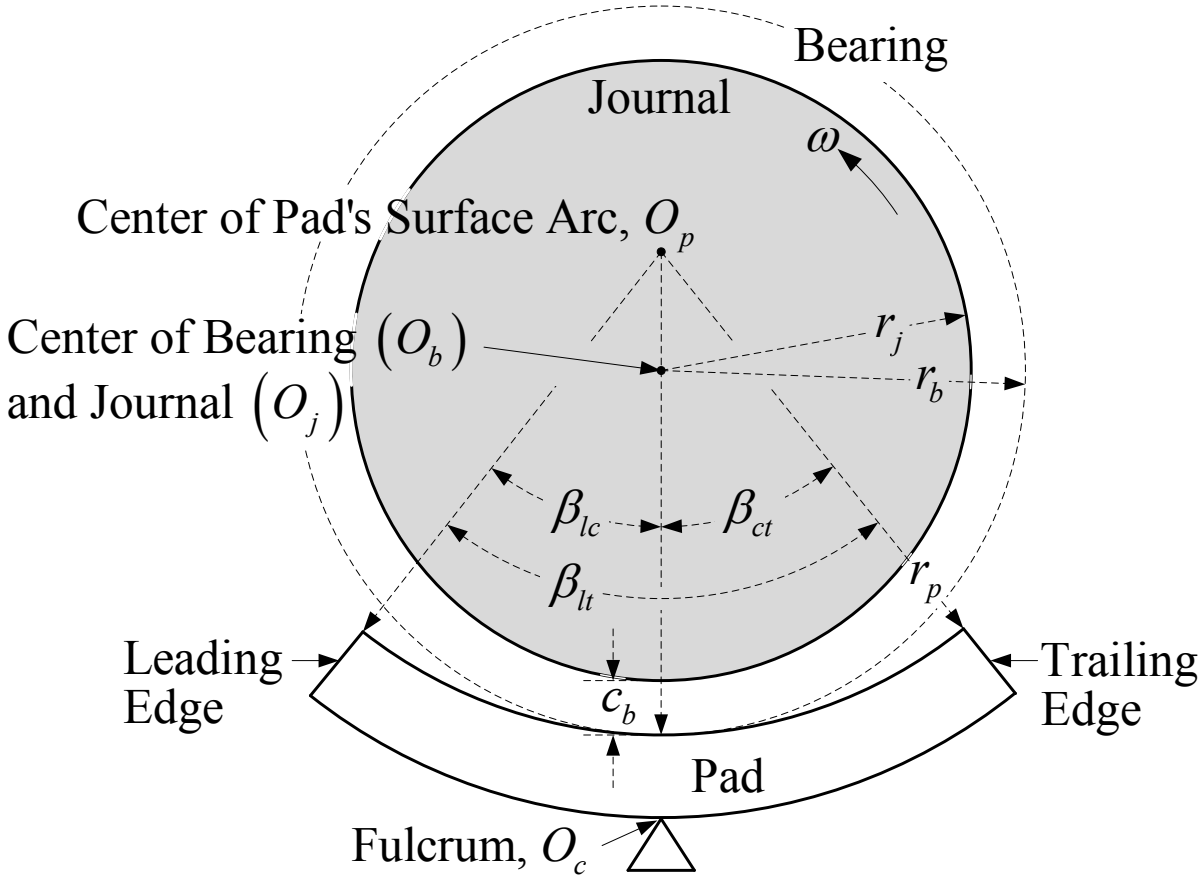

$$Offset := \frac{\beta_{lc}}{\beta_{lc}+\beta_{ct}} = \frac{\beta_{lc}}{\beta_{lt}}$$

$$c_p = r_p - r_j \qquad Preload = 1 - \frac{c_b}{c_p}$$

Introduction: TPJB Theory

- Lund's (1964) Pad Assembly Method
  - Solve for static equilibrium
  - Write *perturbed* equations of motion (EOMs) for a pad and the journal about equilibrium
  - Assume harmonic rotor motion (initially assumed synchronous)

$$\left(\tilde{x}_j, \tilde{y}_j\right) = \left(\tilde{x}_j, \tilde{y}_j\right) e^{j\Omega t}$$

  - Eliminate pad motion using a harmonic reduction (solve for pad motion as a function of the assumed rotor motion)
  - Calculate reduced direct and cross-coupled stiffness and damping coefficients for the pad
  - Sum impedances for all pads to determine bearing impedance

TPJB Theory (Improvements)

- Pad Flexibility: Nilsson (1978)
  - Approximates pad deformation using curved beam theory such that fluid film pressures result in a change in pad radius
  - Asserts that pad compliance having a small impact on static characteristics can dramatically affect dynamic characteristics (stiffness and damping)
  - Shows a 90°arc pad to have 40% less damping than a rigid pad when heavily loaded

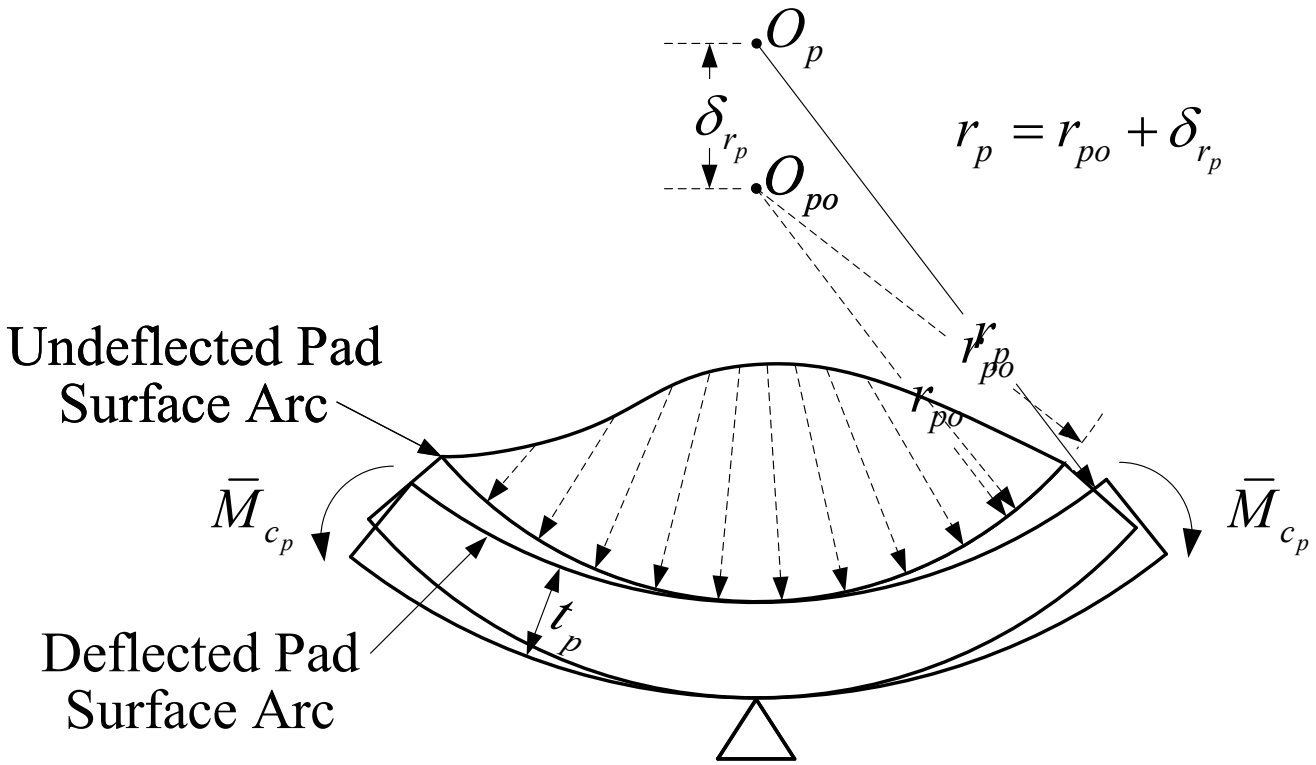

TPJB Theory (Improvements)

- Pad and Pivot Flexibility: Lund and Pederson (1987)
  - Include pad and pivot compliance
  - Analytically perturbed Reynolds equation to obtain stiffness and damping coefficients of the oil film
  - Shows a significant reduction in bearing damping with increasing pivot flexibility
  - Assert that stability calculations should be performed using the systems damped eigenvalue, not the synchronous frequency.

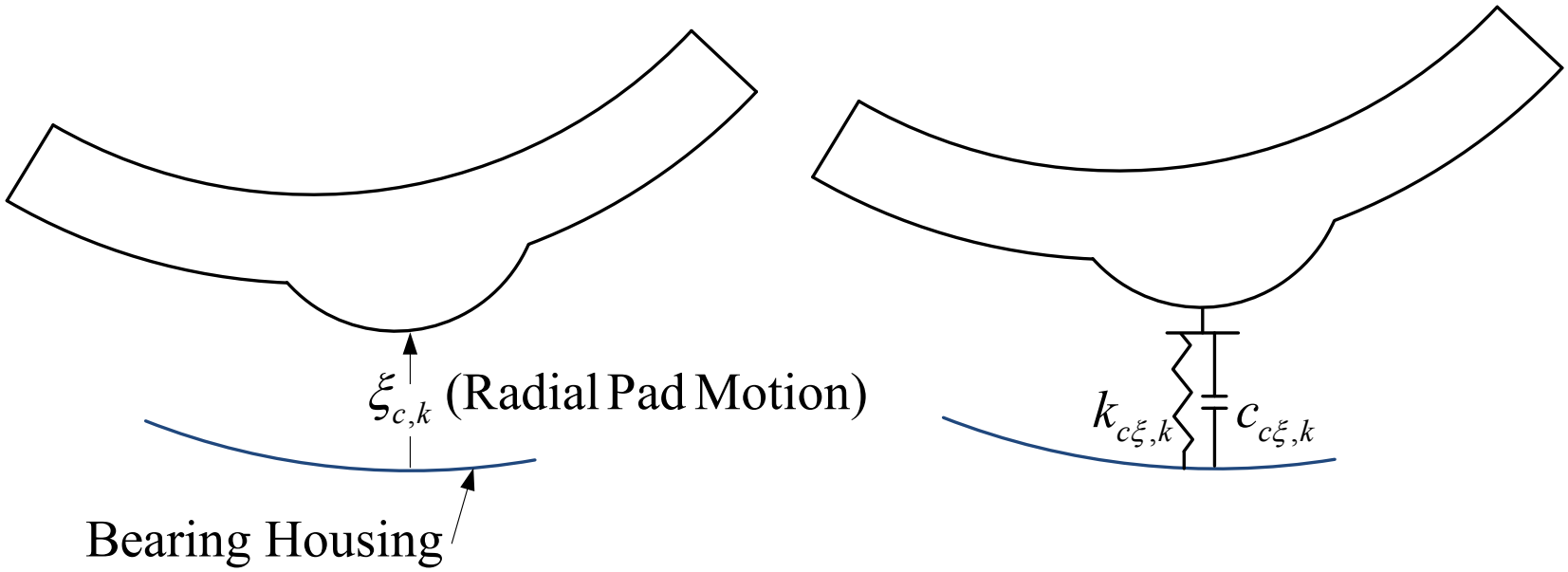

Introduction: Predicted Damping

- Dmochowski (2005, 2007)
  - Damping was reduced at higher excitation frequencies by as much as 75% for spherical pivots and 25% for rocker pivots.
  - Obtained moderately good agreement between experiments and predictions using a model having pivot flexibility (though his data showed significant scatter)
- Carter (2007) and Kulhanek (2010)
  - Measured damping was independent of frequency, speed, and load.
  - Principal damping was significantly over-predicted by codes, especially at low speeds and high loads.

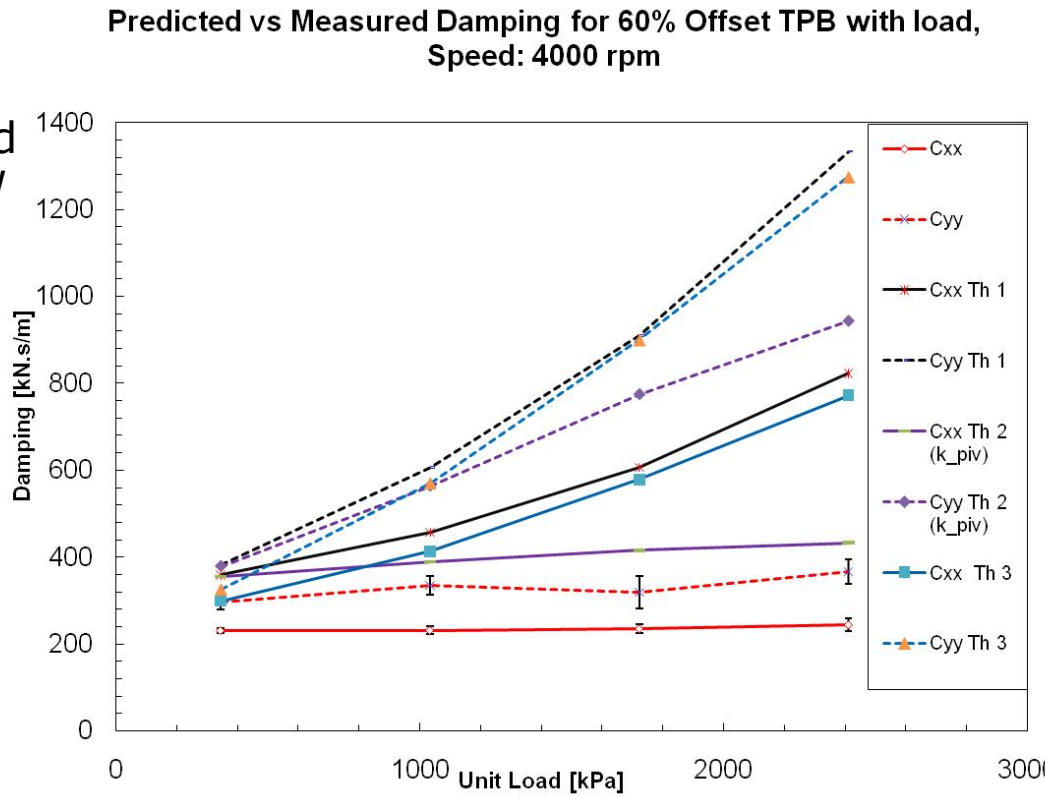

Objective:

- Determine the underlying sources responsible for the discrepancy between measured and predicted tilting-pad bearing damping.
- Approach
  - Reevaluate the fundamental assumptions governing theoretical and experimental practices
  - Focus on comparisons between predicted and measured pad motion (an adequate pad perturbation model should produce accurate bearing coefficients)

Model: The *Reference State*

- Coordinate Transformation

$$\begin{Bmatrix} \boldsymbol{b}_{\eta,k} \\ \boldsymbol{b}_{\xi,k} \end{Bmatrix} = \begin{bmatrix} \cos(\alpha_k) & \sin(\alpha_k) \\ -\sin(\alpha_k) & \cos(\alpha_k) \end{bmatrix} \begin{Bmatrix} \boldsymbol{b}_X \\ \boldsymbol{b}_Y \end{Bmatrix}$$

$$= \mathbf{Q}_\mathbf{k} \begin{Bmatrix} \boldsymbol{b}_X \\ \boldsymbol{b}_Y \end{Bmatrix}$$

- Arbitrary Pad Center of Gravity (C.G.)
- Attention to Physical Dimensions

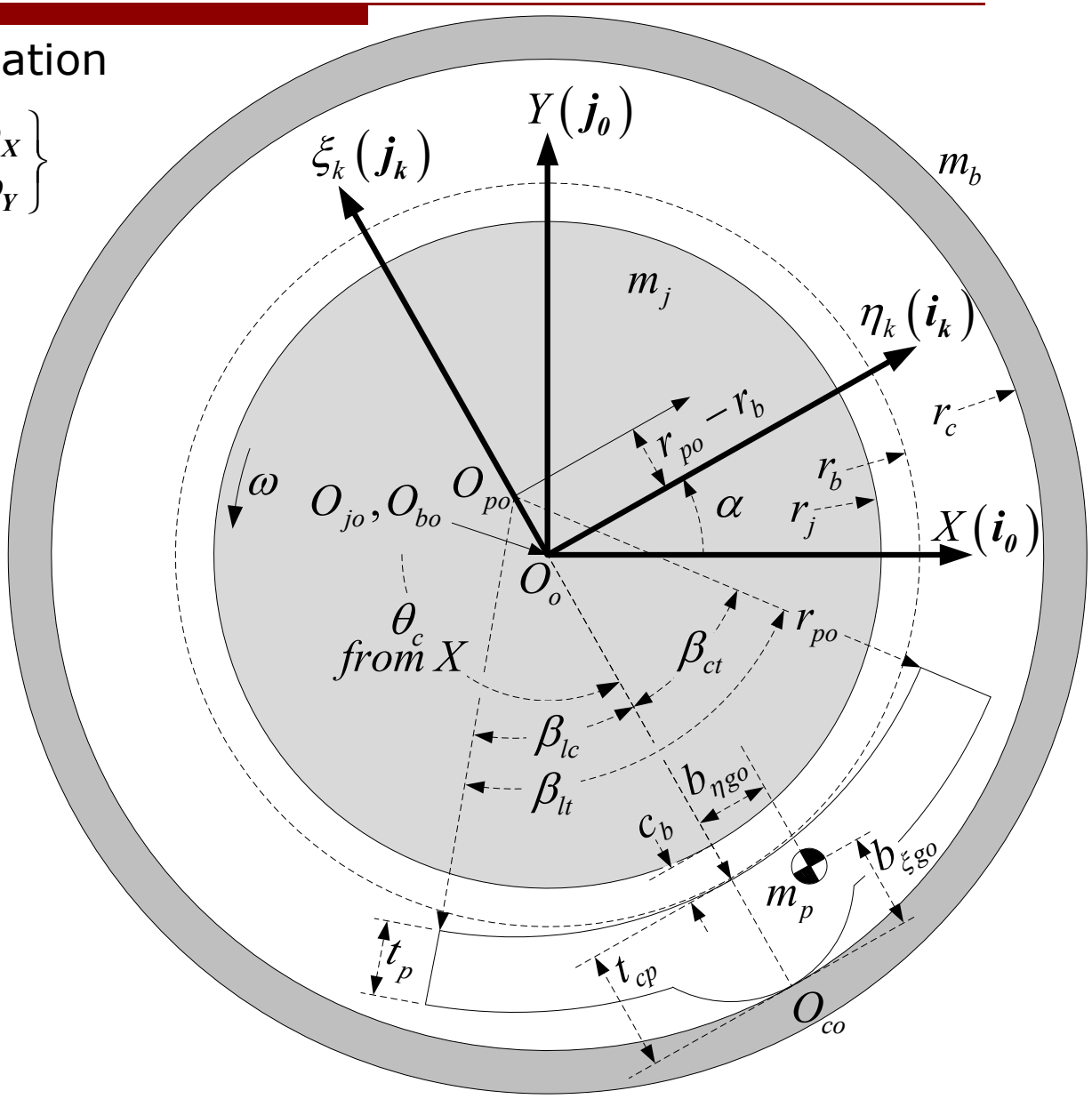

Rigid Body Pad DOFs, Pivot Reaction Forces

- Angular Reaction Force

$$M_{cz,k} = M_{cz0,k} + M_{cz1,k}$$

$$= M_{cz0,k}\left(\xi_{c0,k}, \phi_{0,k}\right) + \left.\frac{\partial M_{cz,k}}{\partial \phi_{1,k}}\right| \phi_{1,k} + \frac{\partial M_{cz,k}}{\partial \dot{\phi}_{1,k}} \dot{\phi}_{1,k}$$

- Radial Reaction Force

$$f_{c\xi,k} = f_{c\xi 0,k} + f_{c\xi 1,k}$$

$$= f_{c\xi 0,k}\left(\xi_{c0,k}\right) + \left.\frac{\partial f_{c\xi,k}}{\partial \xi_{c1,k}}\right|_0 \xi_{c1,k} + \left.\frac{\partial f_{c\xi,k}}{\partial \dot{\xi}_{c1,k}}\right|_0 \dot{\xi}_{c1,k}$$

- Transverse Reaction Force

$$f_{c\eta,k} = f_{c\eta 0,k} + f_{c\eta 1,k}$$

$$= f_{c\eta 0,k}\left(\xi_{c0,k}, \eta_{c0,k}\right) + \left.\frac{\partial f_{c\eta,k}}{\partial \eta_{c1,k}}\right|_0 \eta_{c1,k} + \left.\frac{\partial f_{c\eta,k}}{\partial \dot{\eta}_{c1,k}}\right|_0 \dot{\eta}_{c1,k}$$

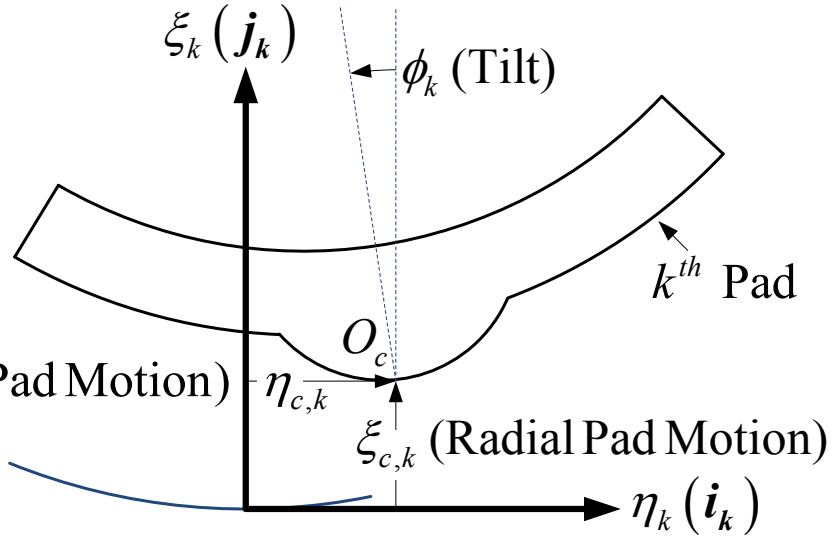

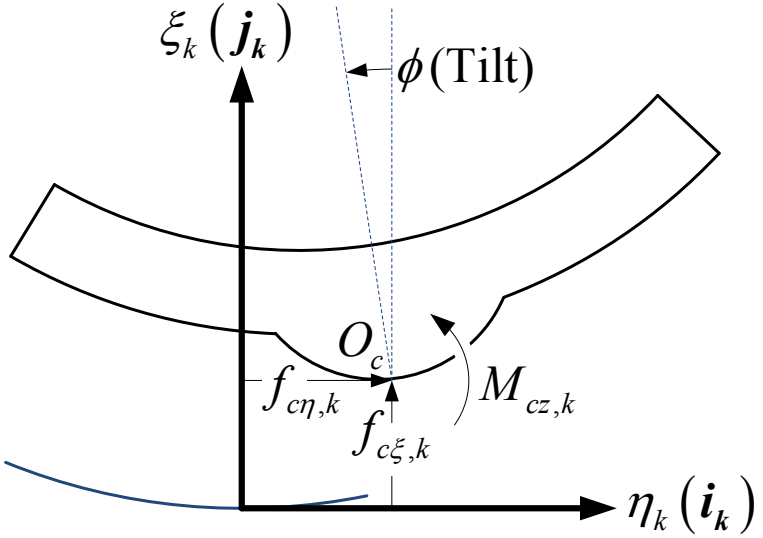

Equilibrium Pivot Reaction Forces

- Angular Stiffness and Damping

$$k_{cz,k} = \left.\frac{\partial M_{cz,k}}{\partial \phi_{1,k}}\right|_0 , \; c_{cz,k} = \left.\frac{\partial M_{cz,k}}{\partial \dot{\phi}_{1,k}}\right|_0$$

- Radial Stiffness and Damping

$$k_{c\xi,k} = \left.\frac{\partial f_{c\xi,k}}{\partial \xi_{c1,k}}\right|_0 , \; c_{c\xi,k} = \left.\frac{\partial f_{c\xi,k}}{\partial \dot{\xi}_{c1,k}}\right|_0$$

- Transverse Stiffness and Damping

$$k_{c\eta,k} = \left.\frac{\partial f_{c\eta,k}}{\partial \eta_{c1,k}}\right|_0 , \; c_{c\eta,k} = \left.\frac{\partial f_{c\eta,k}}{\partial \dot{\eta}_{c1,k}}\right|_0$$

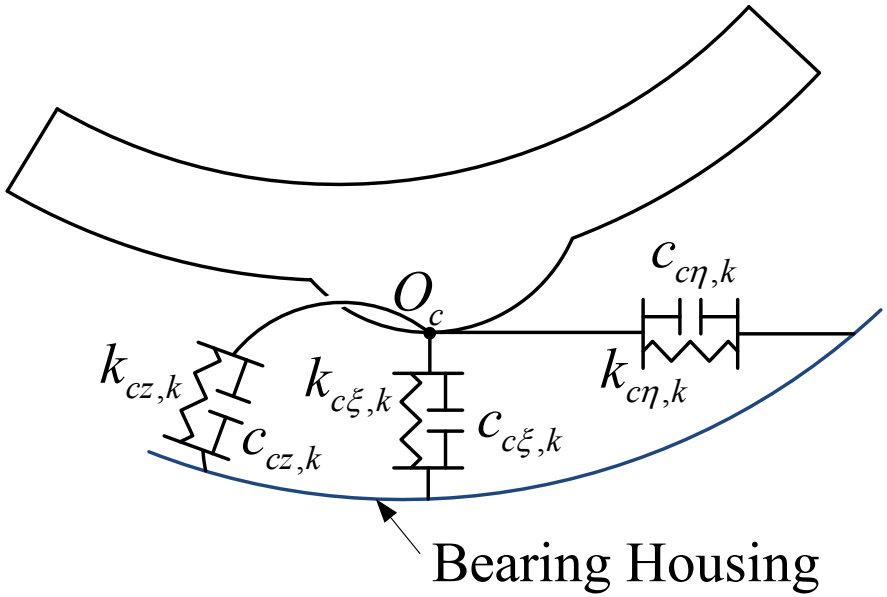

Bending Moment in a Pad

- Pressure induced bending moment

$$M_{c_p,n}(\beta)=\begin{cases}-\int_{-L_p/2}^{L_p/2}\int_{-\beta_{lc}}^{\beta} p(\beta)r_{p,n}\sin(\beta)r_p\,d\beta dZ\,,\ \beta<0\\ -\int_{-L_p/2}^{L_p/2}\int_{\beta}^{\beta_{ct}} p(\beta)r_{p,n}\sin(\beta)r_p\,d\beta dZ\,,\ \beta>0\end{cases}$$

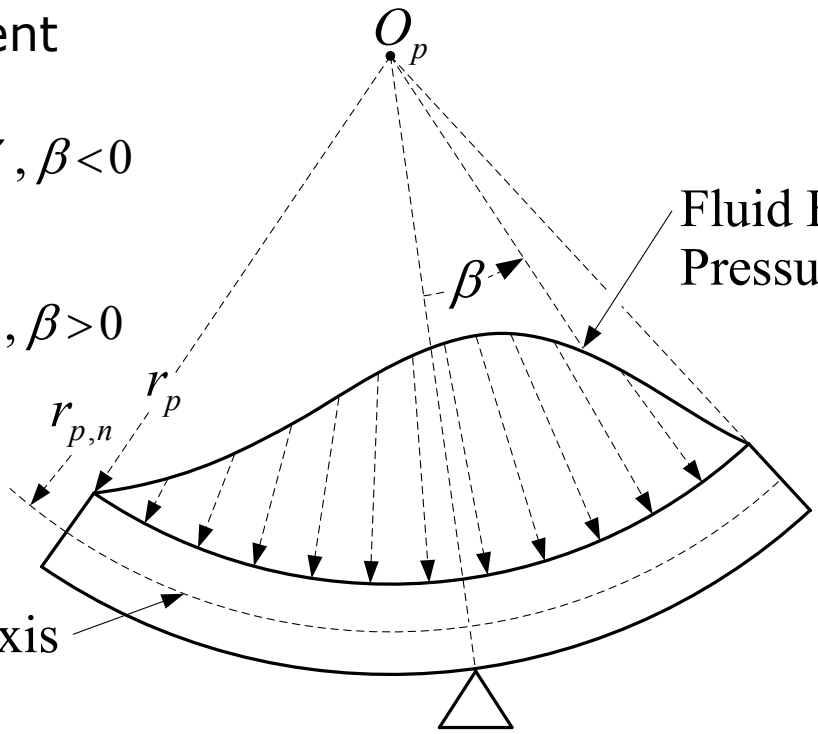

- Pivot Discontinuity

$$M_{c_p,n}(0^-)+M_{cz}=M_{c_p,n}(0^+)$$

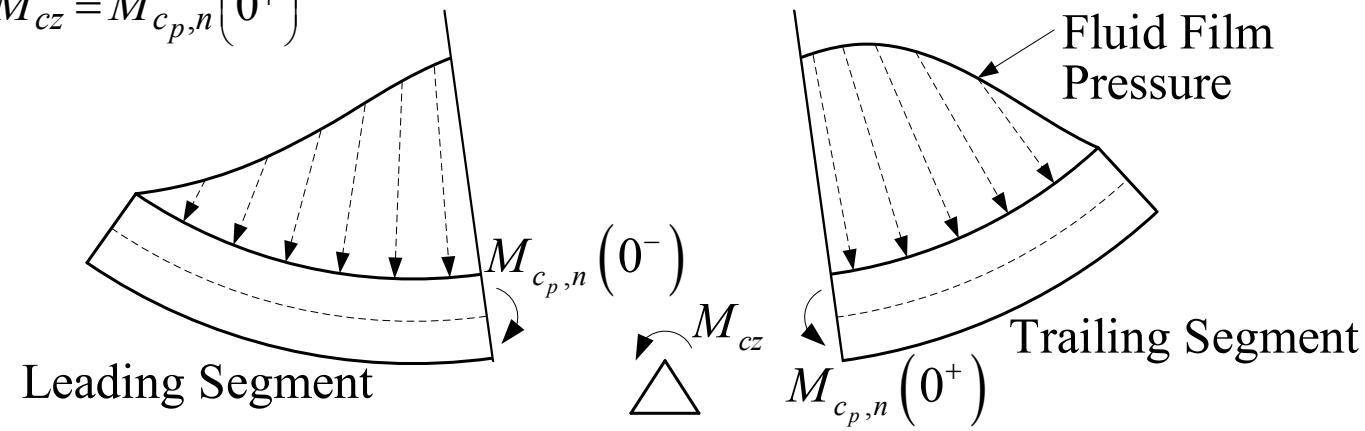

Approach taken by Nilsson, & Lund and Pederson

- Average Bending Moment (to be applied as an end moment on a curved beam)

$$\bar{M}_{c_p,n} = \frac{1}{\beta_{lt}} \int_{-\beta_l}^{\beta_t} M_{c_p,n}(\beta)\, d\beta$$

- The deflected pad radius given by

$$r_p = r_{po} + \delta_{r_p}$$

- where

$$\delta_{r_p} = r_{p0} + r_{p1} = \frac{\bar{M}_{c_p,n}}{\bar{k}_{sc_p}}$$

- and $\bar{k}_{sc_p}$ is the pad's bending stiffness taken from curved beam theory.

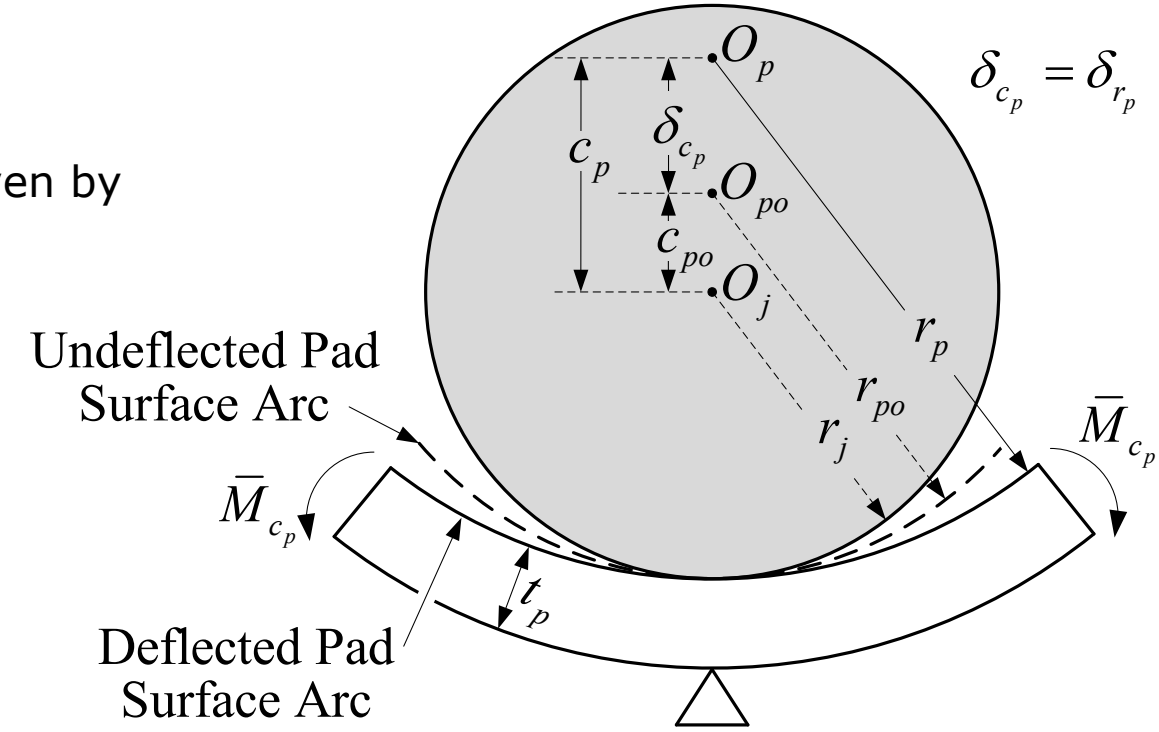

Pad deflection in the Current Work

- Nonlinearity present in the current work requires the development of a slightly different pad bending model.

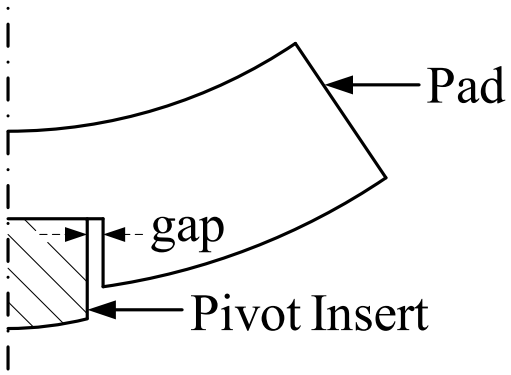

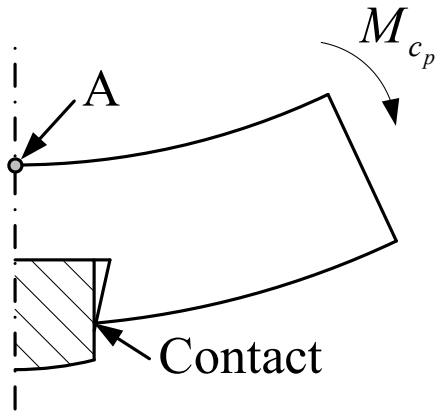

- We will assume that changes in pad clearance are given by

$$\delta_{c_p} = \frac{M_{c_p}}{k_{sc_p}}$$

- $M_{c_p} = \frac{1}{2}\left[M_{c_p}\left(\beta^-\right) + M_{c_p}\left(\beta^+\right)\right]$ is the applied fluid film moment at "A"
- Finite element analysis (FEA) is used to determine the nonlinear bending stiffness

$$k_{sc_p} = \frac{M_{c_p}}{\delta_{c_p}}$$

Theoretical Model: DOF

- Journal, O_j: $\boldsymbol{e_{j,k}} = \eta_{j,k}\boldsymbol{i_k} + \xi_{j,k}\boldsymbol{j_k}$
- Bearing, O_b: $\boldsymbol{e_{b,k}} = \eta_{b,k}\boldsymbol{i_k} + \xi_{b,k}\boldsymbol{j_k}$
- Pad pivot location, O_c:

$$\boldsymbol{e_{c,k}} = \left(\eta_{b,k} + \eta_{c,k}\right)\boldsymbol{i_k} + \left(\xi_{b,k} + \xi_{c,k}\right)\boldsymbol{j_k}$$

- Center of pad surface arc, O_p

$$\begin{aligned}\boldsymbol{e_{p,k}} &= \eta_{p,k}\boldsymbol{i_k} + \xi_{p,k}\boldsymbol{j_k} \\ &= \left(\eta_{b,k} + \eta_{c,k} - r_{cp,k}\phi_k\right)\boldsymbol{i_k} \\ &+ \left(\xi_{b,k} + \xi_{c,k} + c_p - c_b\right)\boldsymbol{j_k}\end{aligned}$$

- Relative Rotor-Pad Motion

$$\begin{aligned}\boldsymbol{e_{pj,k}} &= \boldsymbol{e_{j,k}} - \boldsymbol{e_{p,k}} = \eta_{pj,k}\boldsymbol{i_k} + \xi_{pj,k}\boldsymbol{j_k} \\ &= \left(\eta_{j,k} - \eta_{b,k} - \eta_{c,k} + r_{cp,k}\phi_k\right)\boldsymbol{i_k} + \left(\xi_{j,k} - \xi_{b,k} - \xi_{c,k} - c_p + c_b\right)\boldsymbol{j_k}\end{aligned}$$

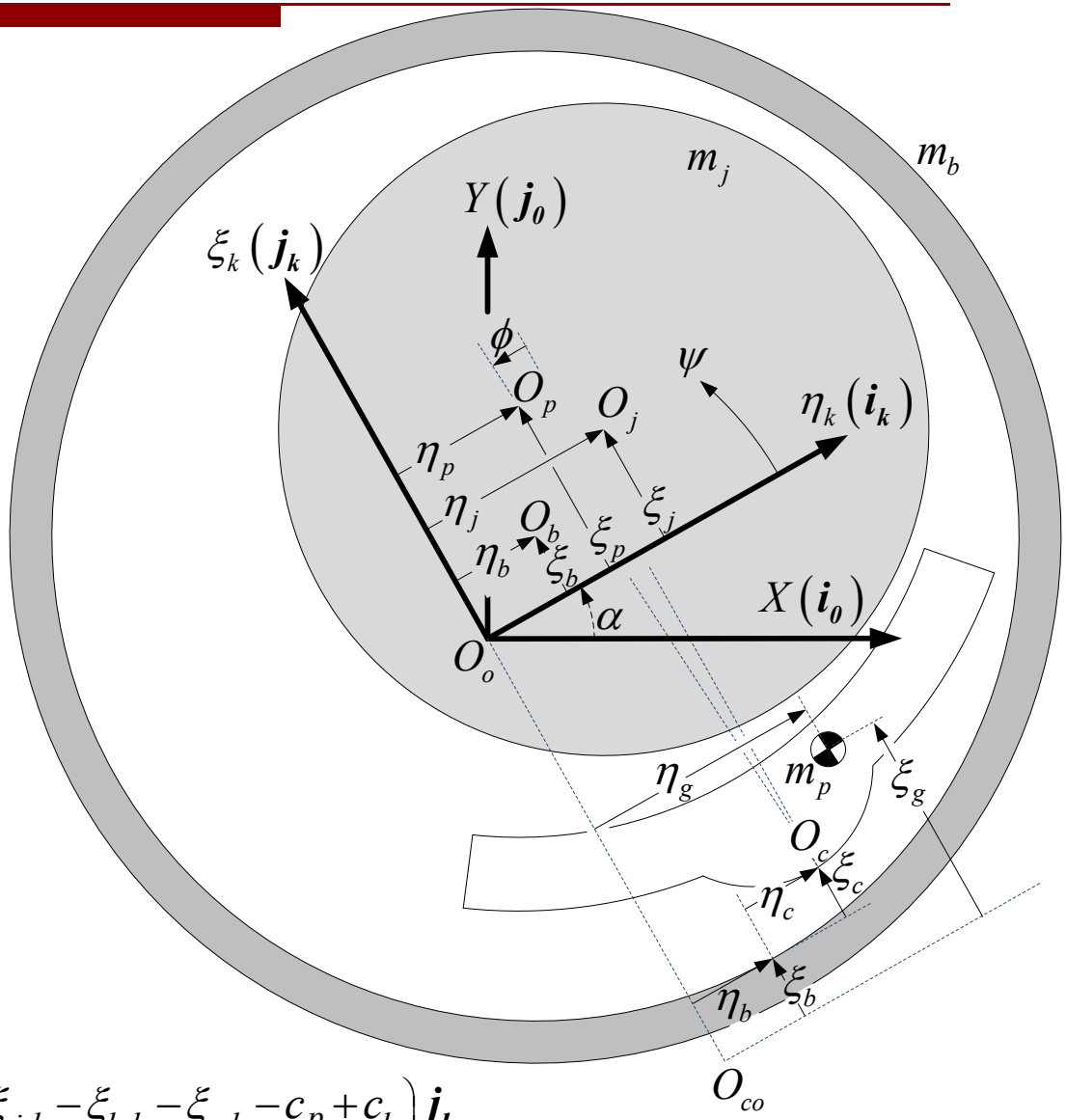

Theoretical Model: Fluid Film

- Reynolds Equation (variable viscosity)

$$\Re\left[p_k\right] := \frac{1}{r_j}\frac{\partial}{\partial\psi_k}\left\{\frac{h_k^3}{12\mu\, r_j}\frac{\partial}{\partial\psi_k}\right\} + \frac{\partial}{\partial z}\left\{\frac{h_k^3}{12\mu}\frac{\partial}{\partial z}\right\}\left[p_k\right] = \frac{\omega}{2}\frac{\partial h_k}{\partial\psi_k} + \frac{\partial h_k}{\partial t}$$

where h_k is the fluid film height

$$h_k\left(\psi_k\right) = h_{0,k}\left(\psi_k\right) + h_{1,k}\left(\psi_k\right) = c_{p,k} - \left|\boldsymbol{e_{pj,k}}\right|\cos\left(\psi_k - \psi_{pj,k}\right)$$

- Pressure perturbation

$$p_k = p_{0,k} + p_{\eta 1,k}\eta_{1,k} + p_{\xi 1,k}\xi_{1,k} + p_{c_p 1,k}c_{p1,k} + p_{\dot\eta 1,k}\dot\eta_{1,k} + p_{\dot\xi 1,k}\dot\xi_{1,k} + p_{\dot c_p 1,k}\dot c_{p1,k}$$

- Transverse and radial fluid-film reaction forces

$$\begin{Bmatrix} f_{\eta,k} \\ f_{\xi,k} \end{Bmatrix} = \begin{Bmatrix} f_{\eta 0,k} \\ f_{\xi 0,k} \end{Bmatrix} + \begin{Bmatrix} f_{\eta 1,k} \\ f_{\xi 1,k} \end{Bmatrix} = -2\int_0^{L_{p,k}/2}\int_{\psi_{l,k}}^{\psi_{t,k}} p_k \begin{Bmatrix} \cos\left(\psi_k\right) \\ \sin\left(\psi_k\right) \end{Bmatrix} r_{p0,k}\, d\psi_k\, dZ$$

- Bending moment applied by the zeroth and first order fluid-film pressures

$$M_{c_p,k} = M_{c_p 0,k} + M_{c_{p1}1,k} = -r_{p0,k}\int_0^{L_{p,k}/2}\int_{\psi_{l,k}}^{\psi_{c,k}} p_k \left|\cos\left(\psi_k\right)\right| r_{p0,k}\, d\psi_k\, dZ$$

Equilibrium Fluid Film Reaction Forces/Moments

- Static Equilibrium: Net body forces and moments on the journal, bearing, and each pad are zero.

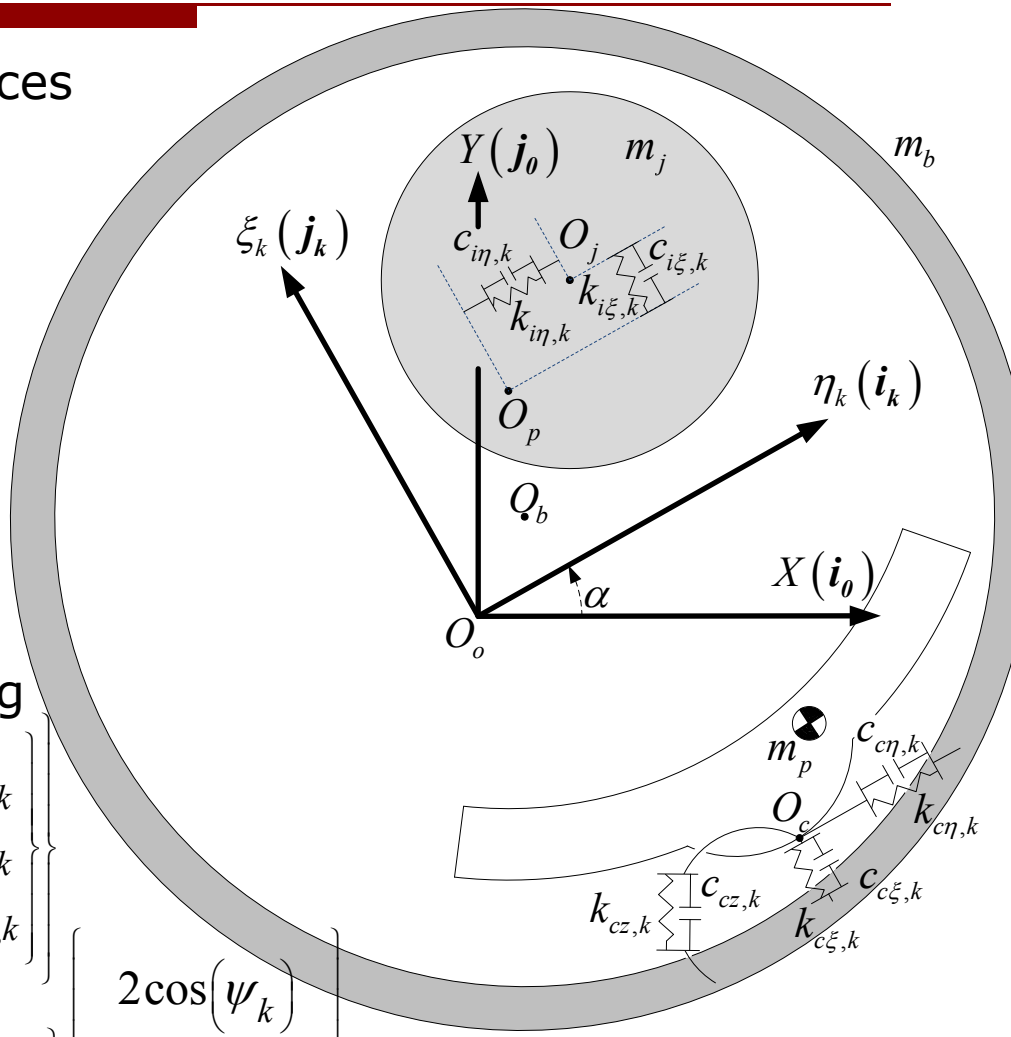

- Fluid Film Stiffness and Damping

$$\left\{\begin{Bmatrix} k_{\eta\eta,k} \\ k_{\xi\eta,k} \\ k_{c_p\eta,k} \end{Bmatrix}, \begin{Bmatrix} k_{\eta\xi,k} \\ k_{\xi\xi,k} \\ k_{c_p\xi,k} \end{Bmatrix}, \begin{Bmatrix} k_{\eta c_p,k} \\ k_{\xi c_p,k} \\ k_{c_p c_p,k} \end{Bmatrix}, \begin{Bmatrix} c_{\eta\eta,k} \\ c_{\xi\eta,k} \\ c_{c_p\eta,k} \end{Bmatrix}, \begin{Bmatrix} c_{\eta\xi,k} \\ c_{\xi\xi,k} \\ c_{c_p\xi,k} \end{Bmatrix}, \begin{Bmatrix} c_{\eta c_p,k} \\ c_{\xi c_p,k} \\ c_{c_p c_p,k} \end{Bmatrix}\right\}$$

$$= \int_0^{L_{p,k}/2\psi_{t,k}} \int_{\psi_{l,k}} \left\{p_{\eta 1,k}, p_{\xi 1,k}, p_{c_p 1,k}, p_{\dot{\eta} 1,k}, p_{\dot{\xi} 1,k}, p_{\dot{c}_p 1,k}\right\} \begin{Bmatrix} 2\cos(\psi_k) \\ 2\sin(\psi_k) \\ r_{p0,k}\left|\cos(\psi_k)\right| \end{Bmatrix} r_{p0,k} d\psi_k dz$$

Journal/Bearing/Pad Perturbed EOMs

- For a single pad, the reaction force components arising from the k^{th} pad are given for the

Journal	Bearing
$\sum F_{\eta j,k} = m_j \ddot{\eta}_{j,k} = f_{\eta,k}$	$\sum F_{\eta b,k} = m_b \ddot{\eta}_{b,k} = -f_{c\eta,k}$
$\sum F_{\xi j,k} = m_j \ddot{\xi}_{j,k} = f_{\xi,k}$	$\sum F_{\xi b,k} = m_b \ddot{\xi}_{b,k} = -f_{c\xi,k}$

- And for the k^{th} pad

$$\sum F_{\eta g,k} = m_{p,k} \ddot{\eta}_{g,k} = -f_{\eta,k} + f_{c\eta,k}$$
$$\sum F_{\xi g,k} = m_{p,k} \ddot{\xi}_{g,k} = -f_{\xi,k} + f_{c\xi,k}$$
$$\sum M_{zc,k} = I_{c,k} \ddot{\phi}_k + m_{p,k} \left(\boldsymbol{b}_{\boldsymbol{cgo,k}} \times \ddot{\boldsymbol{e}}_{\boldsymbol{c,k}} \right) = r_{cp,k} f_{\eta,k} + M_{cz,k}$$
$$\sum M_{c_p,k} = m_{c_p,k} \ddot{c}_{p1,k} = M_{c_p 1,k} - k_{sc_p,k} c_{p1,k}$$

$$\mathbf{U_{1,k}} = \left\{ \begin{array}{c} \mathbf{U_{j1,k}} \\ \hline \mathbf{U_{p1,k}} \\ \hline \mathbf{U_{b1,k}} \end{array} \right\} = \left\{ \begin{array}{c} \eta_{j1,k} \\ \xi_{j1,k} \\ \hline \phi_{1,k} \\ \eta_{c1,k} \\ \xi_{c1,k} \\ c_{p1,k} \\ \hline \eta_{b1,k} \\ \xi_{b1,k} \end{array} \right\}$$

- In matrix notation

$$\begin{bmatrix} \mathbf{M_{jj}} & \mathbf{0} & \mathbf{0} \\ \mathbf{0} & \mathbf{M_{pp,k}} & \mathbf{M_{pb,k}} \\ \mathbf{0} & \mathbf{0} & \mathbf{M_{bb}} \end{bmatrix} \begin{Bmatrix} \ddot{\mathbf{U}}_{\mathbf{j1,k}} \\ \ddot{\mathbf{U}}_{\mathbf{p1,k}} \\ \ddot{\mathbf{U}}_{\mathbf{b1,k}} \end{Bmatrix} + \begin{bmatrix} \mathbf{C_{jj,k}} & \mathbf{C_{jp,k}} & \mathbf{C_{jb,k}} \\ \mathbf{C_{pj,k}} & \mathbf{C_{pp,k}} & \mathbf{C_{pb,k}} \\ \mathbf{C_{bj,k}} & \mathbf{C_{bp,k}} & \mathbf{C_{bb,k}} \end{bmatrix} \begin{Bmatrix} \dot{\mathbf{U}}_{\mathbf{j1,k}} \\ \dot{\mathbf{U}}_{\mathbf{p1,k}} \\ \dot{\mathbf{U}}_{\mathbf{b1,k}} \end{Bmatrix} + \begin{bmatrix} \mathbf{K_{jj,k}} & \mathbf{K_{jp,k}} & \mathbf{K_{jb,k}} \\ \mathbf{K_{pj,k}} & \mathbf{K_{pp,k}} & \mathbf{K_{pb,k}} \\ \mathbf{K_{bj,k}} & \mathbf{K_{bp,k}} & \mathbf{K_{bb,k}} \end{bmatrix} \begin{Bmatrix} \mathbf{U_{j1,k}} \\ \mathbf{U_{p1,k}} \\ \mathbf{U_{b1,k}} \end{Bmatrix} = \begin{Bmatrix} \mathbf{F_{j0,k}} \\ \mathbf{F_{p0,k}} \\ \mathbf{F_{b0,k}} \end{Bmatrix}$$

Options for Including Pad in a System

- Full/Unreduced Bearing Model: Explicitly include all pad degrees of freedom in the structural model
  - Benefits
    - More Accurate
    - Frequency Independent
  - Drawbacks
    - Complexity (Requires $4n_p$ additional degrees of)
- Reduced Bearing Model: Eliminate pad degrees of freedom using a harmonic reduction to produce 2×2 stiffness, damping, (and possibly virtual-mass) coefficients
  - Benefits
    - Simplicity
    - Readily Identifiable
  - Drawbacks
    - Frequency Dependence

Full/Unreduced Bearing Model

- For the journal and bearing, the sum of reaction force components on the journal and bearing in the *X*/*Y* directions is

$$\mathbf{M_{jj}}\ddot{\mathbf{U}}_{\mathbf{j1}}+\sum_{k=1}^{n_p}\mathbf{Q_k^T}\left(\mathbf{C_{jj,k}}\mathbf{Q_k}\dot{\mathbf{U}}_{\mathbf{j1}}+\mathbf{C_{jp,k}}\dot{\mathbf{U}}_{\mathbf{p1,k}}+\mathbf{C_{jb,k}}\mathbf{Q_k}\dot{\mathbf{U}}_{\mathbf{b1}}\right)$$
$$+\sum_{k=1}^{n_p}\mathbf{Q_k^T}\left(\mathbf{K_{jj,k}}\mathbf{Q_k}\mathbf{U}_{\mathbf{j1}}+\mathbf{K_{jp,k}}\mathbf{U}_{\mathbf{p1,k}}+\mathbf{K_{jb,k}}\mathbf{Q_k}\mathbf{U}_{\mathbf{b1}}\right)=\mathbf{F}_{\mathbf{j1}}$$
$$\mathbf{M_{bb}}\ddot{\mathbf{U}}_{\mathbf{b1}}+\sum_{k=1}^{n_p}\mathbf{Q_k^T}\left(\mathbf{C_{bj,k}}\mathbf{Q_k}\dot{\mathbf{U}}_{\mathbf{j1}}+\mathbf{C_{bp,k}}\dot{\mathbf{U}}_{\mathbf{p1,k}}+\mathbf{C_{bb,k}}\mathbf{Q_k}\dot{\mathbf{U}}_{\mathbf{b1}}\right)$$
$$+\sum_{k=1}^{n_p}\mathbf{Q_k^T}\left(\mathbf{K_{bj,k}}\mathbf{Q_k}\mathbf{U}_{\mathbf{j1}}+\mathbf{K_{bp,k}}\mathbf{U}_{\mathbf{p1,k}}+\mathbf{K_{bb,k}}\mathbf{Q_k}\mathbf{U}_{\mathbf{b1}}\right)=\mathbf{F}_{\mathbf{b1}}$$

and for the k^{th} pad,

$$\mathbf{M_{pp,k}}\ddot{\mathbf{U}}_{\mathbf{p1,k}}+\mathbf{M_{pb,k}}\mathbf{Q_k}\ddot{\mathbf{U}}_{\mathbf{b1}}+\mathbf{C_{pj,k}}\mathbf{Q_k}\dot{\mathbf{U}}_{\mathbf{j1}}+\mathbf{C_{pp,k}}\dot{\mathbf{U}}_{\mathbf{p1,k}}+\mathbf{C_{pb,k}}\mathbf{Q_k}\dot{\mathbf{U}}_{\mathbf{b1}}$$
$$+\mathbf{K_{pj,k}}\mathbf{Q_k}\mathbf{U}_{\mathbf{j1}}+\mathbf{K_{pp,k}}\mathbf{U}_{\mathbf{p1,k}}+\mathbf{K_{pb,k}}\mathbf{Q_k}\mathbf{U}_{\mathbf{b1}}=\mathbf{0}\ ,\ k=1\ldots n_p$$

Full/Unreduced Bearing Model

- In matrix notation

$$\begin{bmatrix} \mathbf{M}_{jj} & \mathbf{0} & \cdots & \mathbf{0} \\ \mathbf{0} & \mathbf{M}_{pp,k} & \cdots & \mathbf{M}_{pb,k}\mathbf{Q}_k \\ \vdots & \vdots & \ddots & \vdots \\ \mathbf{0} & \mathbf{0} & \cdots & \mathbf{M}_{bb} \end{bmatrix} \begin{Bmatrix} \ddot{\mathbf{U}}_{j1} \\ \ddot{\mathbf{U}}_{p1,k} \\ \vdots \\ \ddot{\mathbf{U}}_{b1} \end{Bmatrix} + \begin{bmatrix} \sum_{k=1}^{n_p} \mathbf{Q}_k^{\mathrm{T}}\mathbf{C}_{jj,k}\mathbf{Q}_k & \mathbf{Q}_k^{\mathrm{T}}\mathbf{C}_{jp,k} & \cdots & \sum_{k=1}^{n_p} \mathbf{Q}_k^{\mathrm{T}}\mathbf{C}_{jb,k}\mathbf{Q}_k \\ \mathbf{C}_{pj,k}\mathbf{Q}_k & \mathbf{C}_{pp,k} & \cdots & \mathbf{C}_{pb,k}\mathbf{Q}_k \\ \vdots & \vdots & \ddots & \vdots \\ \sum_{k=1}^{n_p} \mathbf{Q}_k^{\mathrm{T}}\mathbf{C}_{bj,k}\mathbf{Q}_k & \mathbf{Q}_k^{\mathrm{T}}\mathbf{C}_{bp,k} & \cdots & \sum_{k=1}^{n_p} \mathbf{Q}_k^{\mathrm{T}}\mathbf{C}_{bb,k}\mathbf{Q}_k \end{bmatrix} \begin{Bmatrix} \dot{\mathbf{U}}_{j1} \\ \dot{\mathbf{U}}_{p1,k} \\ \vdots \\ \dot{\mathbf{U}}_{b1} \end{Bmatrix}$$

$$+ \begin{bmatrix} \sum_{k=1}^{n_p} \mathbf{Q}_k^{\mathrm{T}}\mathbf{K}_{jj,k}\mathbf{Q}_k & \mathbf{Q}_k^{\mathrm{T}}\mathbf{K}_{jp,k} & \cdots & \sum_{k=1}^{n_p} \mathbf{Q}_k^{\mathrm{T}}\mathbf{K}_{jb,k}\mathbf{Q}_k \\ \mathbf{K}_{pj,k}\mathbf{Q}_k & \mathbf{K}_{pp,k} & \cdots & \mathbf{K}_{pb,k}\mathbf{Q}_k \\ \vdots & \vdots & \ddots & \vdots \\ \sum_{k=1}^{n_p} \mathbf{Q}_k^{\mathrm{T}}\mathbf{K}_{bj,k}\mathbf{Q}_k & \mathbf{Q}_k^{\mathrm{T}}\mathbf{K}_{bp,k} & \cdots & \sum_{k=1}^{n_p} \mathbf{Q}_k^{\mathrm{T}}\mathbf{K}_{bb,k}\mathbf{Q}_k \end{bmatrix} \begin{Bmatrix} \mathbf{U}_{j1} \\ \mathbf{U}_{p1,k} \\ \vdots \\ \mathbf{U}_{b1} \end{Bmatrix} = \begin{Bmatrix} \mathbf{F}_{j1} \\ \mathbf{0} \\ \vdots \\ \mathbf{F}_{b1} \end{Bmatrix}$$

$$\mathbf{U}_1 = \begin{Bmatrix} \mathbf{U}_{j1} \\ \hline \mathbf{U}_{p1,k=1} \\ \hline \vdots \\ \hline \mathbf{U}_{b1} \end{Bmatrix} = \begin{Bmatrix} x_{j1} \\ y_{j1} \\ \hline \phi_{1,1} \\ \eta_{c1,1} \\ \xi_{c1,1} \\ c_{p1,1} \\ \hline \vdots \\ \hline x_{b1} \\ y_{b1} \end{Bmatrix}$$

Reduced Bearing Model

- Assume that $\left(\tilde{\xi}_i, \tilde{\eta}_i\right) = \left(\tilde{\xi}_i, \tilde{\eta}_i\right) e^{\tilde{s}t} = \left(\tilde{\xi}_i, \tilde{\eta}_i\right) e^{(-\lambda + \tilde{j}\Omega)t}$ where $\tilde{s} = \lambda + \tilde{j}\Omega$ such that

$$\begin{bmatrix} \tilde{\mathbf{I}}_{\mathbf{jj,k}} & \tilde{\mathbf{I}}_{\mathbf{jp,k}} & \tilde{\mathbf{I}}_{\mathbf{jb,k}} \\ \tilde{\mathbf{I}}_{\mathbf{pj,k}} \mathbf{M}_{\mathbf{pp,k}} \tilde{\mathbf{s}}^2 + \mathbf{I}_{\mathbf{pp,k}} \mathbf{M}_{\mathbf{pb,k}} \tilde{\mathbf{s}}^2 + \tilde{\mathbf{I}}_{\mathbf{pb,k}} \\ \tilde{\mathbf{I}}_{\mathbf{bj,k}} & \tilde{\mathbf{I}}_{\mathbf{bp,k}} & \tilde{\mathbf{I}}_{\mathbf{bb,k}} \end{bmatrix} \begin{Bmatrix} \tilde{\mathbf{U}}_{\mathbf{j1,k}} \\ \tilde{\mathbf{U}}_{\mathbf{p1,k}} \\ \tilde{\mathbf{U}}_{\mathbf{b1,k}} \end{Bmatrix} = \begin{bmatrix} \tilde{\mathbf{A}}_{\mathbf{jj,k}} & \tilde{\mathbf{A}}_{\mathbf{jp,k}} & \tilde{\mathbf{A}}_{\mathbf{jb,k}} \\ \tilde{\mathbf{A}}_{\mathbf{pj,k}} & \tilde{\mathbf{A}}_{\mathbf{pp,k}} & \tilde{\mathbf{A}}_{\mathbf{pb,k}} \\ \tilde{\mathbf{A}}_{\mathbf{bj,k}} & \tilde{\mathbf{A}}_{\mathbf{bp,k}} & \tilde{\mathbf{A}}_{\mathbf{bb,k}} \end{bmatrix} \begin{Bmatrix} \tilde{\mathbf{U}}_{\mathbf{j1,k}} \\ \tilde{\mathbf{U}}_{\mathbf{p1,k}} \\ \tilde{\mathbf{U}}_{\mathbf{b1,k}} \end{Bmatrix} = \begin{Bmatrix} -\mathbf{M}_{\mathbf{jj}} \tilde{\mathbf{s}}^2 \tilde{\mathbf{U}}_{\mathbf{j1,k}} \\ \mathbf{0} \\ -\mathbf{M}_{\mathbf{bb}} \tilde{\mathbf{s}}^2 \tilde{\mathbf{U}}_{\mathbf{b1,k}} \end{Bmatrix}$$

  where $\tilde{\mathbf{I}}_{\mathbf{ij,k}} = \mathbf{C}_{\mathbf{ij,k}} \tilde{\mathbf{s}} + \mathbf{K}_{\mathbf{ij,k}}$

- Solve for pad motion $\tilde{\mathbf{U}}_{\mathbf{p1,k}}$ using the second equation yields

$$\tilde{\mathbf{U}}_{\mathbf{p1,k}} = -\tilde{\mathbf{A}}^{-1}_{\mathbf{pp,k}} \tilde{\mathbf{A}}_{\mathbf{pj,k}} \tilde{\mathbf{U}}_{\mathbf{j1,k}} - \tilde{\mathbf{A}}^{-1}_{\mathbf{pp,k}} \tilde{\mathbf{A}}_{\mathbf{pb,k}} \tilde{\mathbf{U}}_{\mathbf{b1,k}} = \tilde{\mathbf{\Gamma}}_{\mathbf{pj,k}} \tilde{\mathbf{U}}_{\mathbf{j1,k}} + \tilde{\mathbf{\Gamma}}_{\mathbf{pb,k}} \tilde{\mathbf{U}}_{\mathbf{b1,k}}$$

  where $\tilde{\mathbf{\Gamma}}_{\mathbf{pj,k}}$ is the *pad-journal* or *pad-rotor* transfer-function matrix

$$\tilde{\mathbf{\Gamma}}_{\mathbf{pj,k}} = \begin{bmatrix} \tilde{\Gamma}^{\eta_j}_{\phi_k} & \tilde{\Gamma}^{\xi_j}_{\phi_k} \\ \tilde{\Gamma}^{\eta_j}_{\eta_{c,k}} & \tilde{\Gamma}^{\xi_j}_{\eta_{c,k}} \\ \tilde{\Gamma}^{\eta_j}_{\xi_{c,k}} & \tilde{\Gamma}^{\xi_j}_{\xi_{c,k}} \\ \tilde{\Gamma}^{\eta_j}_{c_{p,k}} & \tilde{\Gamma}^{\xi_j}_{c_{p,k}} \end{bmatrix} = -\tilde{\mathbf{A}}^{-1}_{\mathbf{pp,k}} \tilde{\mathbf{A}}_{\mathbf{pj,k}} \equiv \begin{bmatrix} \tilde{\phi}^{\eta_j}_{1,k} & \tilde{\phi}^{\xi_j}_{1,k} \\ \tilde{\eta}^{\eta_j}_{c1,k} & \tilde{\eta}^{\xi_j}_{c1,k} \\ \tilde{\xi}^{\eta_j}_{c1,k} & \tilde{\xi}^{\xi_j}_{c1,k} \\ \tilde{c}^{\eta_j}_{p1,k} & \tilde{c}^{\xi_j}_{p1,k} \end{bmatrix} \begin{bmatrix} \tilde{\eta}^{-1}_{j1,k} & 0 \\ 0 & \tilde{\xi}^{-1}_{j1,k} \end{bmatrix}$$

- and $\tilde{\mathbf{\Gamma}}_{\mathbf{pb,k}}$ is similarly defined as the *pad-bearing* transfer-function matrix

Reduced Bearing Model

- Substituting $\tilde{\mathbf{U}}_{\mathbf{p1,k}}$ back into the previous set of equations yields

$$\begin{bmatrix} \tilde{\mathbf{A}}_{\mathbf{jj,k}} + \tilde{\mathbf{A}}_{\mathbf{jp,k}}\tilde{\mathbf{\Gamma}}_{\mathbf{pj,k}} & \tilde{\mathbf{A}}_{\mathbf{jb,k}} + \tilde{\mathbf{A}}_{\mathbf{jp,k}}\tilde{\mathbf{\Gamma}}_{\mathbf{pb,k}} \\ \tilde{\mathbf{A}}_{\mathbf{bj,k}} + \tilde{\mathbf{A}}_{\mathbf{bp,k}}\tilde{\mathbf{\Gamma}}_{\mathbf{pj,k}} & \tilde{\mathbf{A}}_{\mathbf{bb,k}} + \tilde{\mathbf{A}}_{\mathbf{bp,k}}\tilde{\mathbf{\Gamma}}_{\mathbf{pb,k}} \end{bmatrix} \begin{Bmatrix} \tilde{\mathbf{U}}_{\mathbf{j1,k}} \\ \tilde{\mathbf{U}}_{\mathbf{b1,k}} \end{Bmatrix} = \begin{bmatrix} \tilde{\mathbf{H}}_{\mathbf{jj,k}} & \tilde{\mathbf{H}}_{\mathbf{jb,k}} \\ \tilde{\mathbf{H}}_{\mathbf{bj,k}} & \tilde{\mathbf{H}}_{\mathbf{bb,k}} \end{bmatrix} \begin{Bmatrix} \tilde{\mathbf{U}}_{\mathbf{j1,k}} \\ \tilde{\mathbf{U}}_{\mathbf{b1,k}} \end{Bmatrix} = \begin{Bmatrix} -\mathbf{M}_{\mathbf{jj}}\tilde{\mathbf{s}}^{\mathbf{2}}\tilde{\mathbf{U}}_{\mathbf{j1,k}} \\ -\mathbf{M}_{\mathbf{bb}}\tilde{\mathbf{s}}^{\mathbf{2}}\tilde{\mathbf{U}}_{\mathbf{b1,k}} \end{Bmatrix}$$

  where the elements of $\tilde{\mathbf{H}}_{\mathbf{ij,k}}$ are commonly referred to as impedances, or complex dynamic stiffnesses, where

$$\tilde{\mathbf{H}}_{\mathbf{ij,k}}(\Omega) = \begin{bmatrix} \tilde{H}_{\eta\eta,k} & \tilde{H}_{\eta\xi,k} \\ \tilde{H}_{\xi\eta,k} & \tilde{H}_{\xi\xi,k} \end{bmatrix}_{ij,k}, \mathbf{K}_{\mathbf{ij,k}}(\Omega) = \mathrm{Re}\left\{\tilde{\mathbf{H}}_{\mathbf{ij,k}}\right\}, \mathbf{C}_{\mathbf{ij,k}}(\Omega) = \frac{\mathrm{Im}\left\{\tilde{\mathbf{H}}_{\mathbf{ij,k}}\right\}}{\Omega},$$

- Rotating $\tilde{\mathbf{H}}_{\mathbf{ij,k}}$ into the *X*/*Y* coordinate system and summing impedances across all pads nets the journal/bearing impedances

$$\begin{bmatrix} \tilde{\mathbf{H}}_{\mathbf{jj}} & \tilde{\mathbf{H}}_{\mathbf{jb}} \\ \tilde{\mathbf{H}}_{\mathbf{bj}} & \tilde{\mathbf{H}}_{\mathbf{bb}} \end{bmatrix} = \begin{bmatrix} \sum_{k=1}^{n_p} \mathbf{Q}_{\mathbf{k}}^{\mathbf{T}}\tilde{\mathbf{H}}_{\mathbf{jj,k}}\mathbf{Q}_{\mathbf{k}} & \sum_{k=1}^{n_p} \mathbf{Q}_{\mathbf{k}}^{\mathbf{T}}\tilde{\mathbf{H}}_{\mathbf{jb,k}}\mathbf{Q}_{\mathbf{k}} \\ \sum_{k=1}^{n_p} \mathbf{Q}_{\mathbf{k}}^{\mathbf{T}}\tilde{\mathbf{H}}_{\mathbf{bj,k}}\mathbf{Q}_{\mathbf{k}} & \sum_{k=1}^{n_p} \mathbf{Q}_{\mathbf{k}}^{\mathbf{T}}\tilde{\mathbf{H}}_{\mathbf{bb,k}}\mathbf{Q}_{\mathbf{k}} \end{bmatrix}$$

Test Rig: Overview

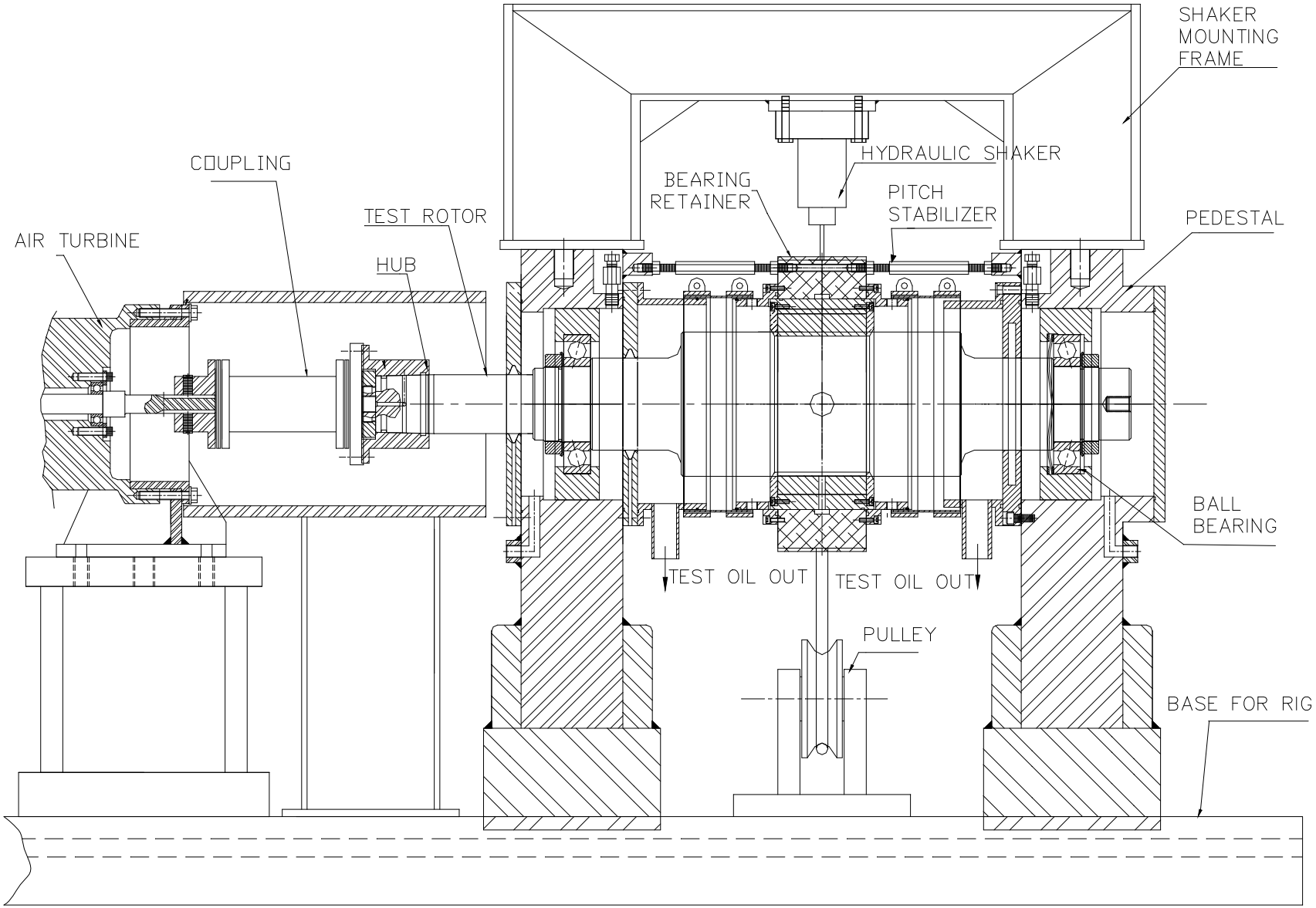

Test Bearing

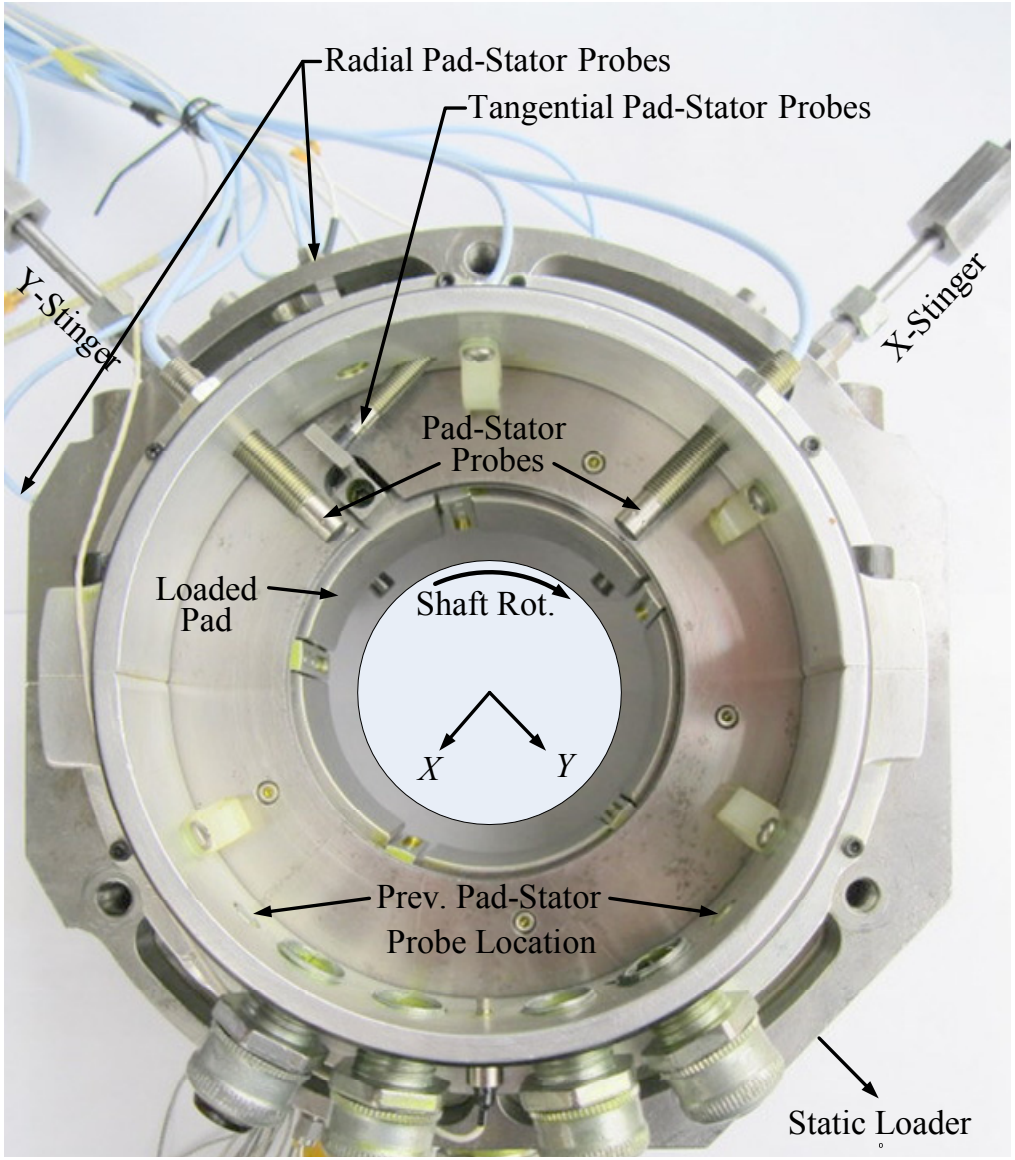

Properties of the bearing at room temp. (24 °C).

Number of Pads	5
Loading Configuration	Load on pad (LOP)
Pad Arc Length (β_{lt})	58.9°
Rotor Diameter	101.587 mm (3.9995 in)
Pad Axial Length	55.88 mm (2.200 in)
Cold Bearing Radial Clearance[1]	68 μm (2.67 mils)
Cold Pad Radial Clearance[1]	120.65 μm (4.75 mils)
Cold Bearing Preload[1]	0.44
Offset	0.50
Pad Mass (m_p)	0.385 kg (0.849 lb)
Pad Inertia about O_c ($I_{c,k}$)	1.807e-4 kg-m^2 (0.851 lb-in^2)
Pad C.G ($b_{\eta go}$,$b_{\xi go}$)	(0,0.0127) m, (0,0.5) in
Bearing Lubricant	DTE 797, ISO VG-32

Operating conditions
Speed: 4400-13100 rpm
Unit Load: 0-3134 kPa (0-454 psi)

Pad Motion Measurement

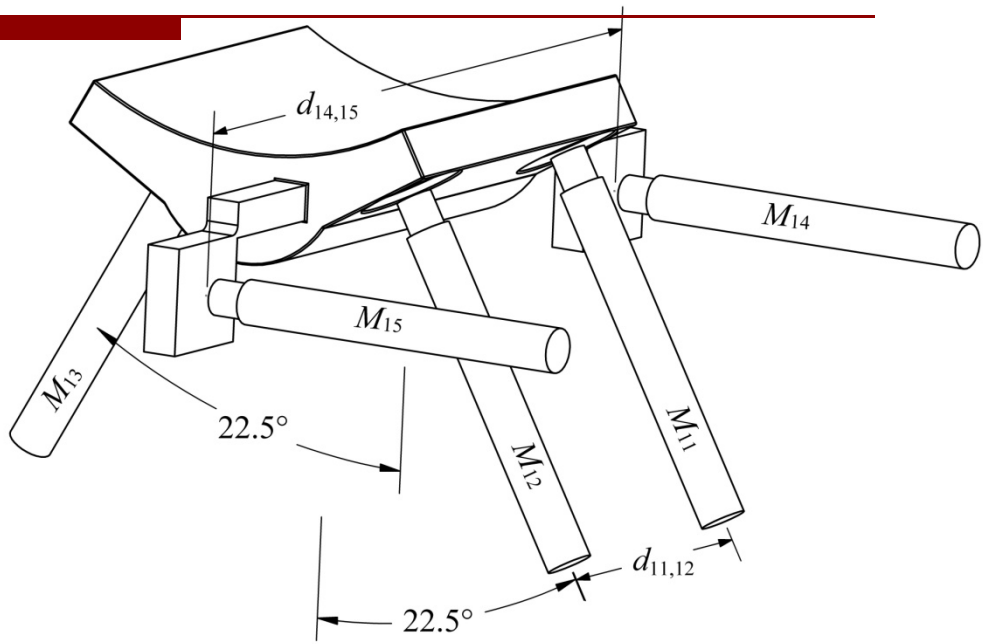

Motion Probe Arrangement

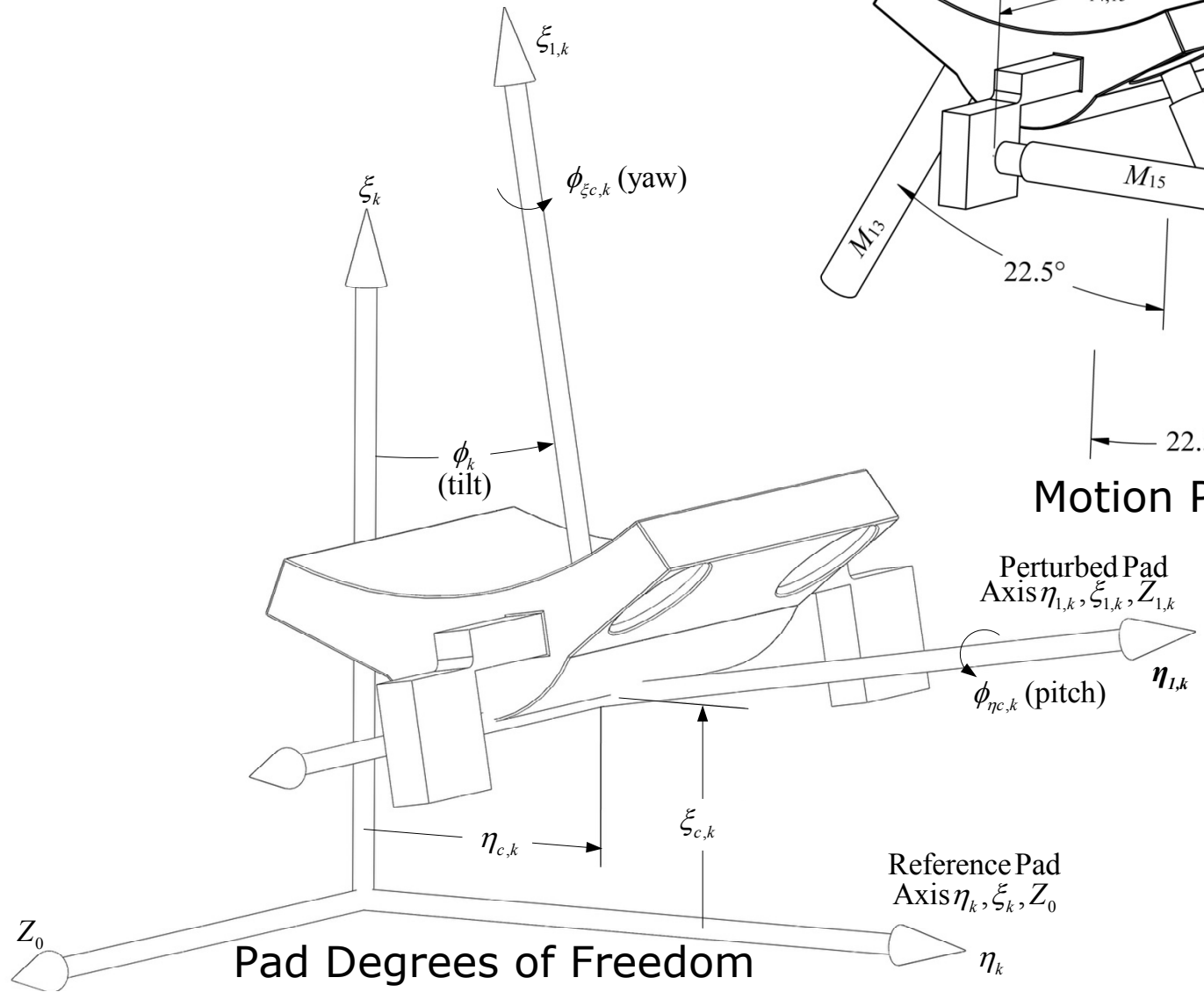

Pad Degrees of Freedom

Pad Strain Measurement

- Strain gages were applied to the side of the loaded pad

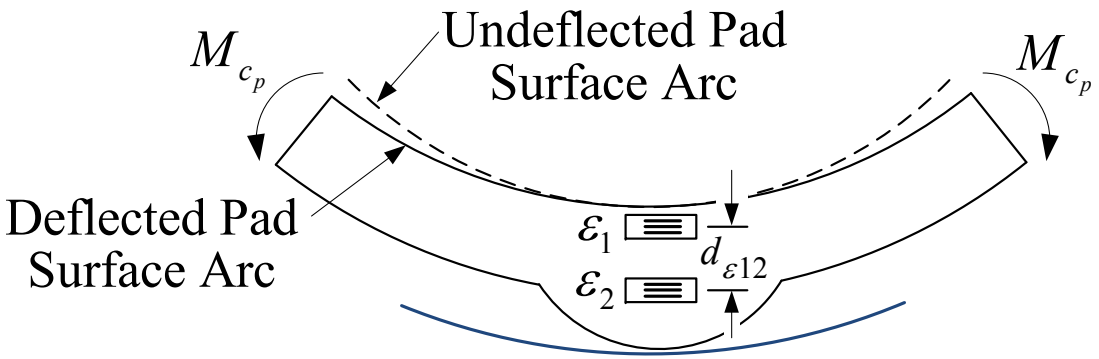

- Differential Wheatstone Bridge Configuration

$$\varepsilon_{12} = \varepsilon_1 - \varepsilon_2 = \left(v_{out} - v_o\right) k_{\varepsilon 12}$$

- Changes in pad clearance were determined using

$$\delta_{c_p} = k_{c_p \varepsilon_{12}} \varepsilon_{12}$$

where $k_{c_p \varepsilon_{12}}$ will be determined by correlating differential strains to changes in pad radius using FEA

Test Rig: Data Analysis

- Writing an EOM for the stator and taking an FFT nets

$$\begin{Bmatrix} \tilde{F}_{ex} - m_{bx}\tilde{A}_{bx} \\ \tilde{F}_{ey} - m_{by}\tilde{A}_{by} \end{Bmatrix} = \begin{bmatrix} \tilde{H}_{xx} & \tilde{H}_{xy} \\ \tilde{H}_{yx} & \tilde{H}_{yy} \end{bmatrix} \begin{Bmatrix} \tilde{U}_x \\ \tilde{U}_y \end{Bmatrix}$$

- Given orthogonal excitations, we can solve for $\tilde{\mathbf{H}}_{\mathbf{ij}}$ using

$$\begin{bmatrix} \tilde{F}_{ex}^{x} - m_{bx}\tilde{A}_{bx}^{x} & \tilde{F}_{ex}^{y} - m_{bx}\tilde{A}_{bx}^{y} \\ \tilde{F}_{ey}^{x} - m_{by}\tilde{A}_{by}^{x} & \tilde{F}_{ey}^{y} - m_{by}\tilde{A}_{by}^{y} \end{bmatrix} \begin{bmatrix} \tilde{U}_x^x & \tilde{U}_x^y \\ \tilde{U}_y^x & \tilde{U}_y^y \end{bmatrix}^{-1} = \begin{bmatrix} \tilde{H}_{xx} & \tilde{H}_{xy} \\ \tilde{H}_{yx} & \tilde{H}_{yy} \end{bmatrix}$$

and likewise for the pad-rotor transfer functions $\tilde{\mathbf{\Gamma}}_{\mathbf{pj,k}}$ using

$$\tilde{\mathbf{\Gamma}}_{\mathbf{pj,k}} = \begin{bmatrix} \tilde{\Gamma}_{\phi_k}^{\eta_j} & \tilde{\Gamma}_{\phi_k}^{\xi_j} \\ \tilde{\Gamma}_{\eta_{c,k}}^{\eta_j} & \tilde{\Gamma}_{\eta_{c,k}}^{\xi_j} \\ \tilde{\Gamma}_{\xi_{c,k}}^{\eta_j} & \tilde{\Gamma}_{c_{p,k}}^{\xi_j} \\ \tilde{\Gamma}_{c_{p,k}}^{\eta_j} & \tilde{\Gamma}_{\phi_{\xi c1,k}}^{\xi_j} \end{bmatrix} = \begin{bmatrix} \tilde{\phi}_{1,k}^{\eta_j} & \tilde{\phi}_{1,k}^{\xi_j} \\ \tilde{\eta}_{c1,k}^{\eta_j} & \tilde{\eta}_{c1,k}^{\xi_j} \\ \tilde{\xi}_{c1,k}^{\eta_j} & \tilde{\xi}_{c1,k}^{\xi_j} \\ \tilde{c}_{p1,k}^{\eta_j} & \tilde{c}_{p1,k}^{\xi_j} \end{bmatrix} \mathbf{Q}_{\mathbf{k}} \begin{bmatrix} \tilde{U}_x^x & \tilde{U}_x^y \\ \tilde{U}_y^x & \tilde{U}_y^y \end{bmatrix}^{-1}$$

where the *x*/*y* superscripts denote data recorded during orthogonal *X*/*Y* stator excitations.

Results: Pivot Load-vs-Deflection

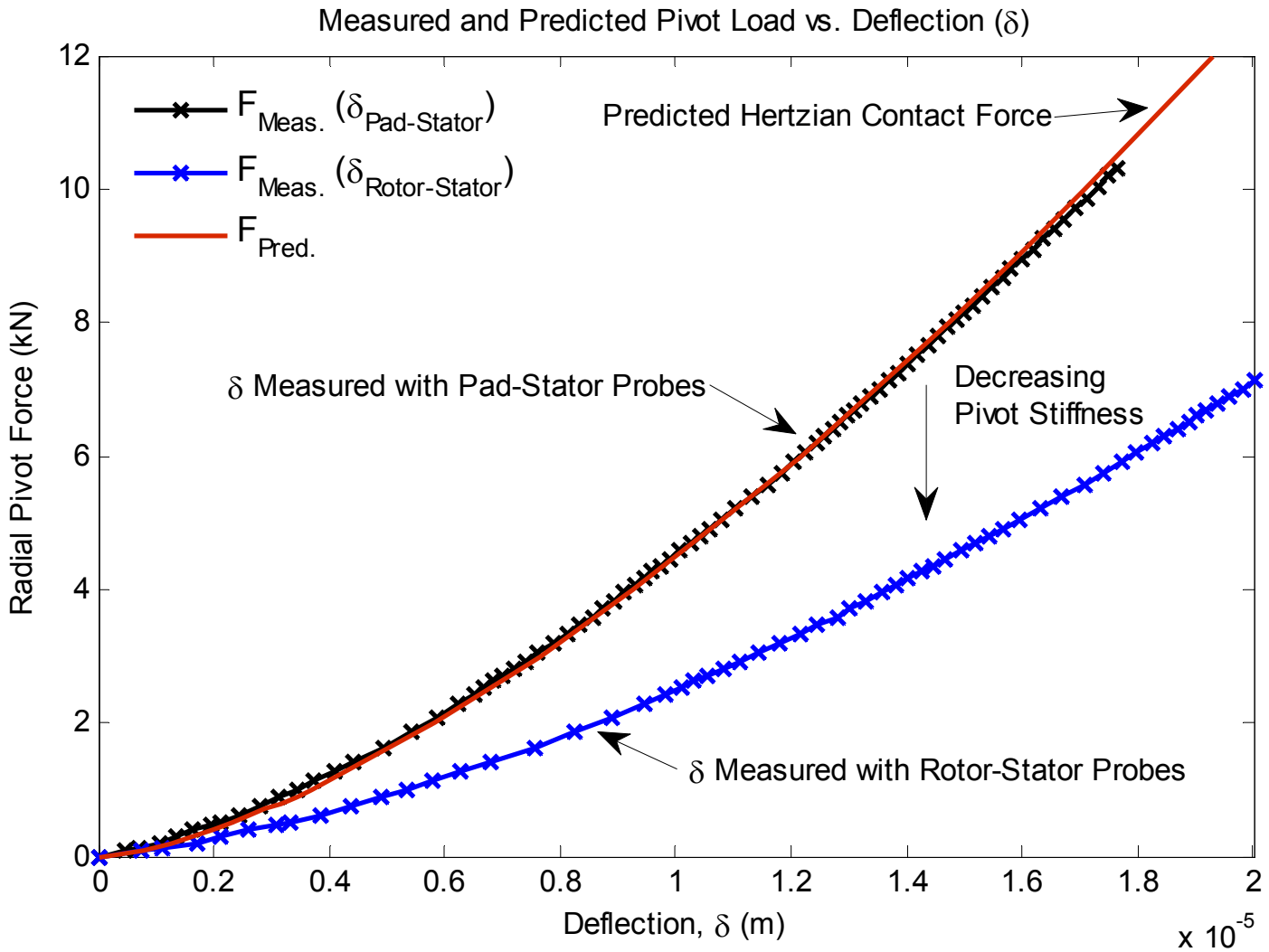

Results: Pivot Stiffness

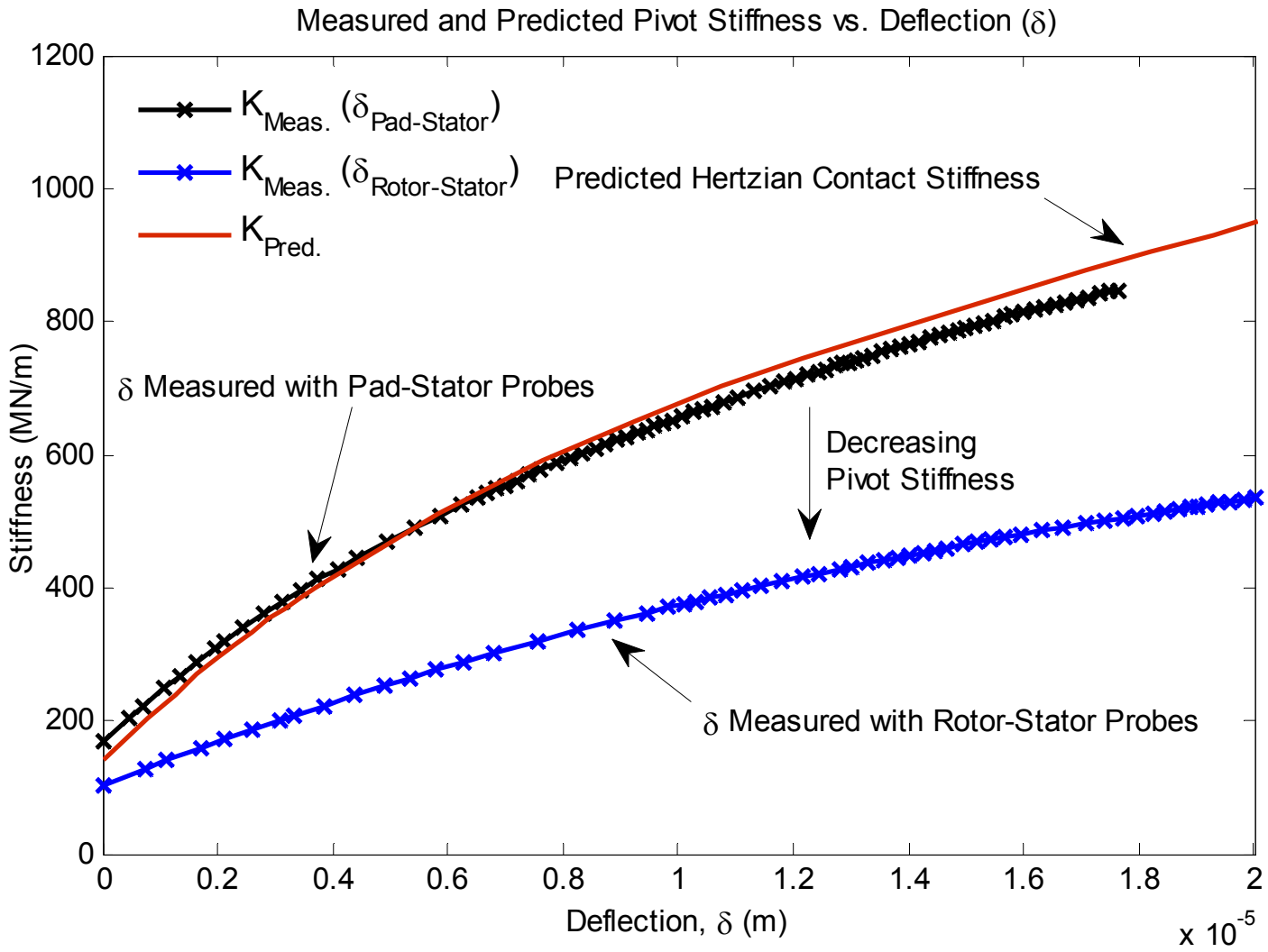

Results: Pivot Stiffness

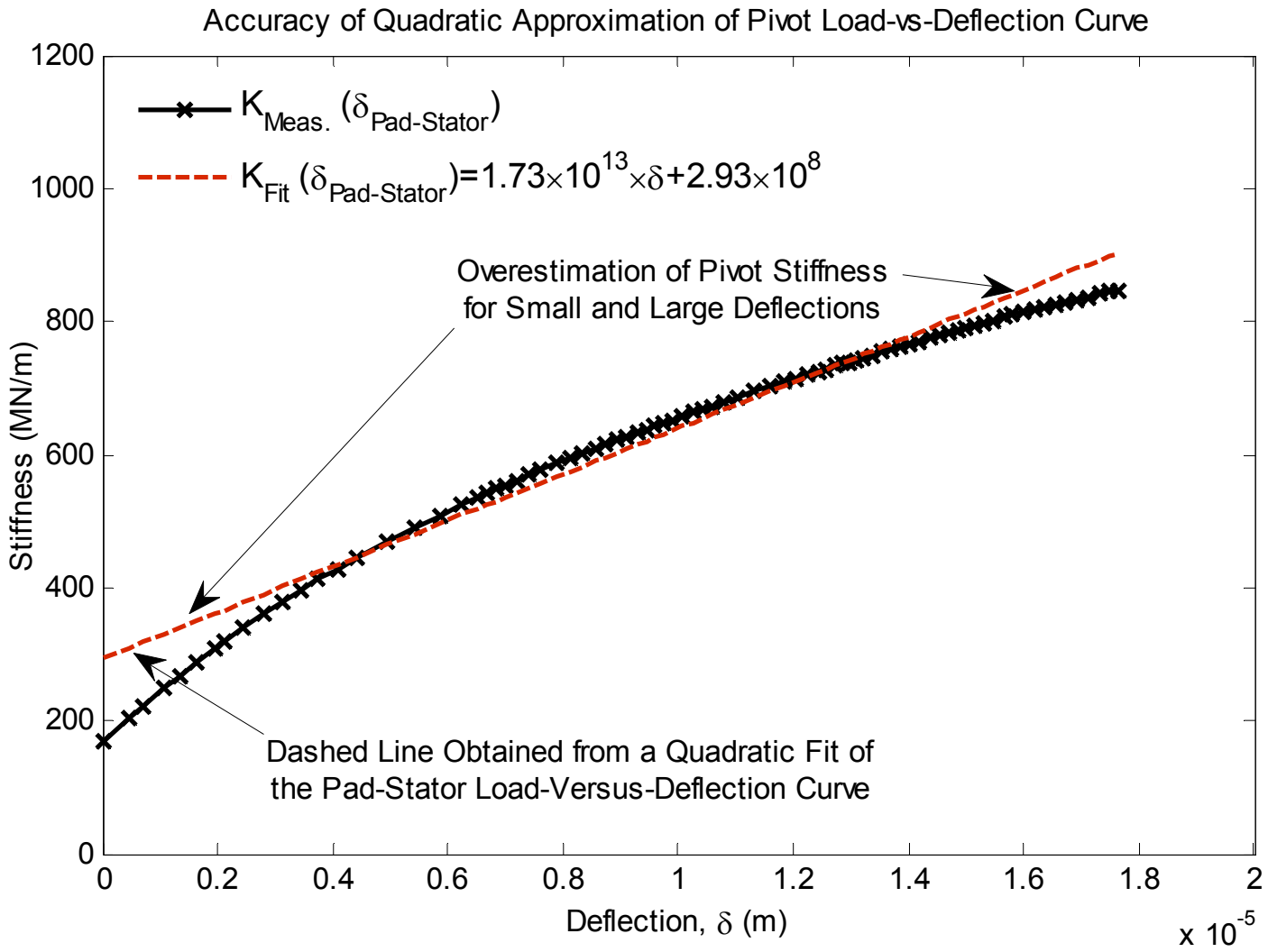

$$f_{c\xi} = 7.321\times10^{21}\delta^4 - 6.653\times10^{17}\delta^3 + 3.339\times10^{13}\delta^2 + 1.773\times10^{8}\delta - 64.44$$

Results: Pad Bending Stiffness

Region 1

(light/no bending moments)

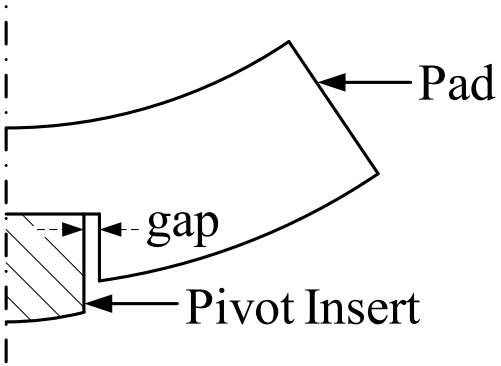

Region 2

(heavy bending moments)

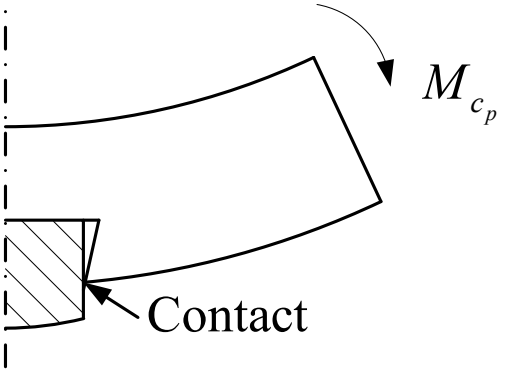

- Pivot insert design
  - Nonlinear bending stiffness
  - Increases with increasing bending moment

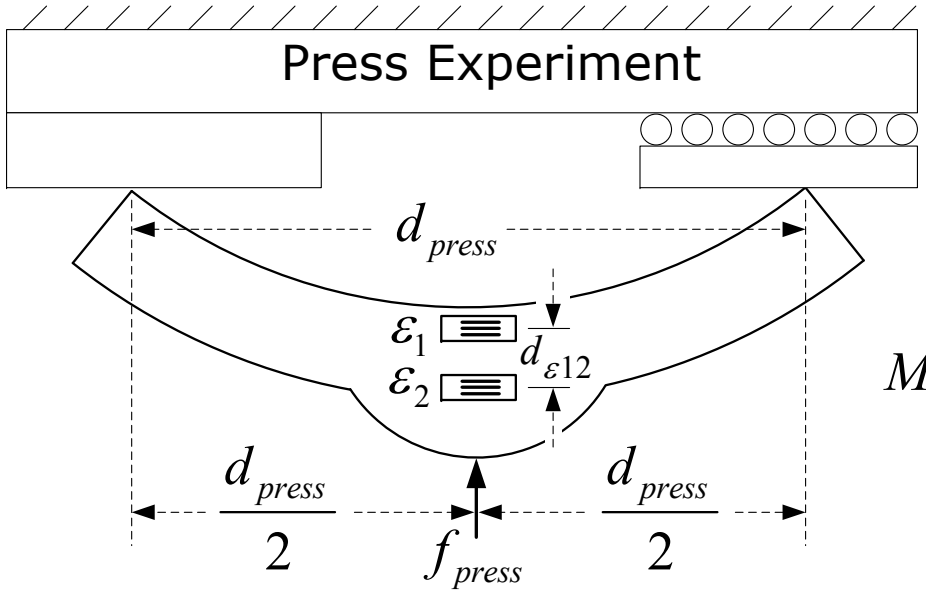

$$M_{c_p} = \frac{f_{press}\, d_{press}}{4}$$

Results: FEA Validation

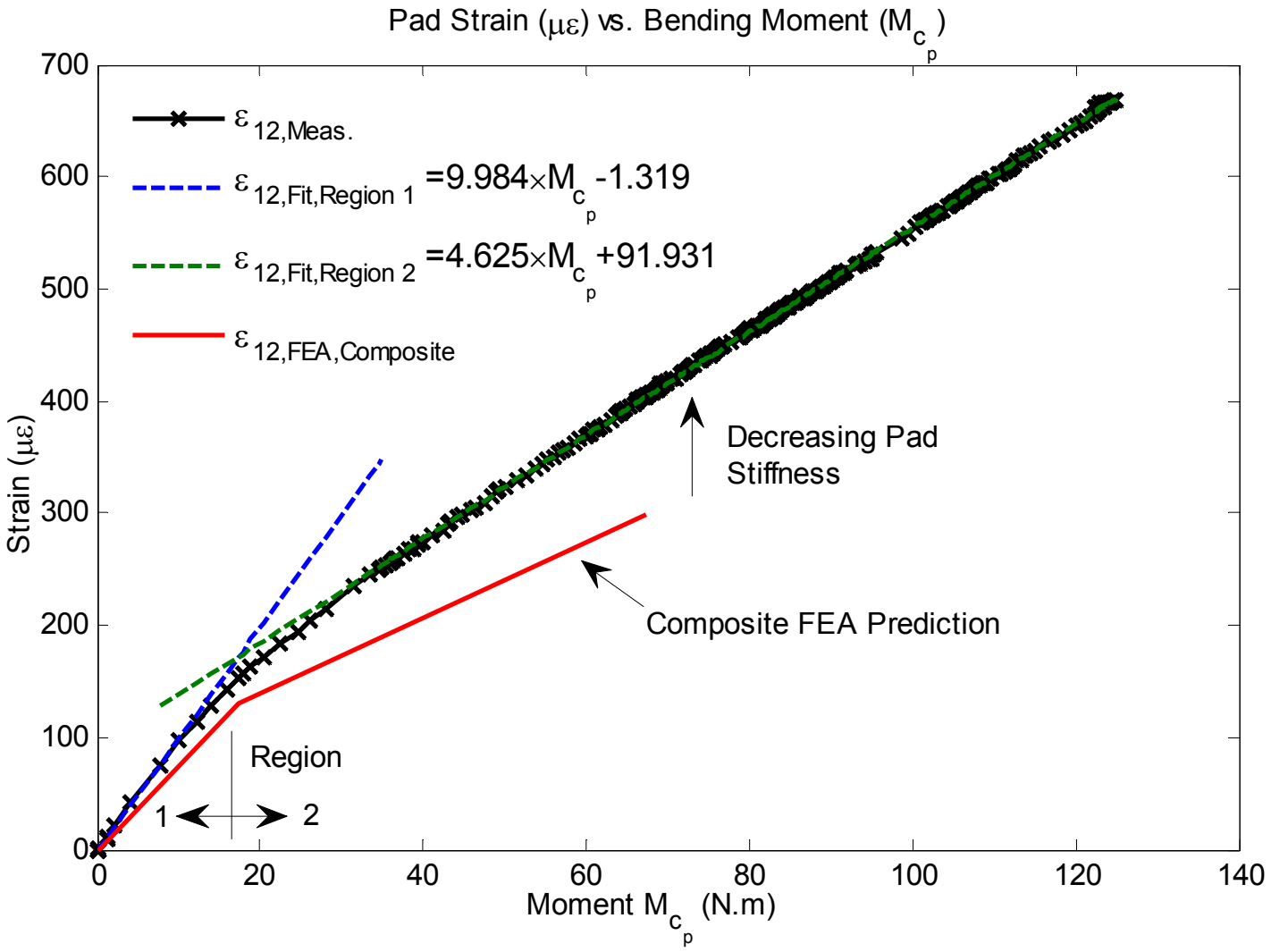

Results: FEA Pad Bending Stiffness

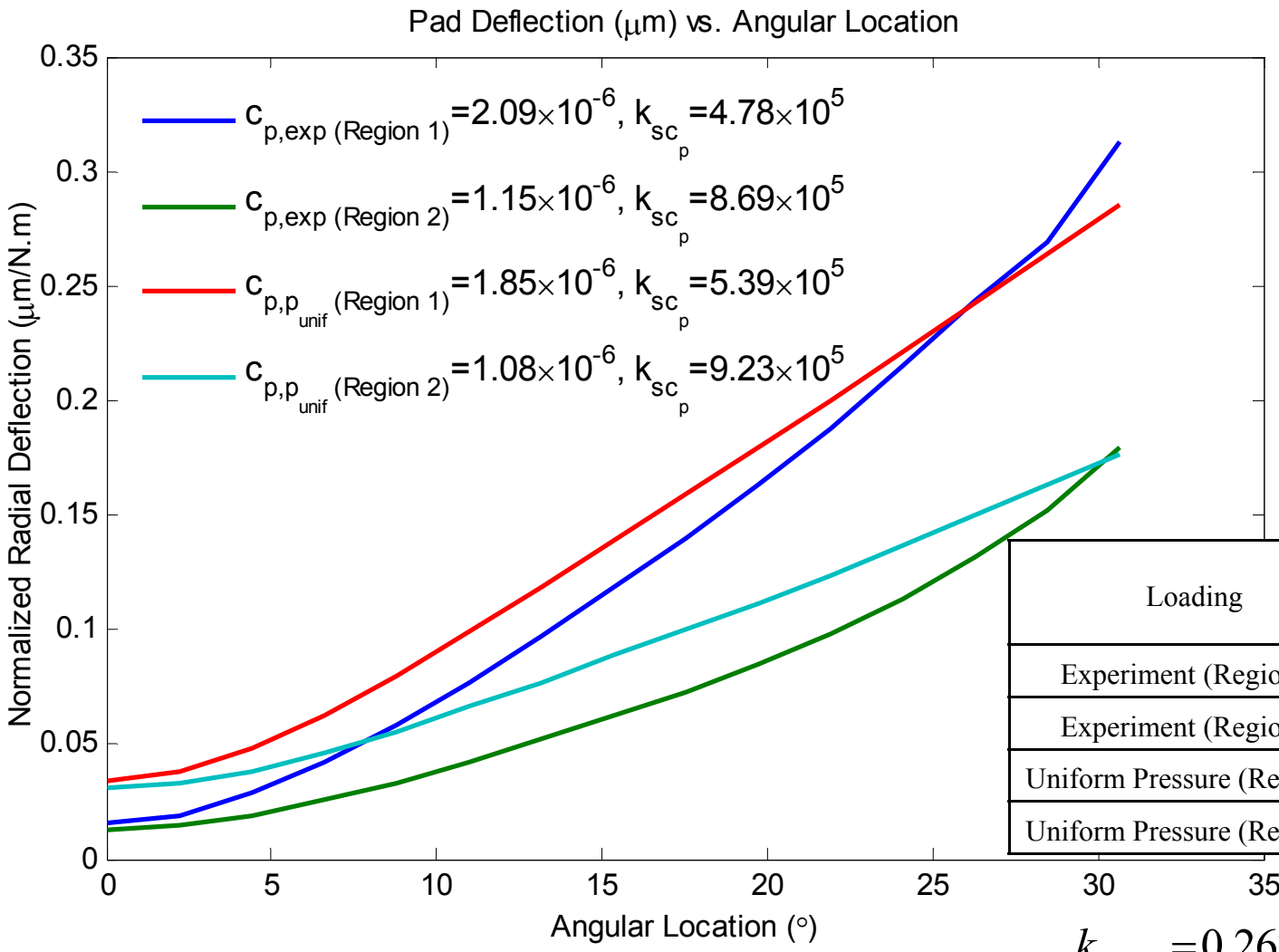

Loading	$k_{cp\varepsilon 12}$ (μm/με)
Experiment (Region 1)	0.2787
Experiment (Region 2)	0.3397
Uniform Pressure (Region 1)	0.2560
Uniform Pressure (Region 2)	0.2782

$$k_{c_p\varepsilon_{12}} = 0.2671 \mu m / \mu\varepsilon$$

Results: Pad Bending Stiffness

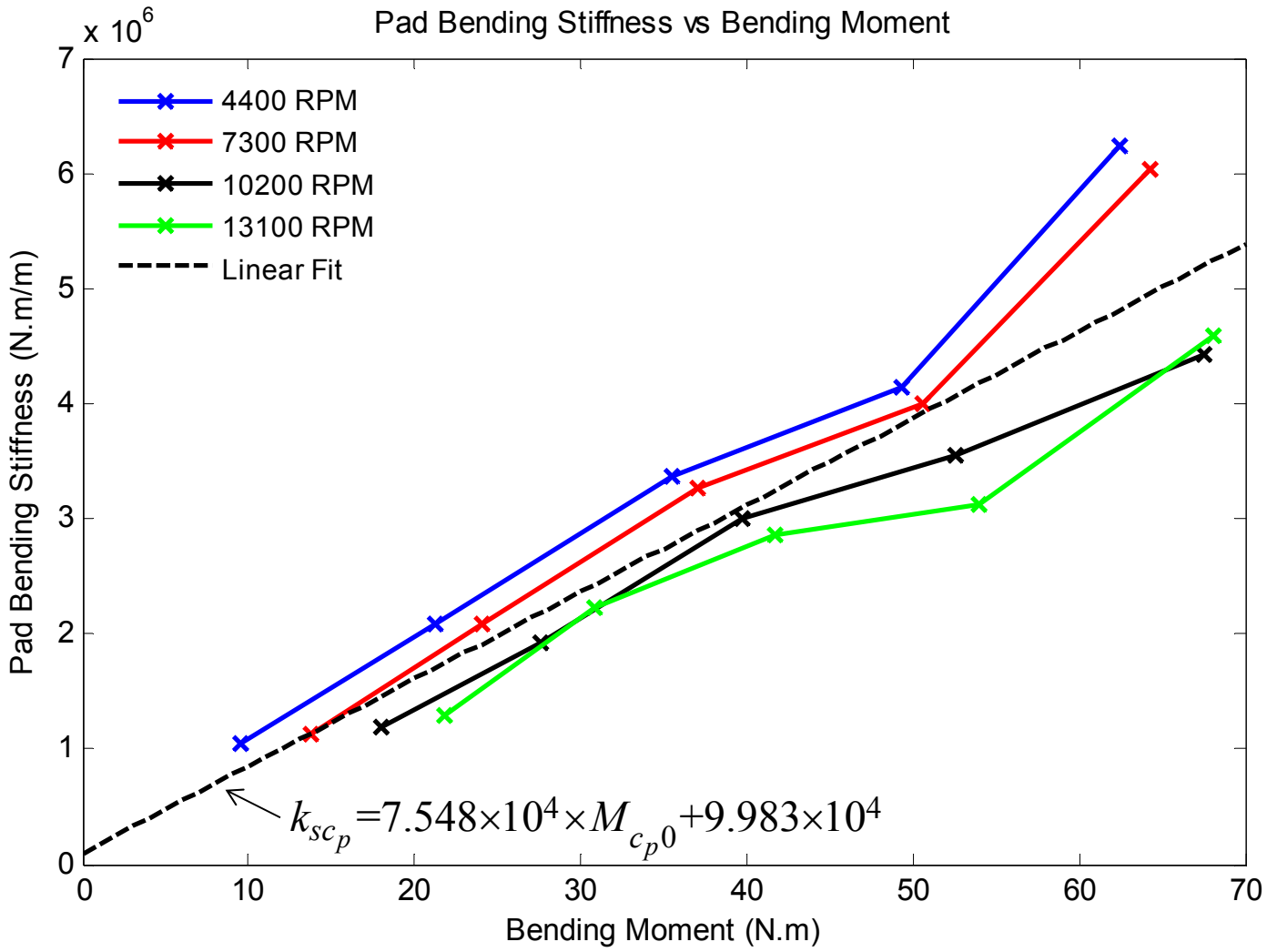

Operating Bearing Clearance

- Large reduction in bearing clearance during experiments.
- Measured after shutdown with slow stator precession

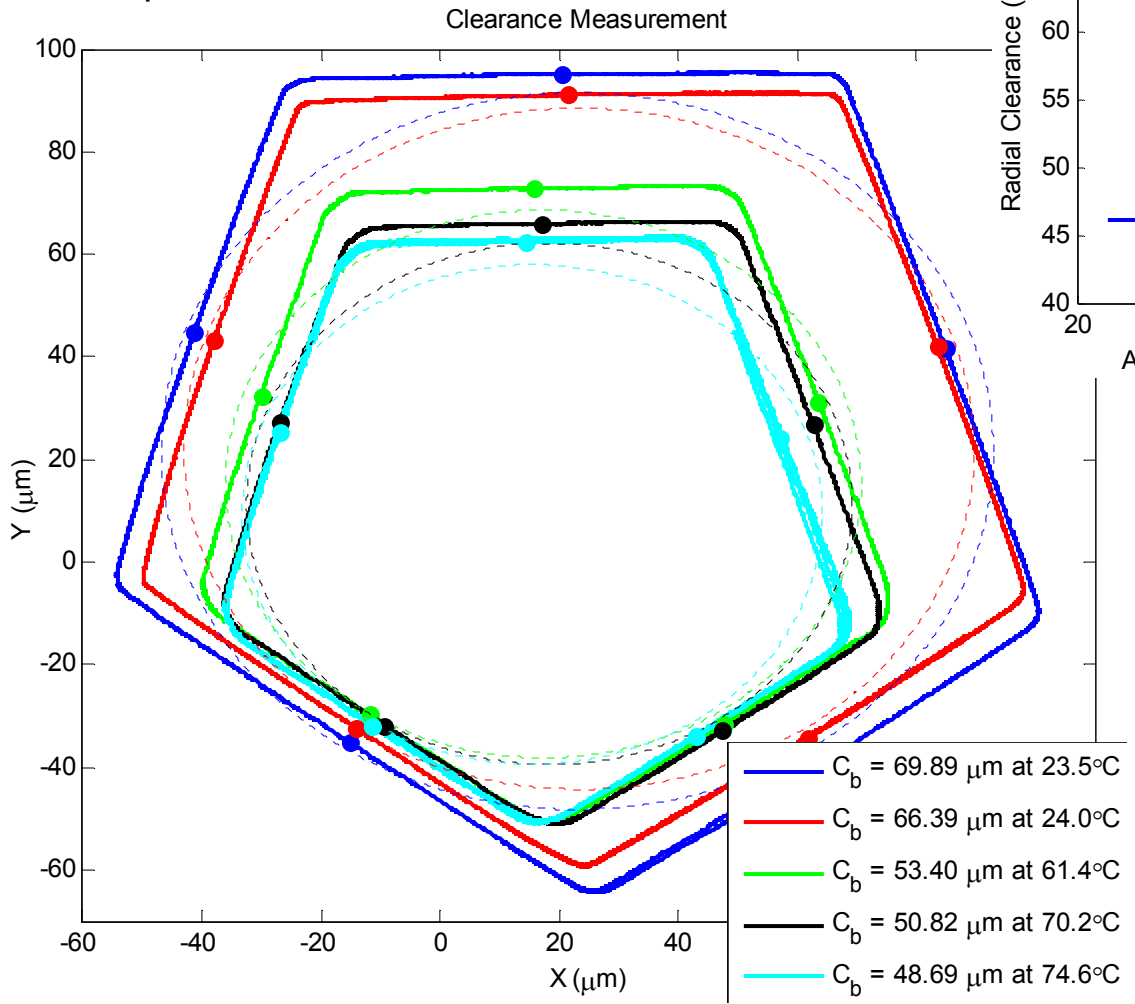

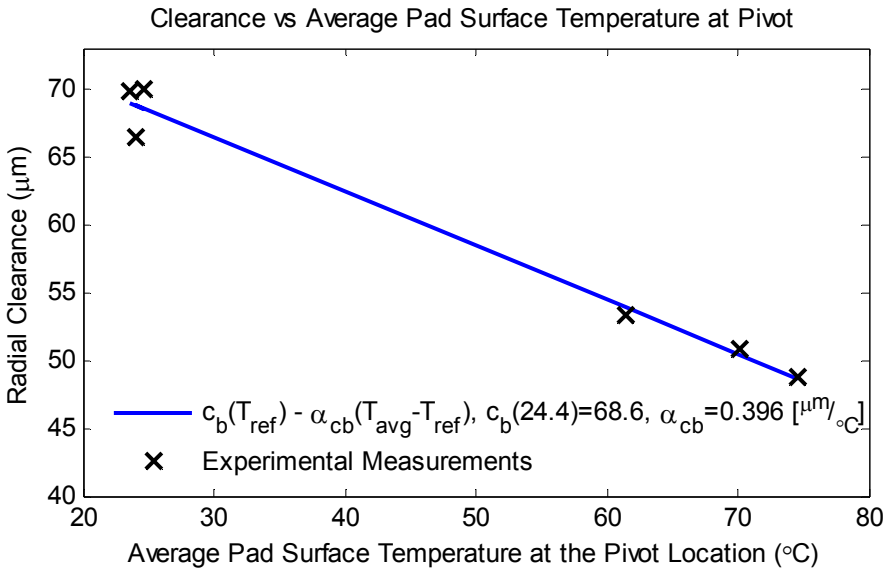

- Squashed clearances at large load
- Decrease in clearance results in increased stiffness and damping predictions
- Clearance inversely proportional to average pivot surface temperature
- Characteristic thermal length

$$l_{T,char} = \frac{\alpha_{c_b}}{\alpha_{mat}} = \frac{0.396\,^{\mu m}/_{\circ C}}{11.4\,^{\mu}/_{\circ C}} = 34.7\,\text{mm}\left(1.37\,\text{in}\right)$$

Static Eccentricity Measurement

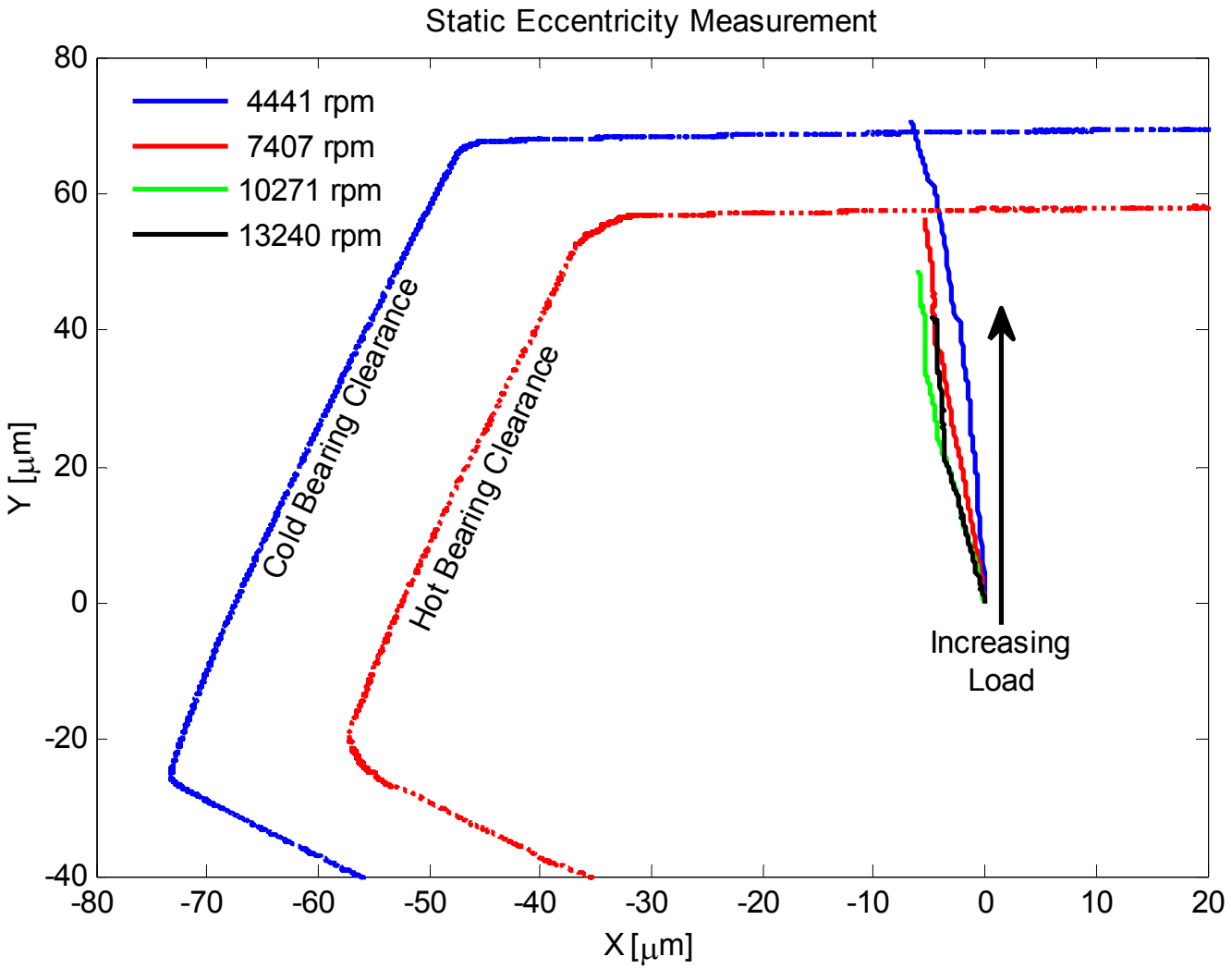

Static Pad Radial Displacement

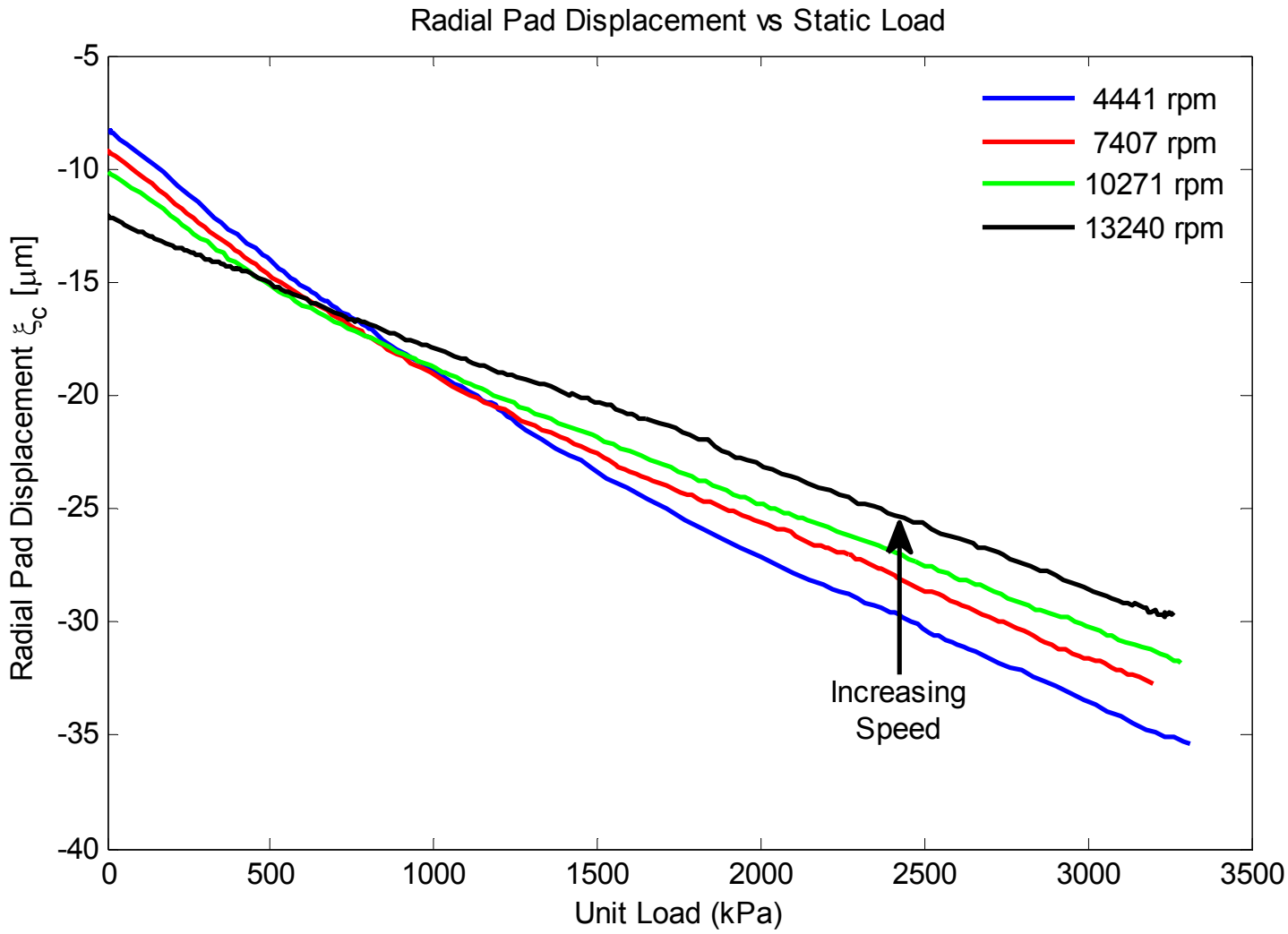

Static Pad Radial Displacement

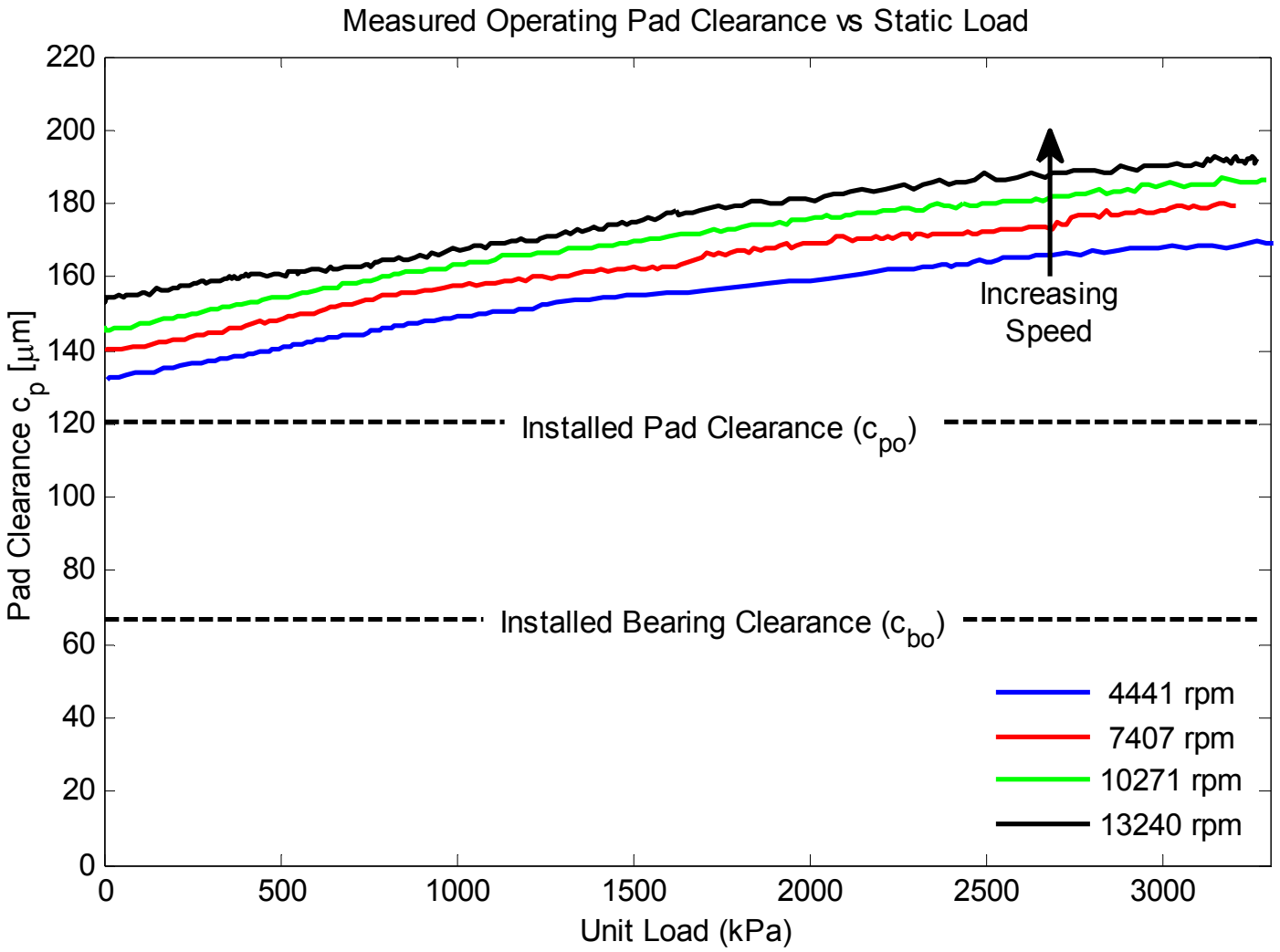

Journal vs. Bearing Impedances

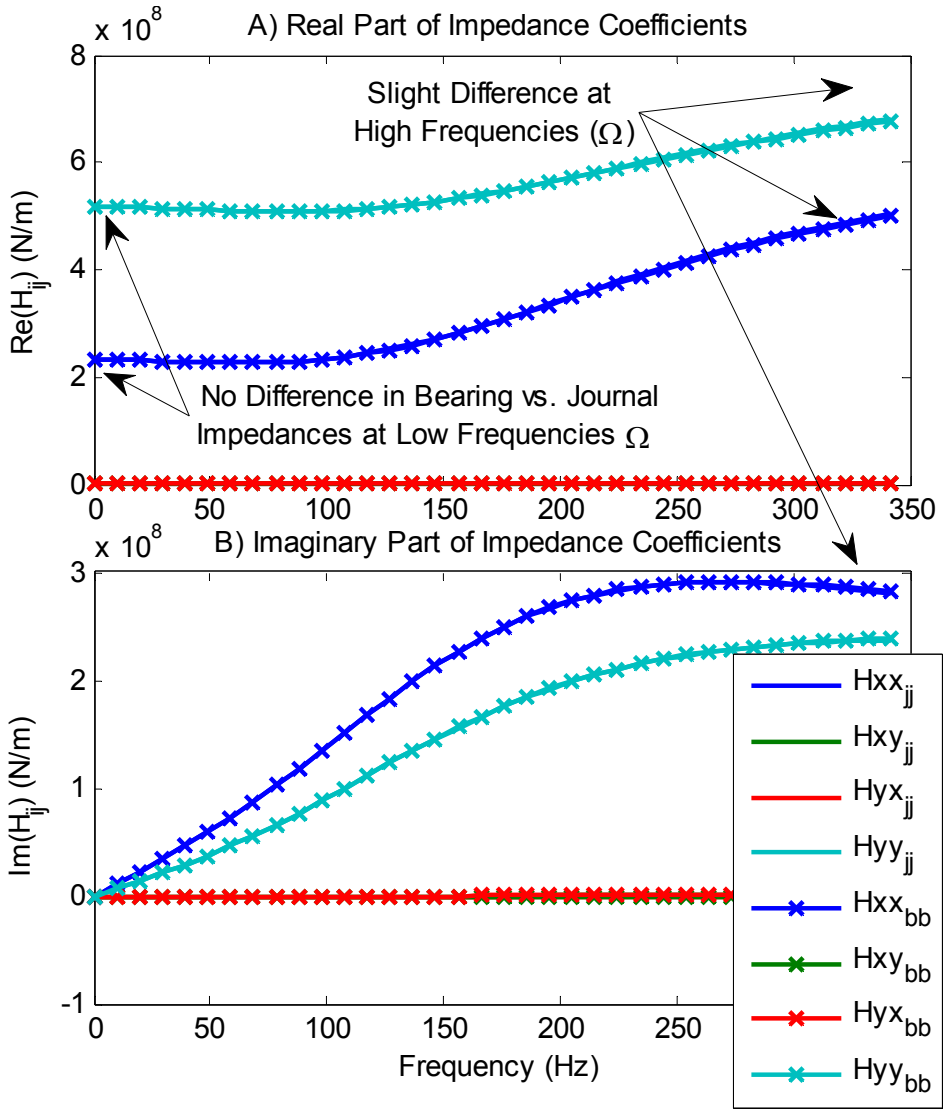

Impedances for the test bearing

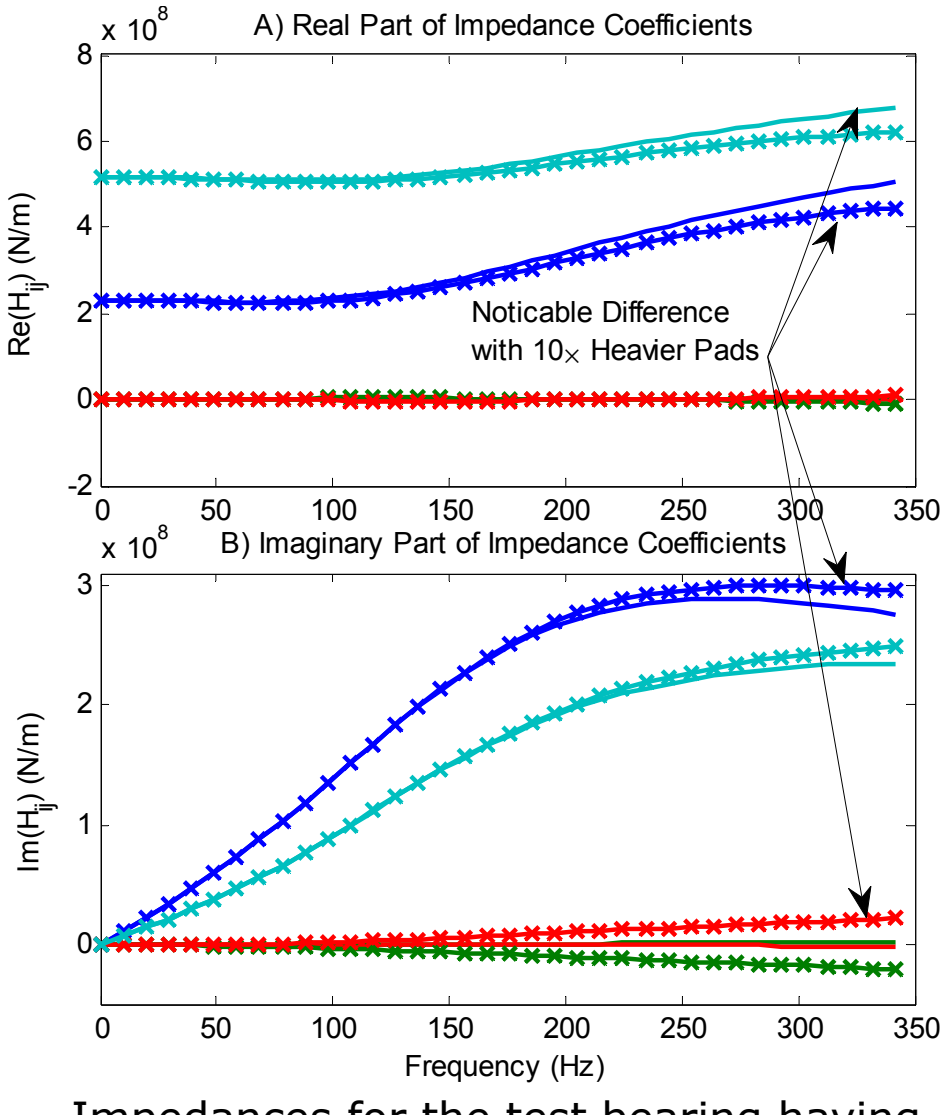

Impedances for the test bearing having 10x heavier pads

Journal vs. Bearing Cross-Impedances

- For the test bearing

$$\begin{bmatrix} \tilde{\mathbf{H}}_{jj} & \tilde{\mathbf{H}}_{jb} \\ \tilde{\mathbf{H}}_{bj} & \tilde{\mathbf{H}}_{bb} \end{bmatrix} \simeq \begin{bmatrix} \tilde{\mathbf{H}}_{jj} & -\tilde{\mathbf{H}}_{jj} \\ -\tilde{\mathbf{H}}_{jj} & \tilde{\mathbf{H}}_{jj} \end{bmatrix}$$

- Reaction forces result from *relative* rotor-stator motions.
- Previous comparisons are valid!

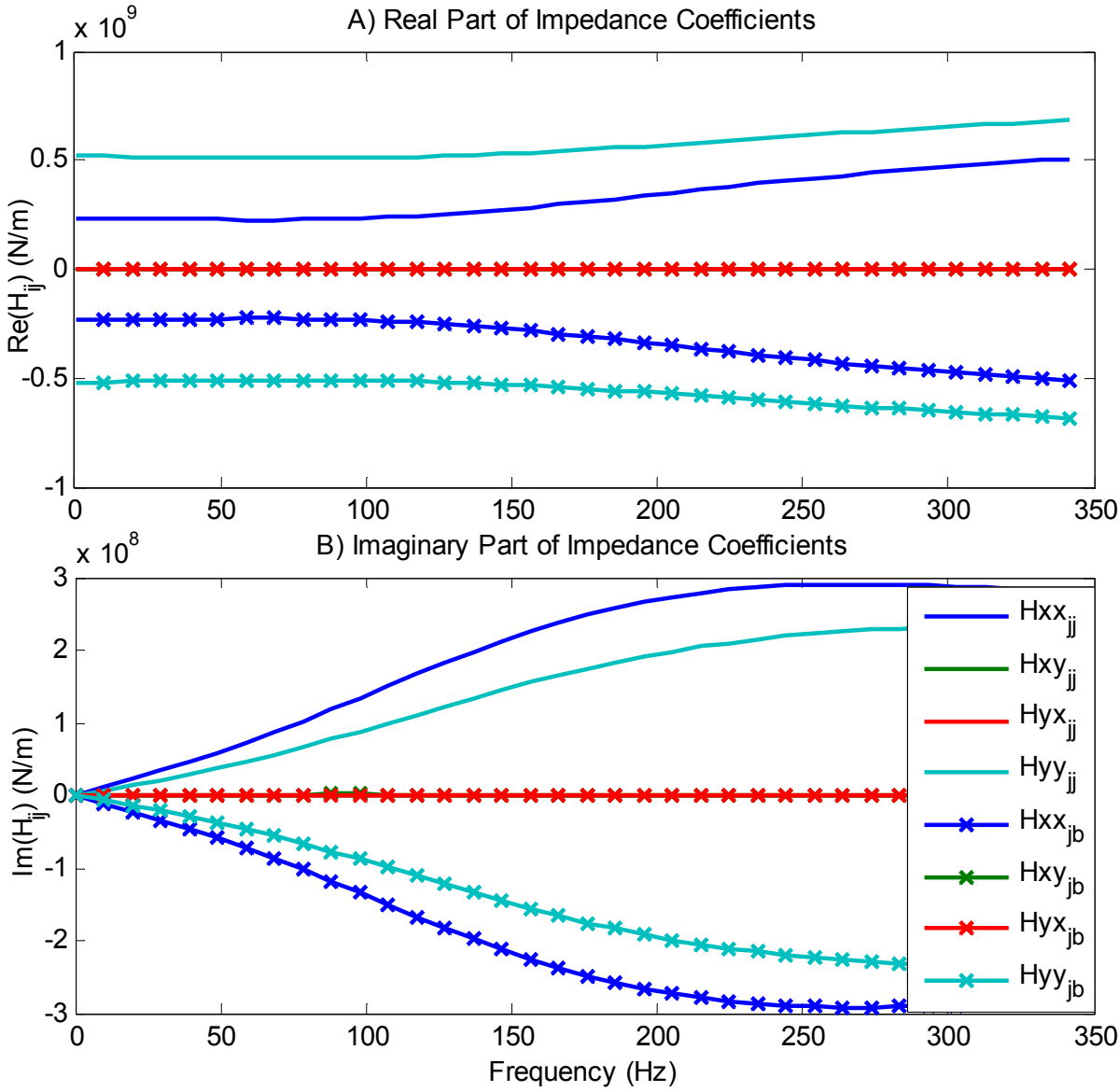

Anatomy of the Pad-Rotor TF

- Normalized Pad Tilt

$$\hat{\phi} = \phi \times 25.4\text{mm}$$

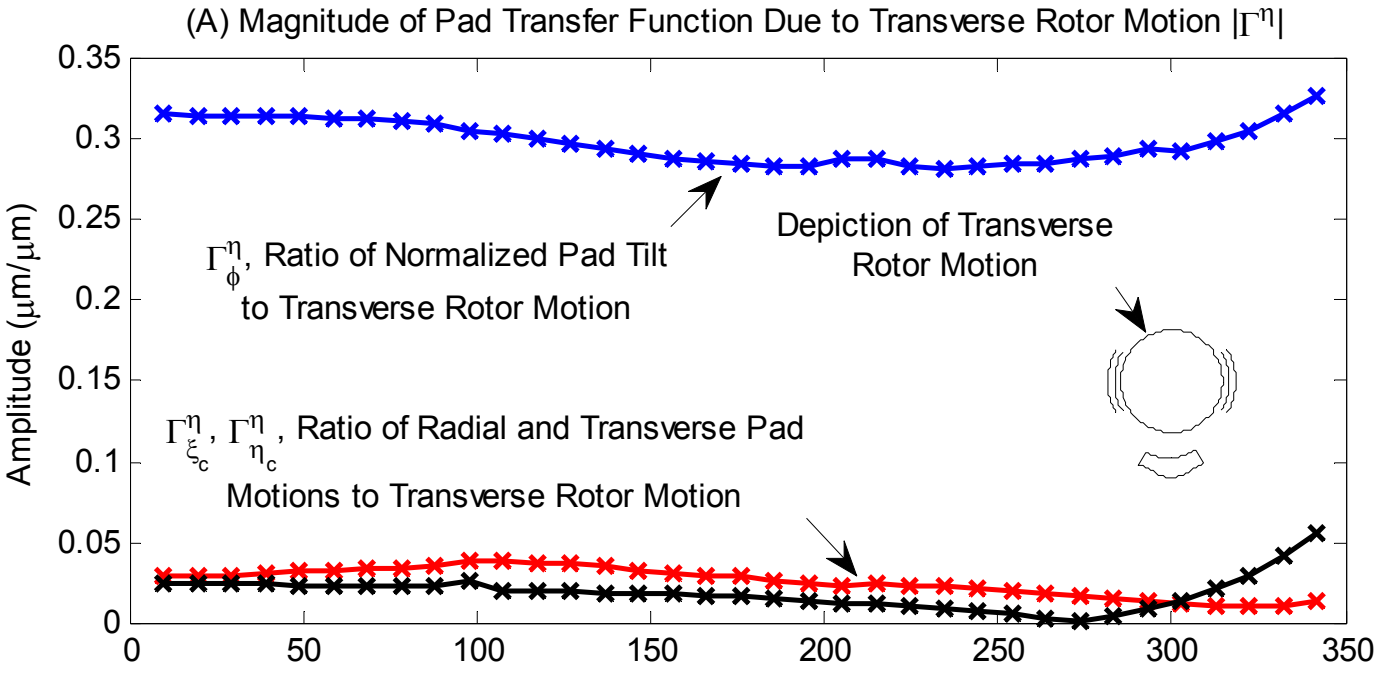

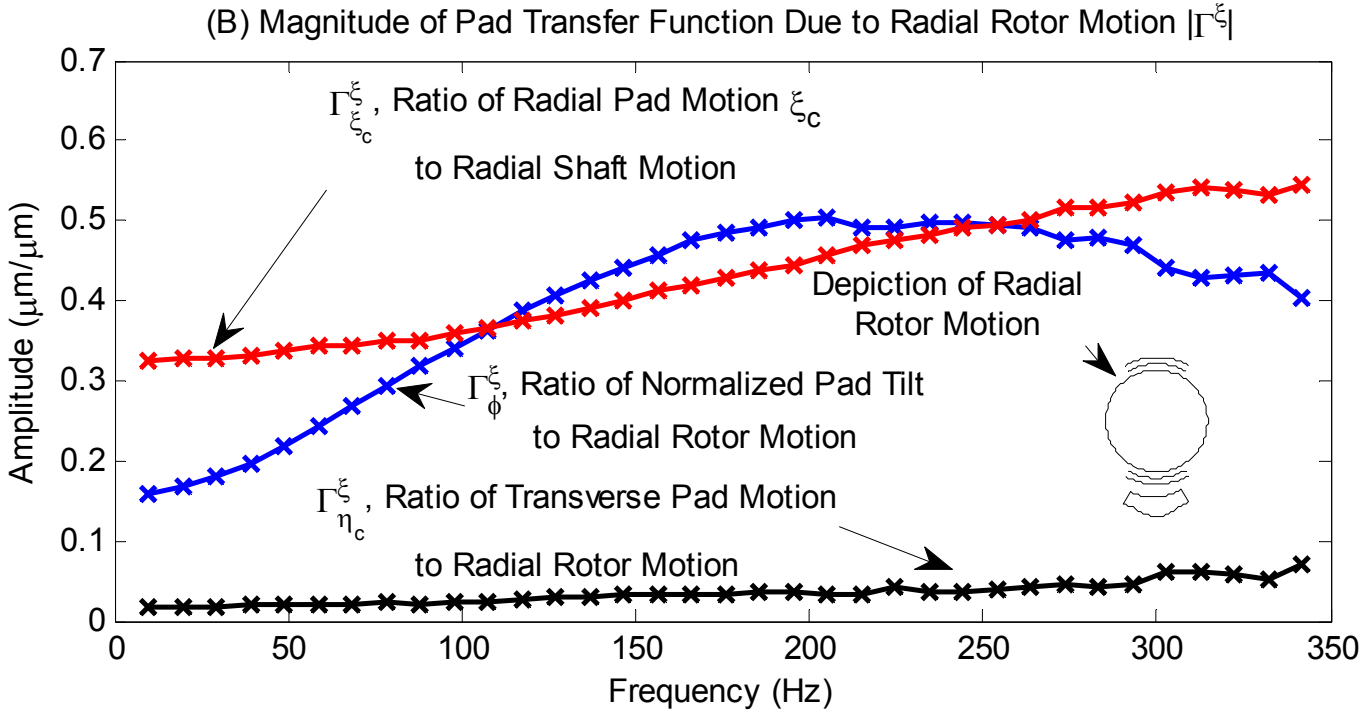

Pad-Rotor TF (4400 RPM, 10 Hz)

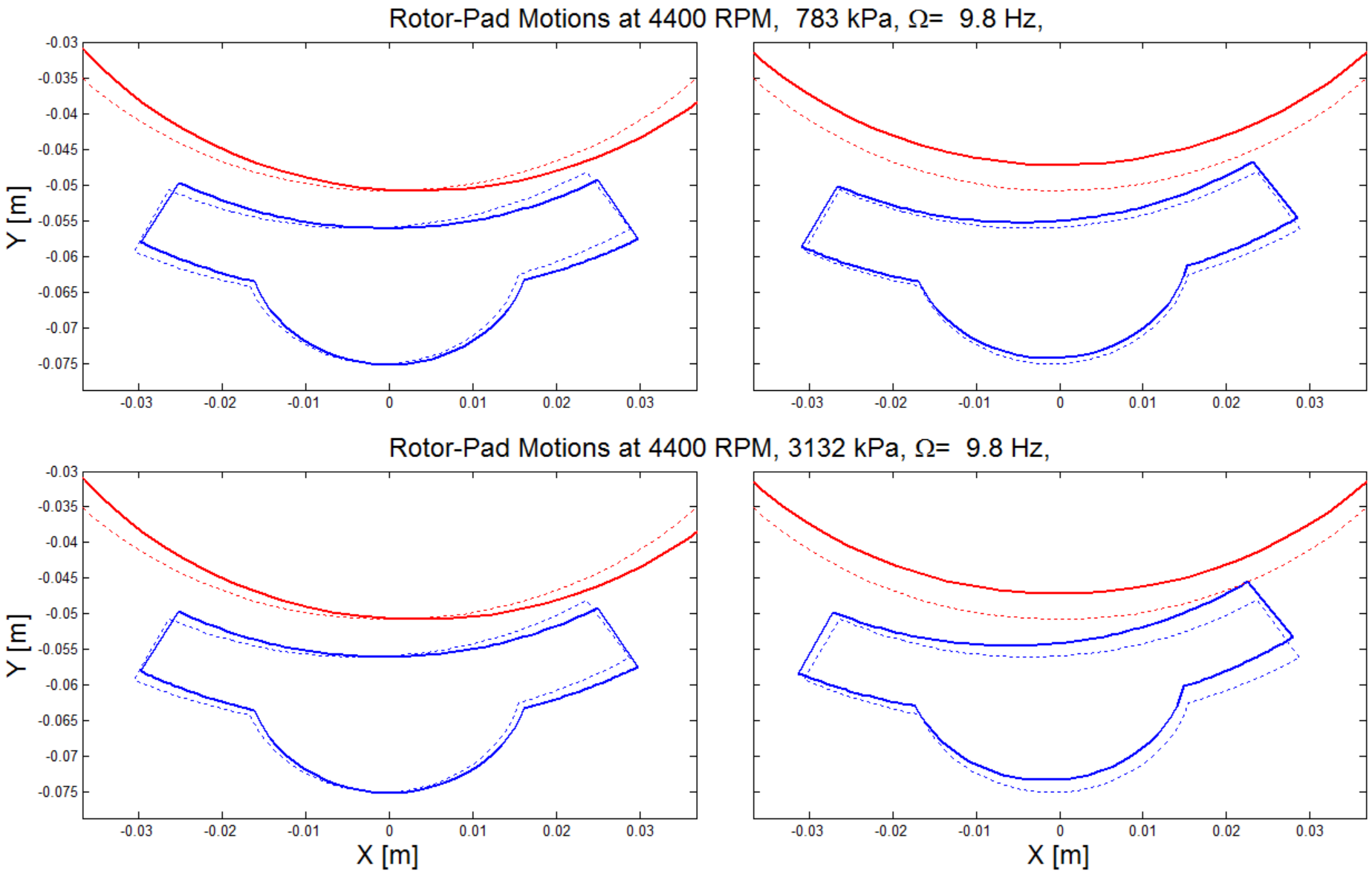

Pad-Rotor TF (4400 RPM, 166 Hz)

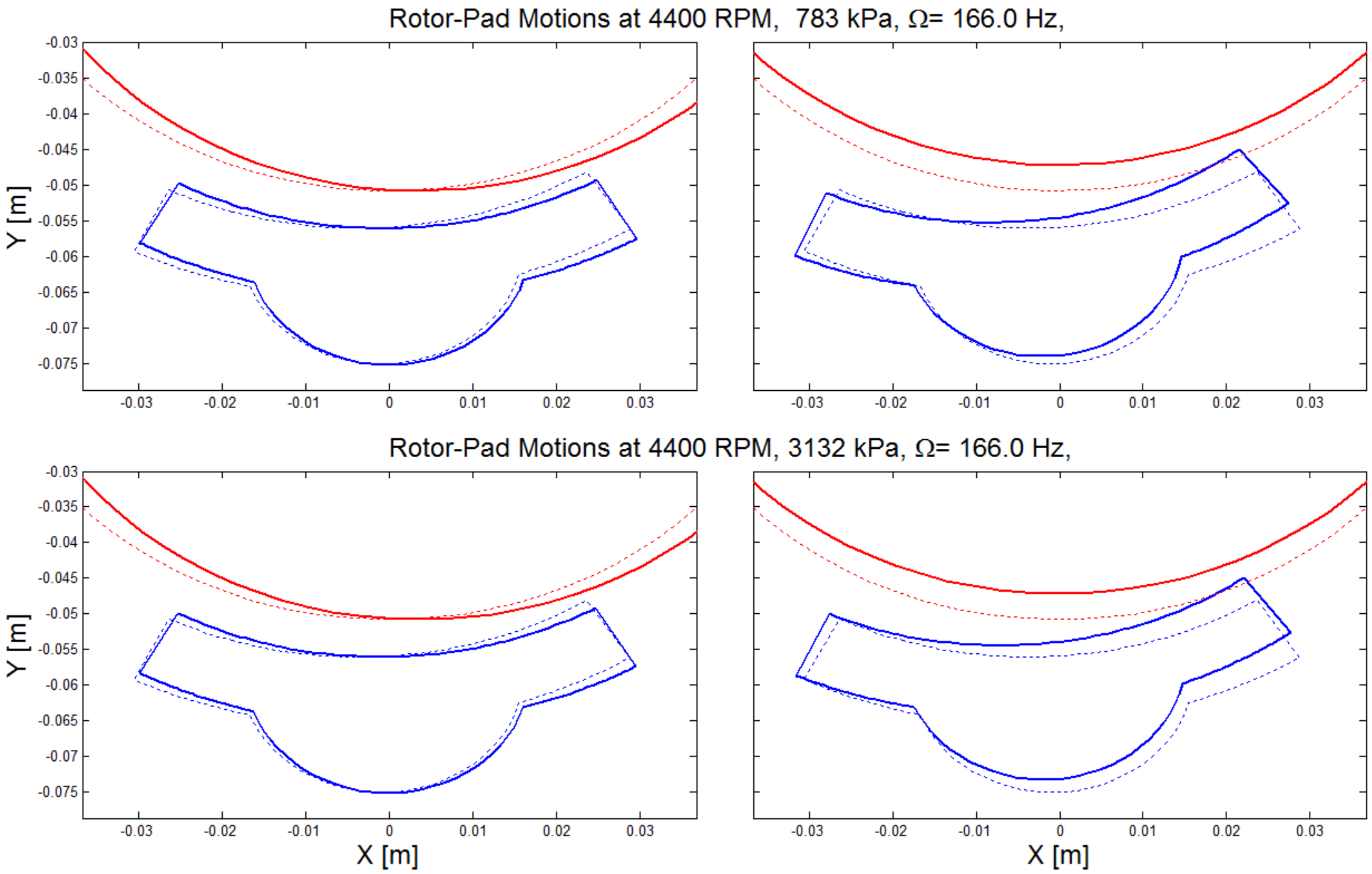

Pad-Rotor TF (4400 RPM, 342 Hz)

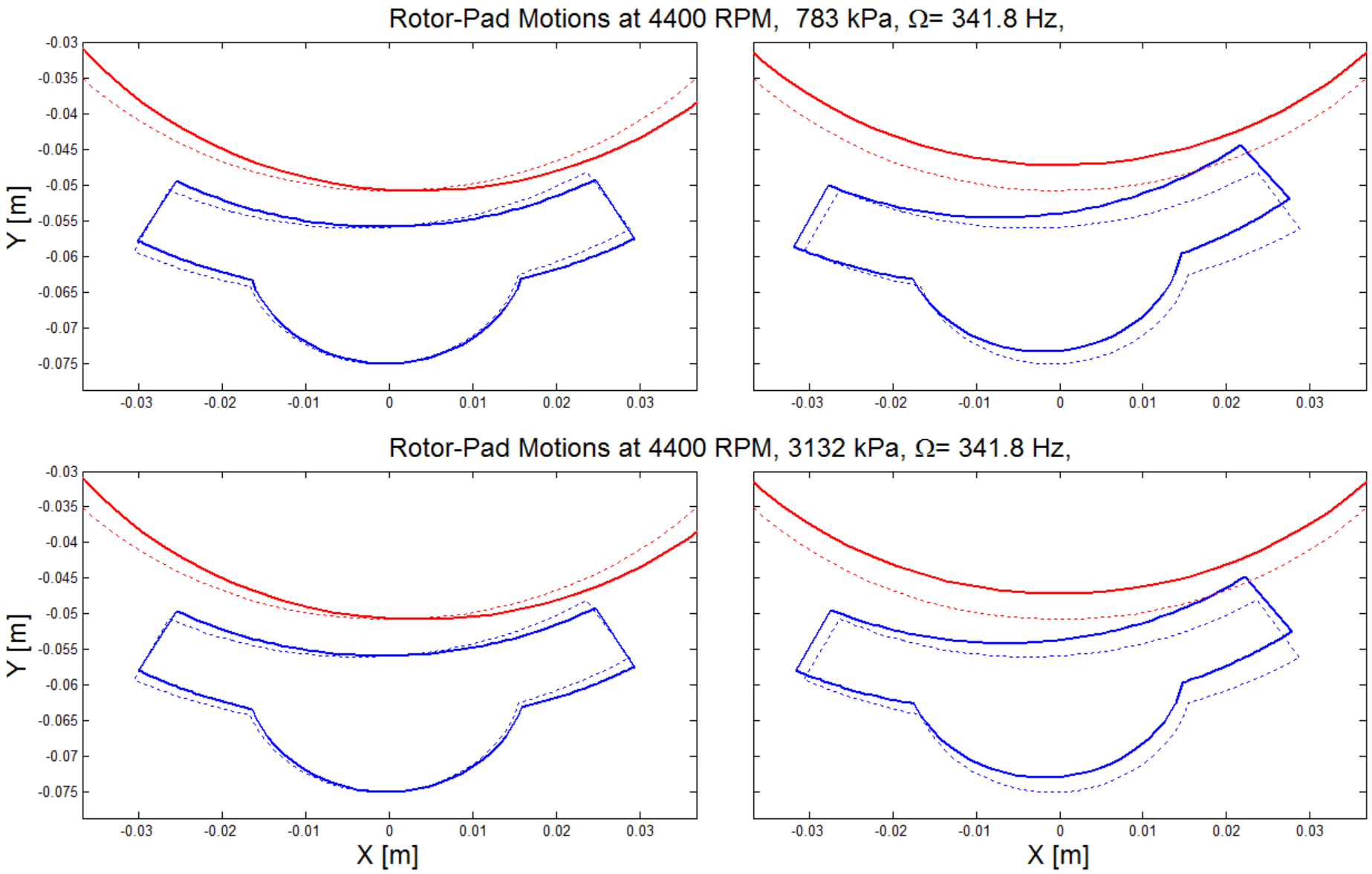

Pad-Rotor TF vs unit load at 4400 rpm

- Pad-Rotor Tracking Anomaly $\left|\tilde{\Gamma}^{\eta_j}_{\hat{\phi}}\right|$
- Ratio of radial pad motion to radial shaft motion **increases** with **increasing** unit load.
- Ratio of pad tilt to radial shaft motion **decreases** with **increasing** unit load.
- Ratio of transverse pad motion to radial and transverse shaft motions is minimal

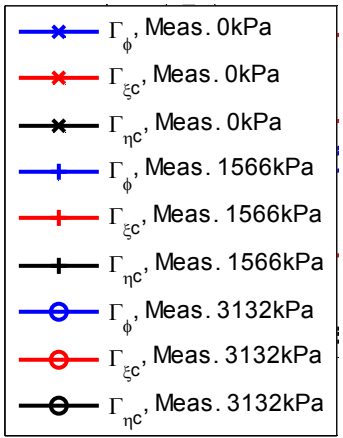

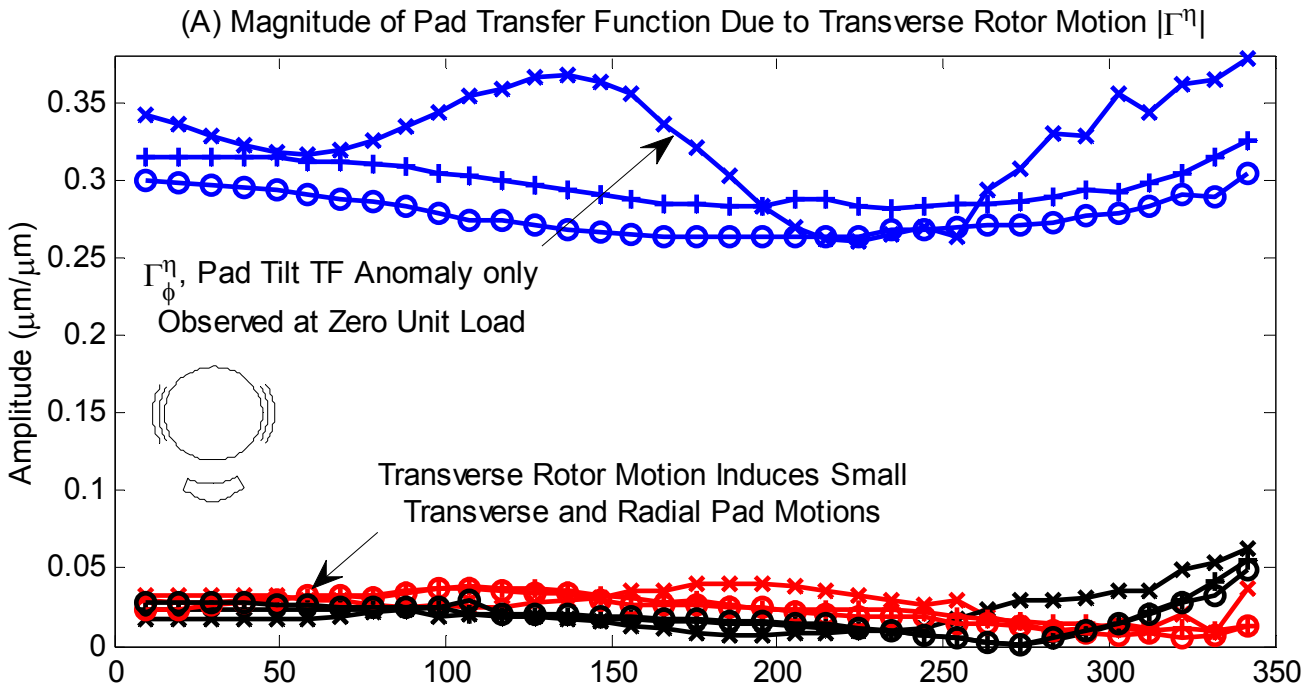

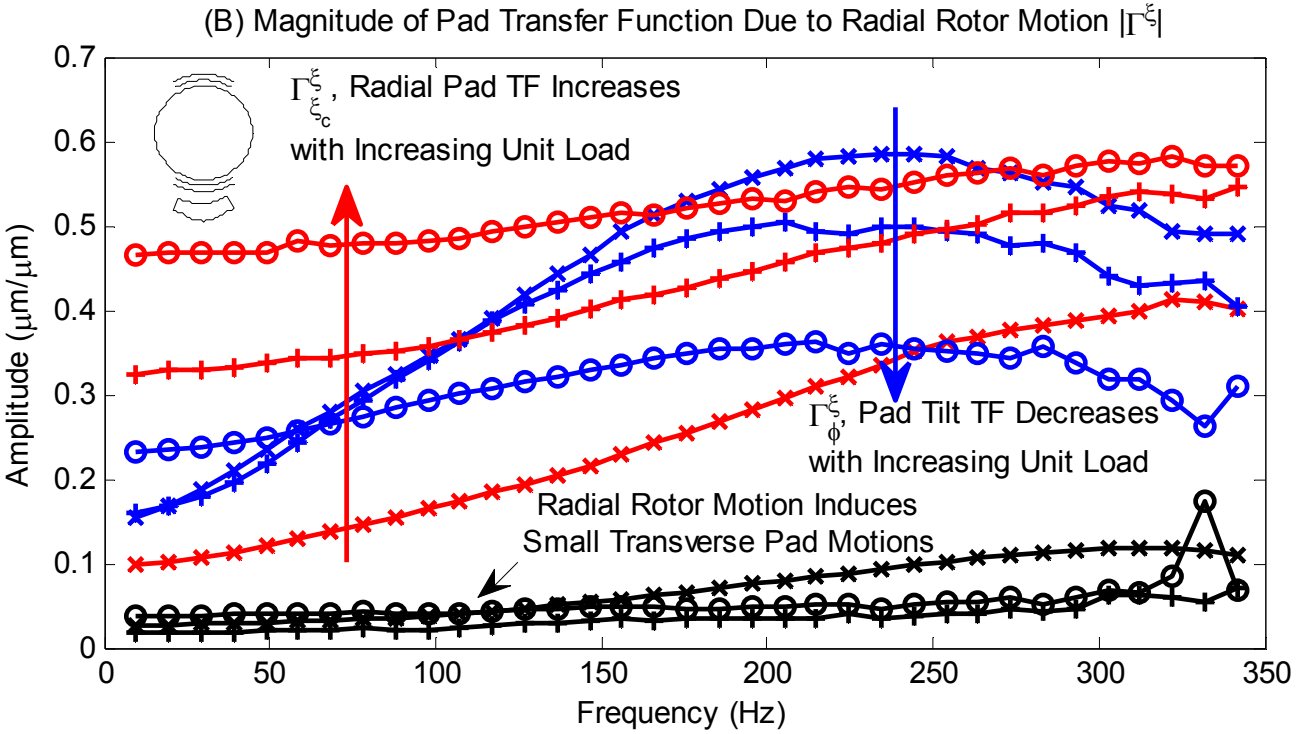

Pad-Rotor TF vs unit load at 10200 rpm

- Pad-Rotor Tracking Anomaly
- Ratio of radial pad motion to radial shaft motion **increases** with **increasing** unit load.
- Ratio of pad tilt to radial shaft motion **increases** with **increasing** unit load
- Ratio of transverse pad motion to radial and transverse shaft motions is minimal
- Less frequency dependence

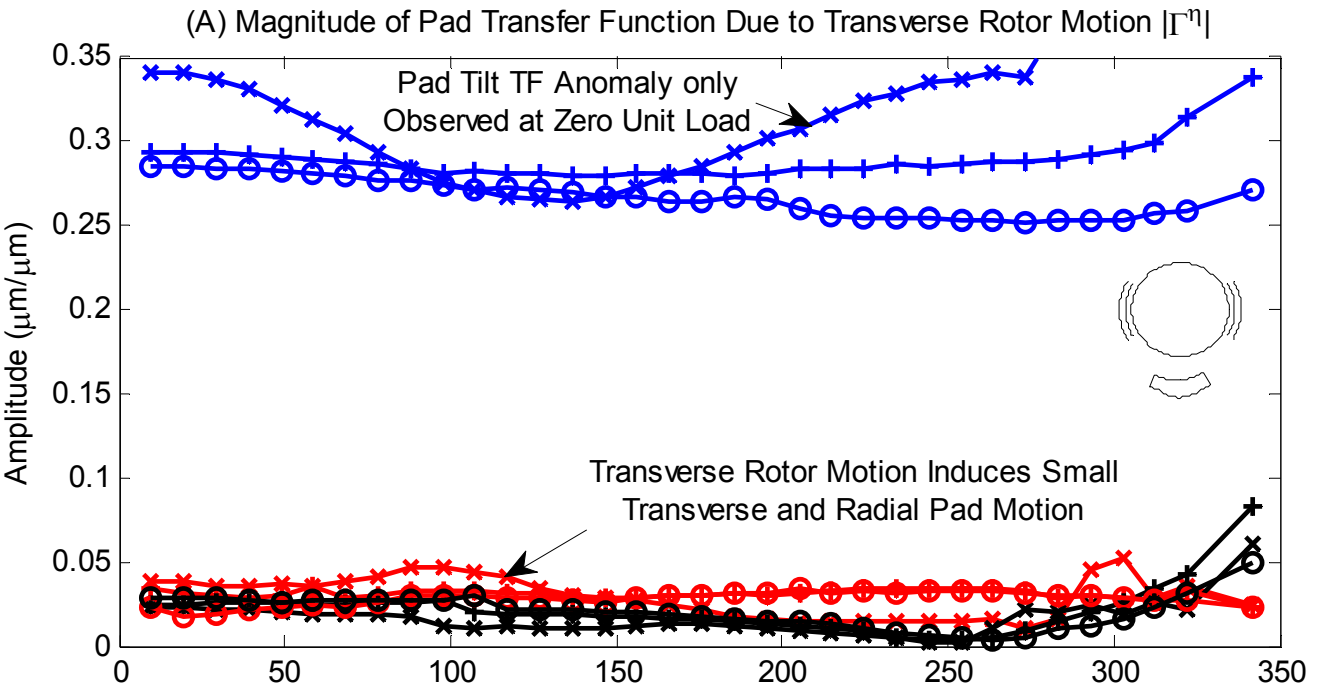

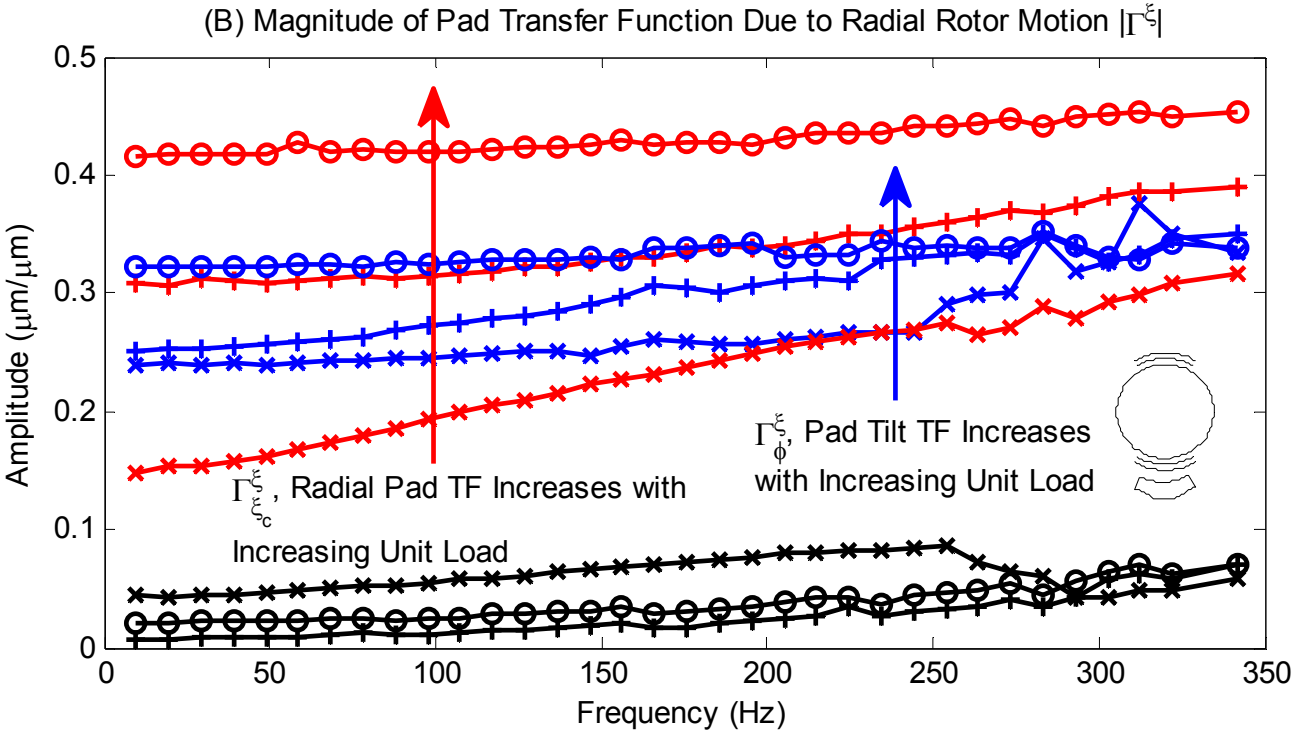

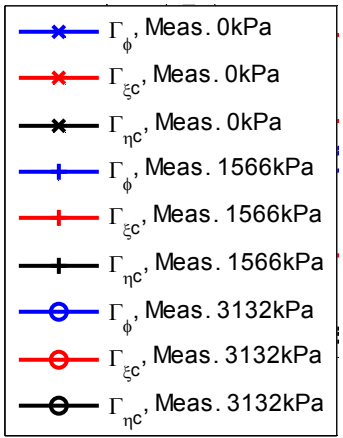

Pad-Rotor TF vs unit load at 4400 rpm

- Ratio of pad clearance change to radial shaft motion **decreases** with **increasing** unit load.
- The pad is much stiffer at high unit loads

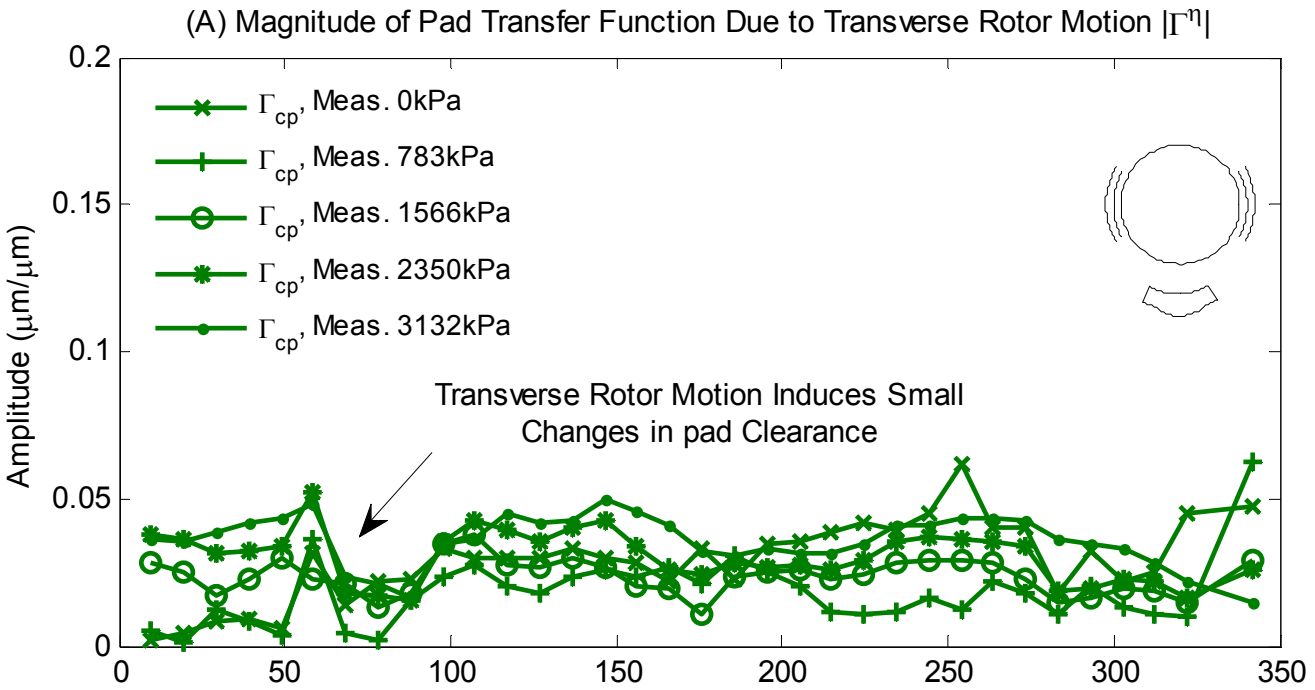

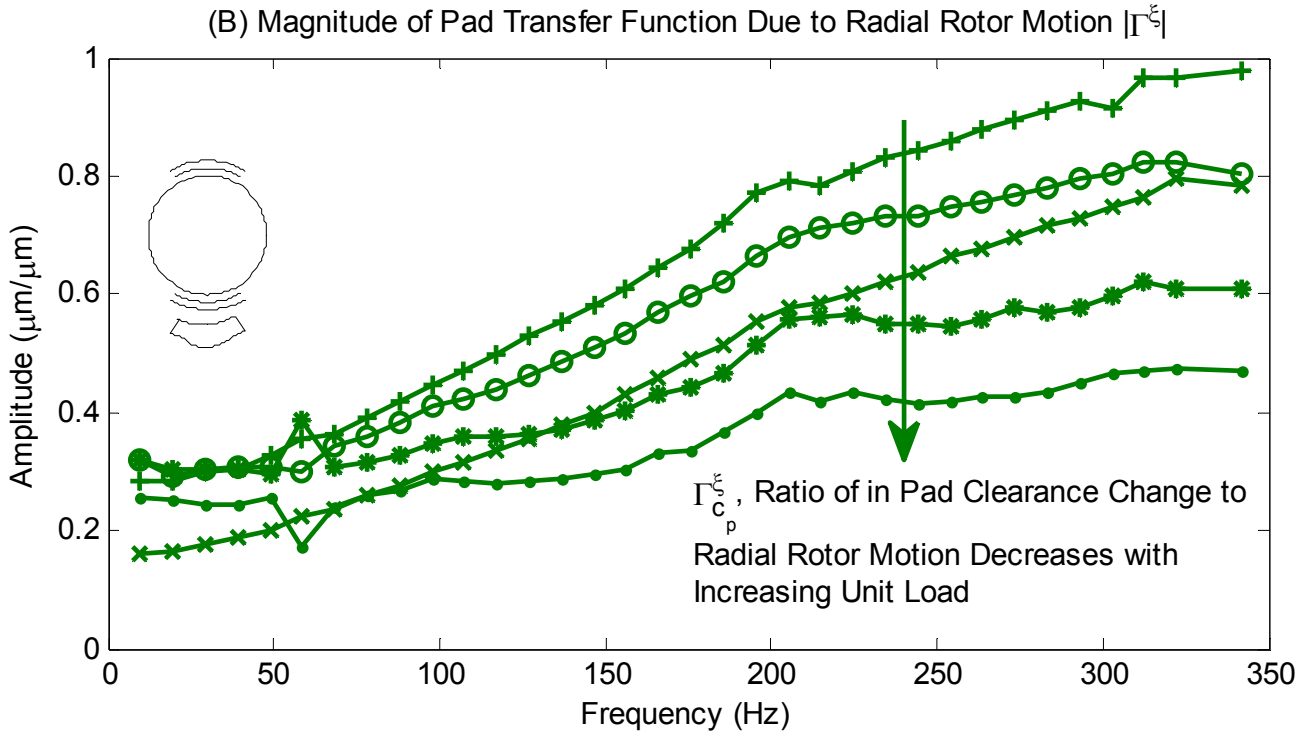

TF Amplitude Meas. vs. Pred.: 4400 rpm, 0 kPa

- Tilt tracking anomaly not predicted.
- Radial pad motion predicted well
- Pad tilt due to radial rotor motion slightly underpredicted
- Predicted transverse pad motions are minimal

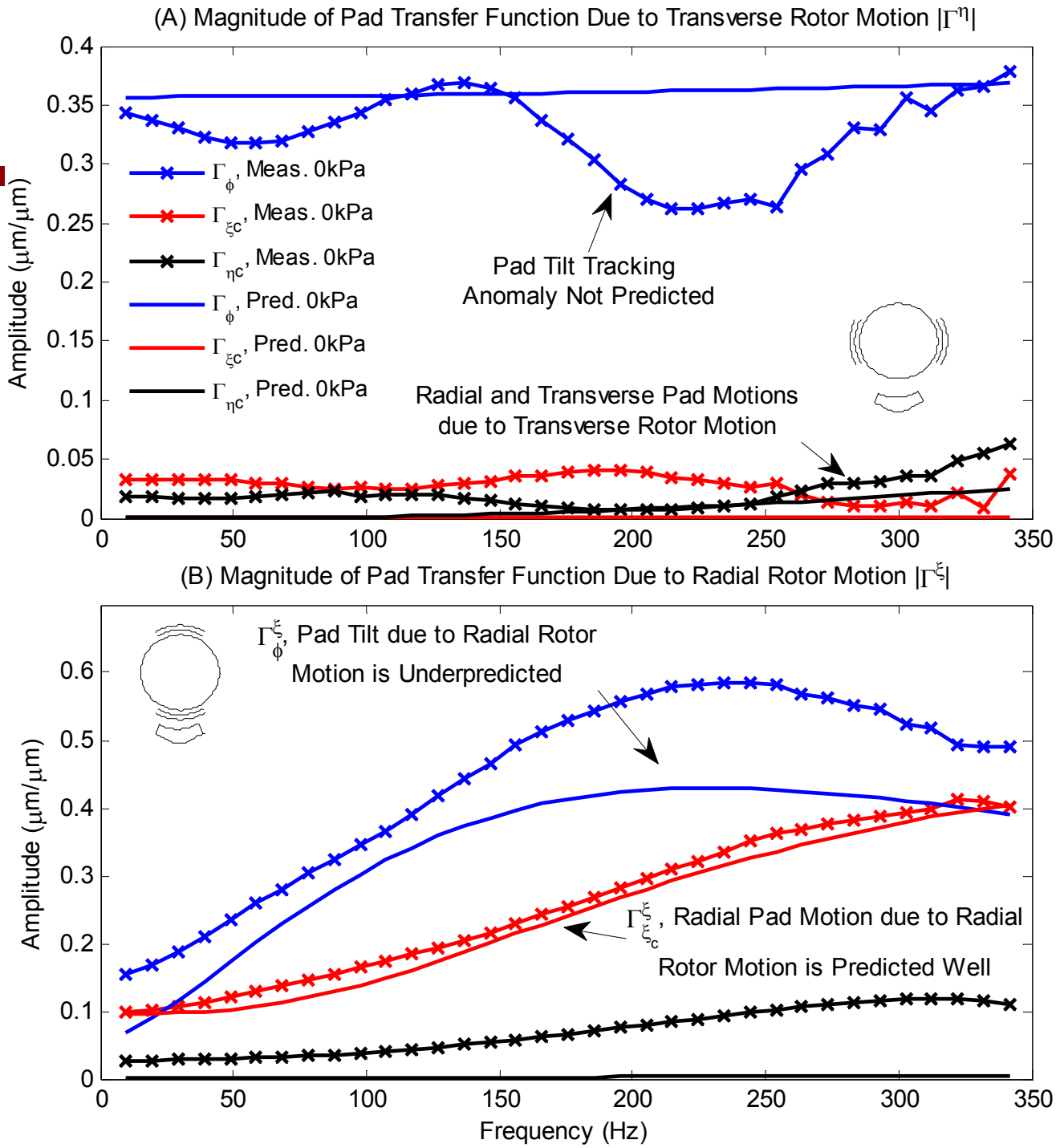

TF Amplitude Meas. vs. Pred.: 4400 rpm, 3132 kPa

- Pad tracking slightly overpredicted
- Radial pad motion predicted well
- Pad tilt due to radial rotor motion moderately underpredicted
- Predicted transverse pad motions are minimal

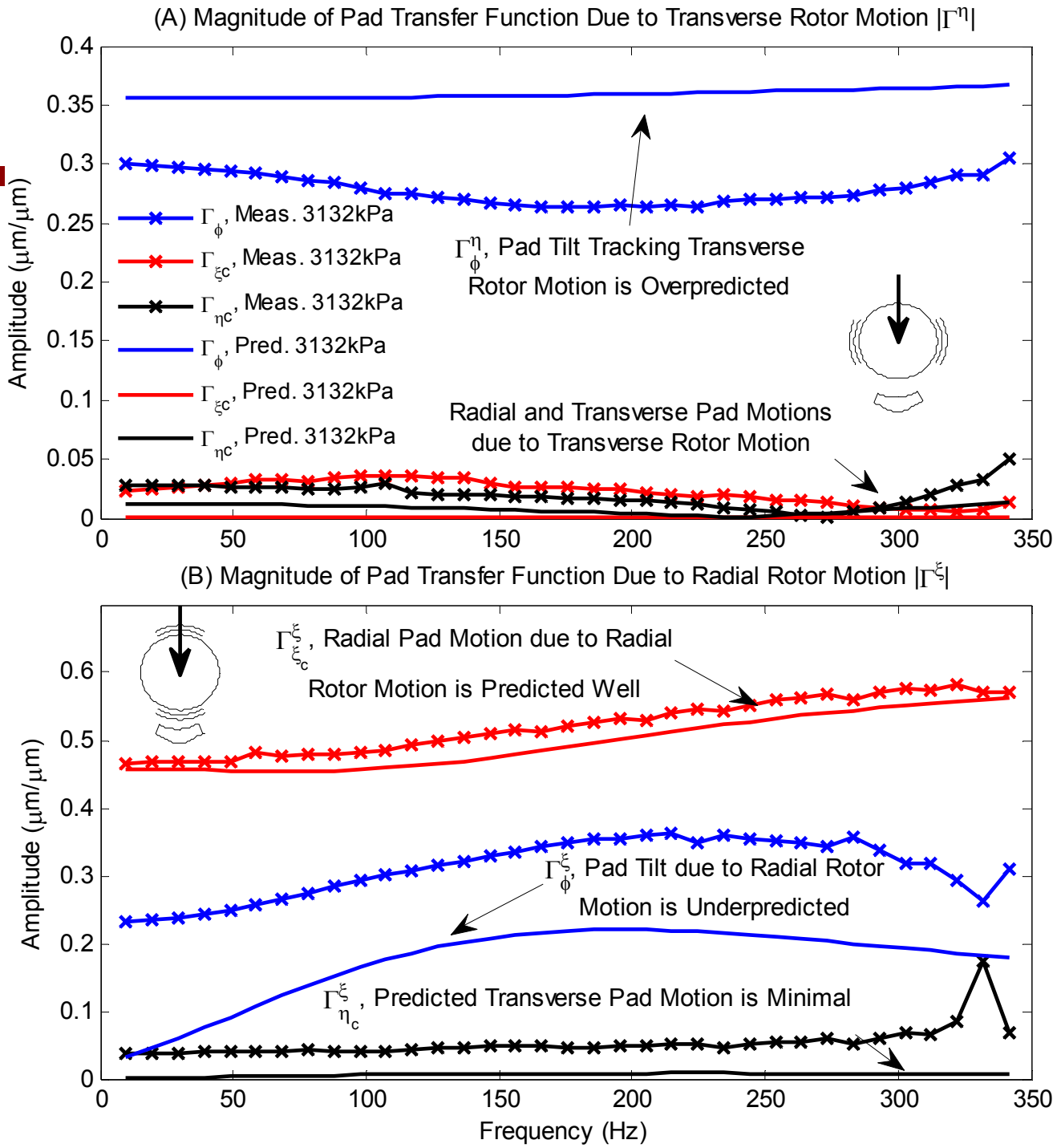

TF Amplitude Meas. vs. Pred.: 10200 rpm, 3132 kPa

- Pad tracking still slightly overpredicted
- Radial pad motion predicted very well
- Pad tilt due to radial rotor motion still underpredicted
- Predicted transverse pad motions are minimal

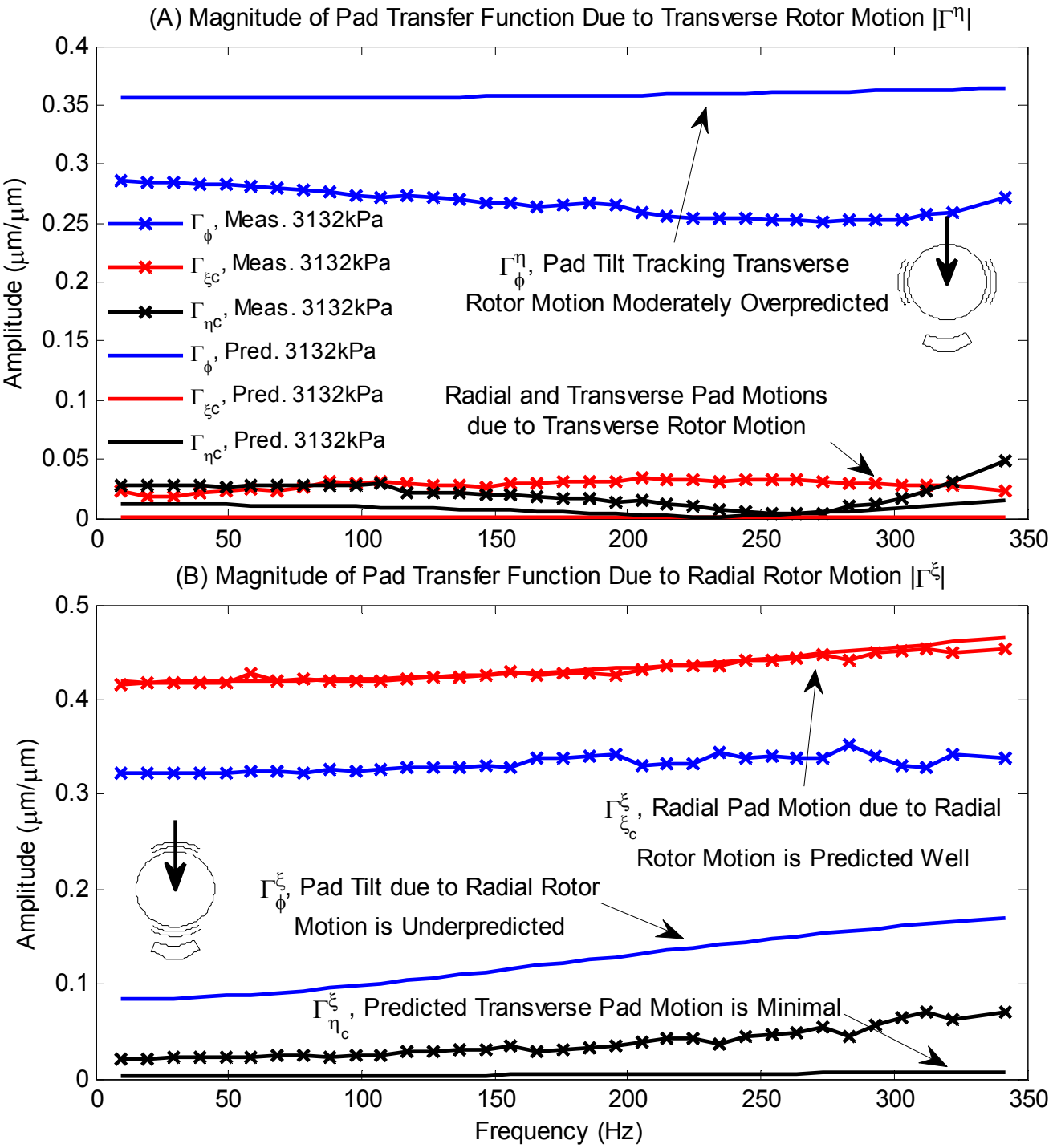

TF Amplitude Meas. vs. Pred.: 4400 rpm, 3132 kPa

- Predicted change in pad clearance due to transverse rotor motion is minimal
- Change in pad clearance due to radial rotor motion predicted well at low frequencies, and slightly underpredicted at higher frequencies.

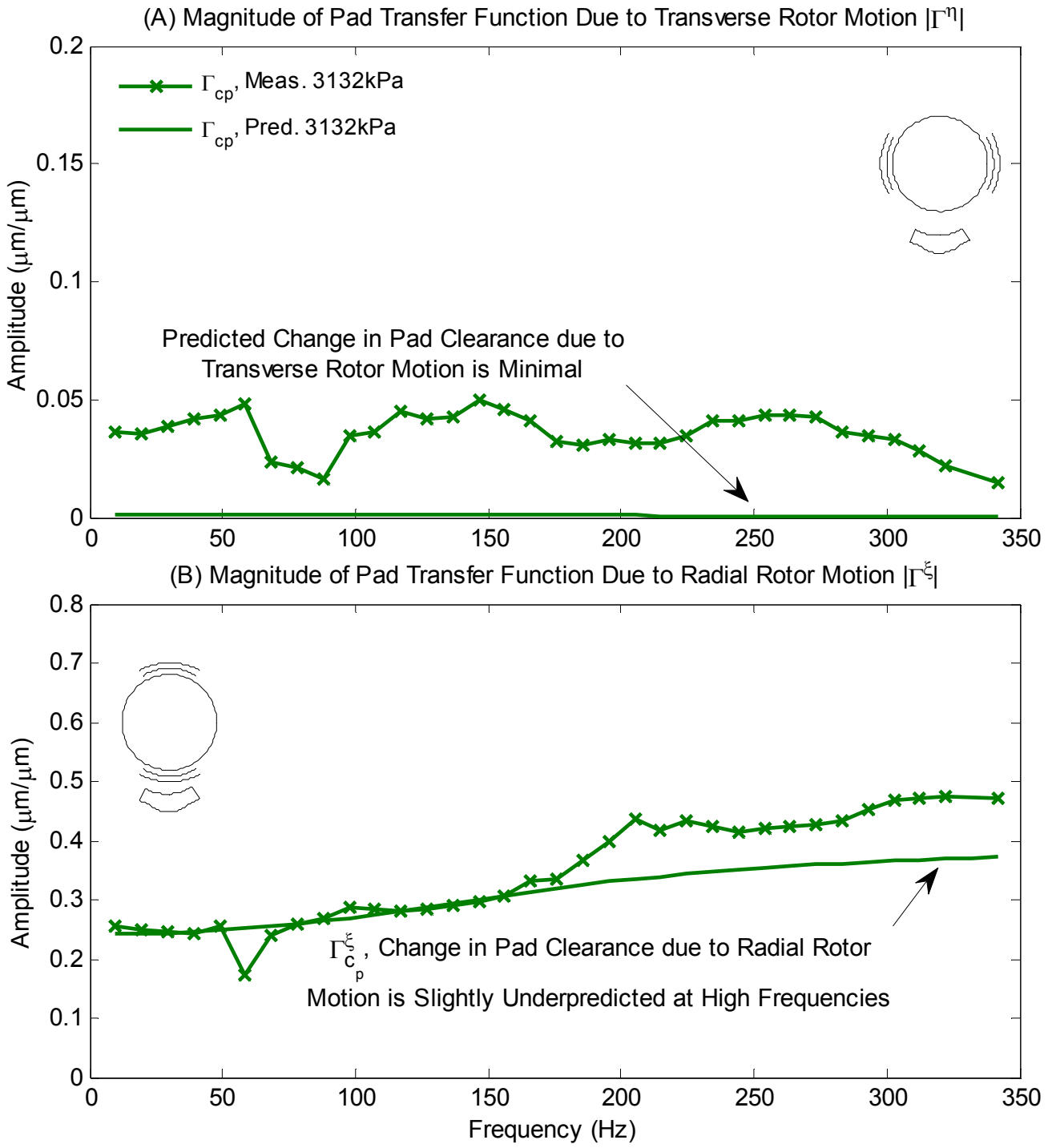

TF Phase Meas. vs. Pred.: 4400 rpm, 1566 kPa

- Sharp phase shift indicates that transverse pad motion is lightly damped (resonance not seen in amplitude)
- Phase of pad tilt and radial pad motion relative to radial rotor motion predicted well

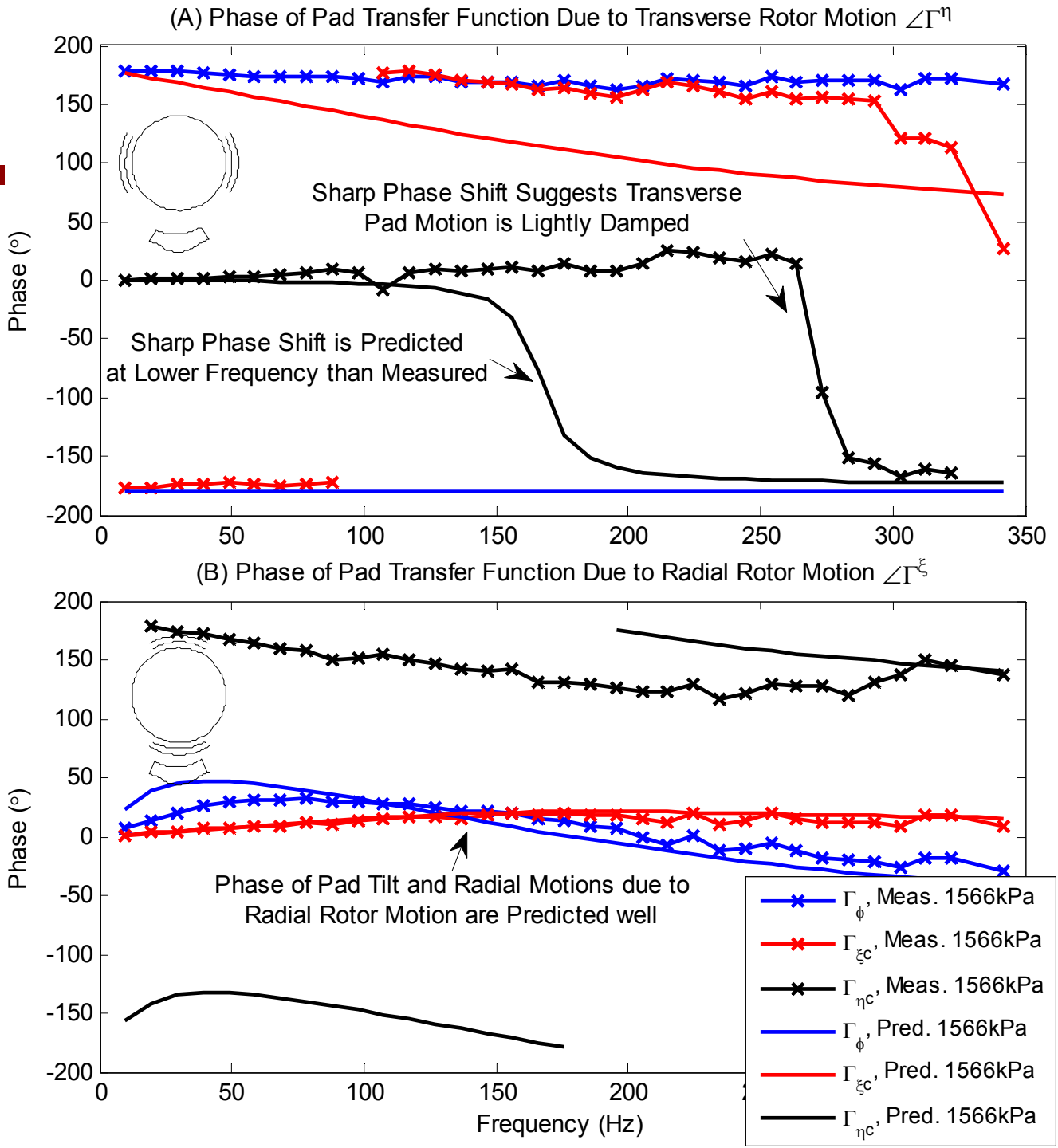

Meas. vs. Pred. Brg. Impedances: 4400 rpm, 3132 kPa

- Real part of direct impedance coefficients slightly **overpredicted** at high frequencies
- Imaginary part of direct impedance coefficients **underpredicted** at high frequencies

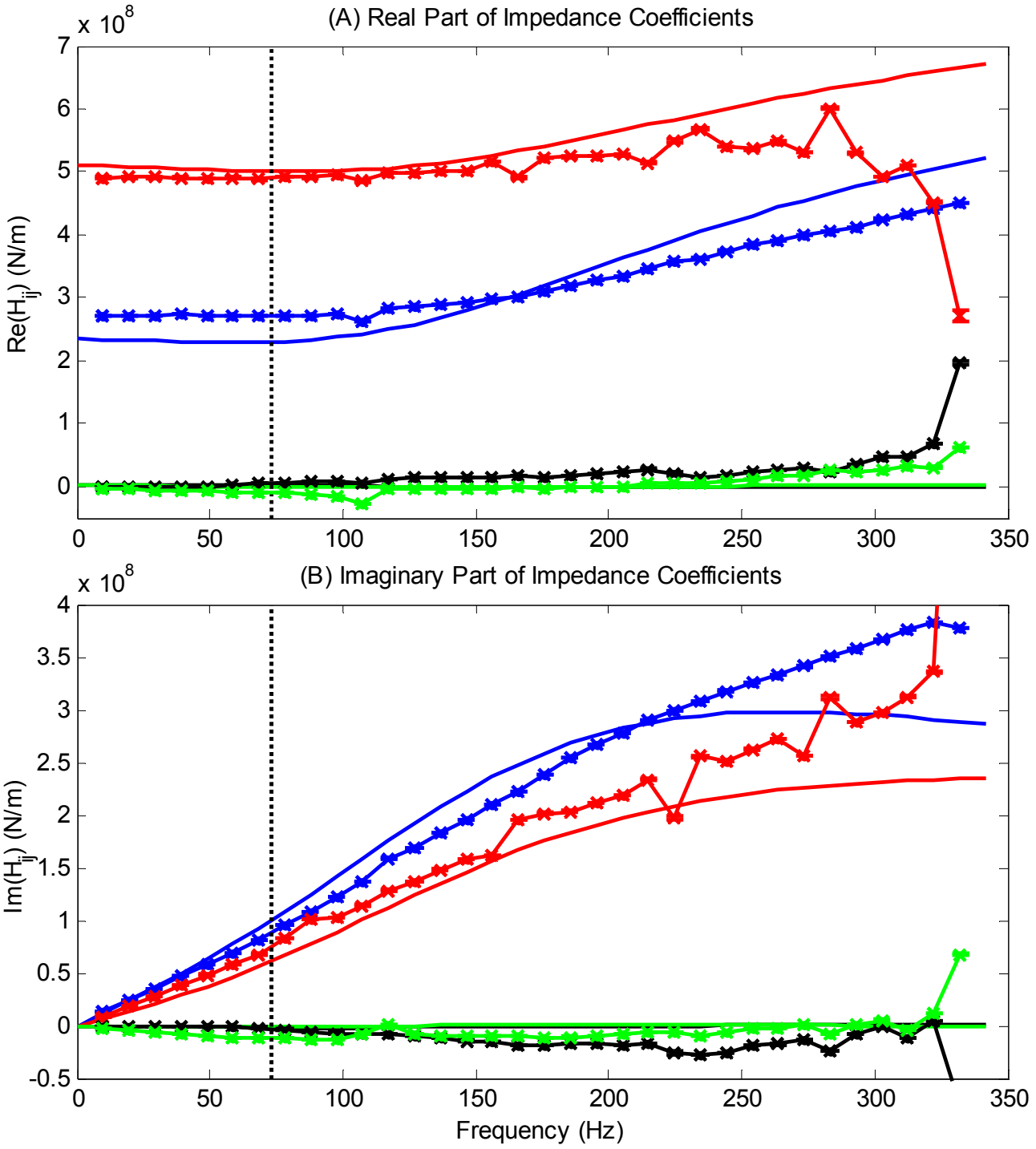

Meas. vs. Pred. Brg. Impedances: 10200 rpm, 783 kPa

- Real and imaginary impedances are predicted quite well
- Slight difference in the frequency dependence of the real part of H_{ij} at high frequencies

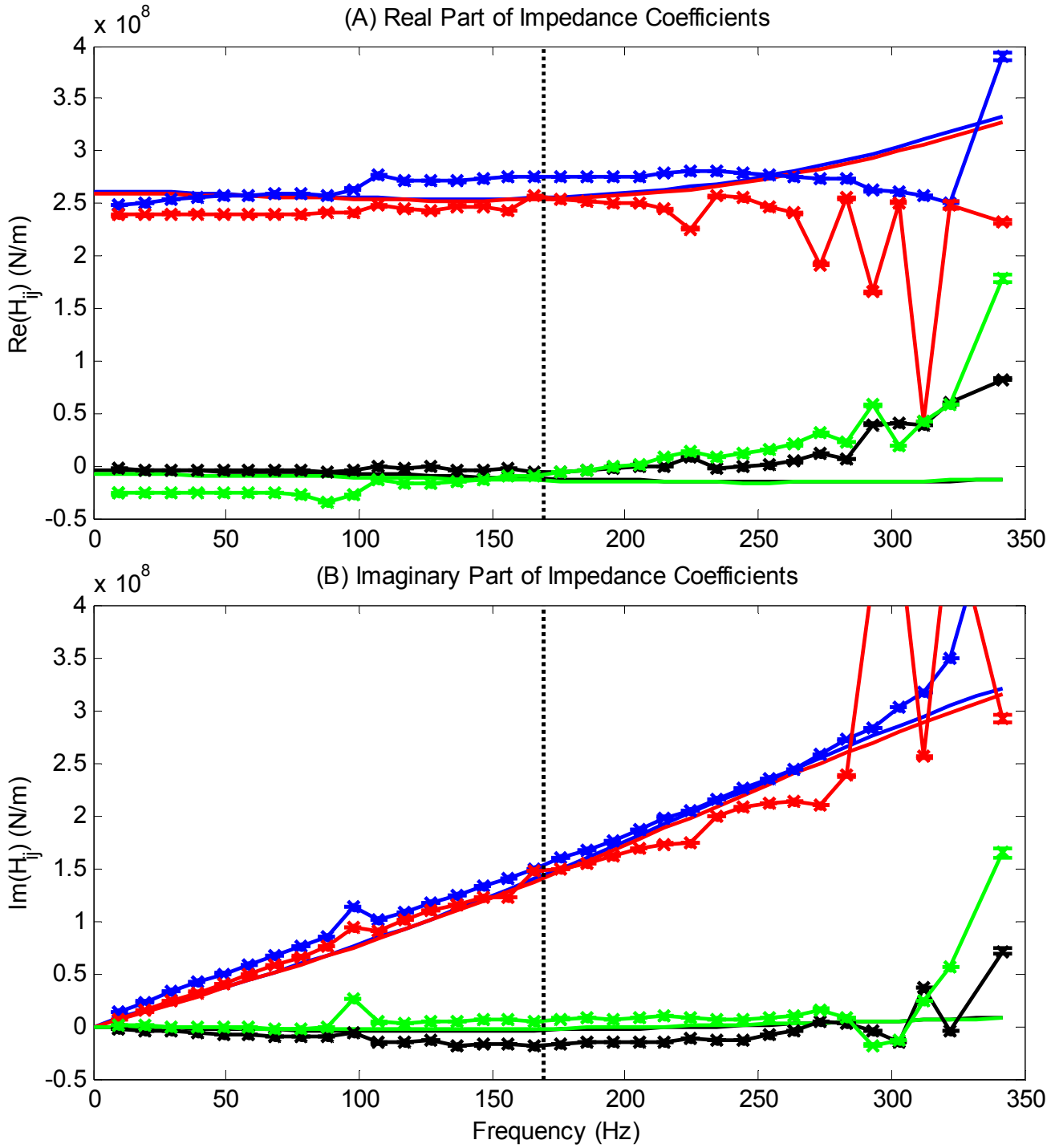

Meas. vs. Pred. Brg. Impedances: 10200 rpm, 3132 kPa

- Real and imaginary impedances are predicted quite well

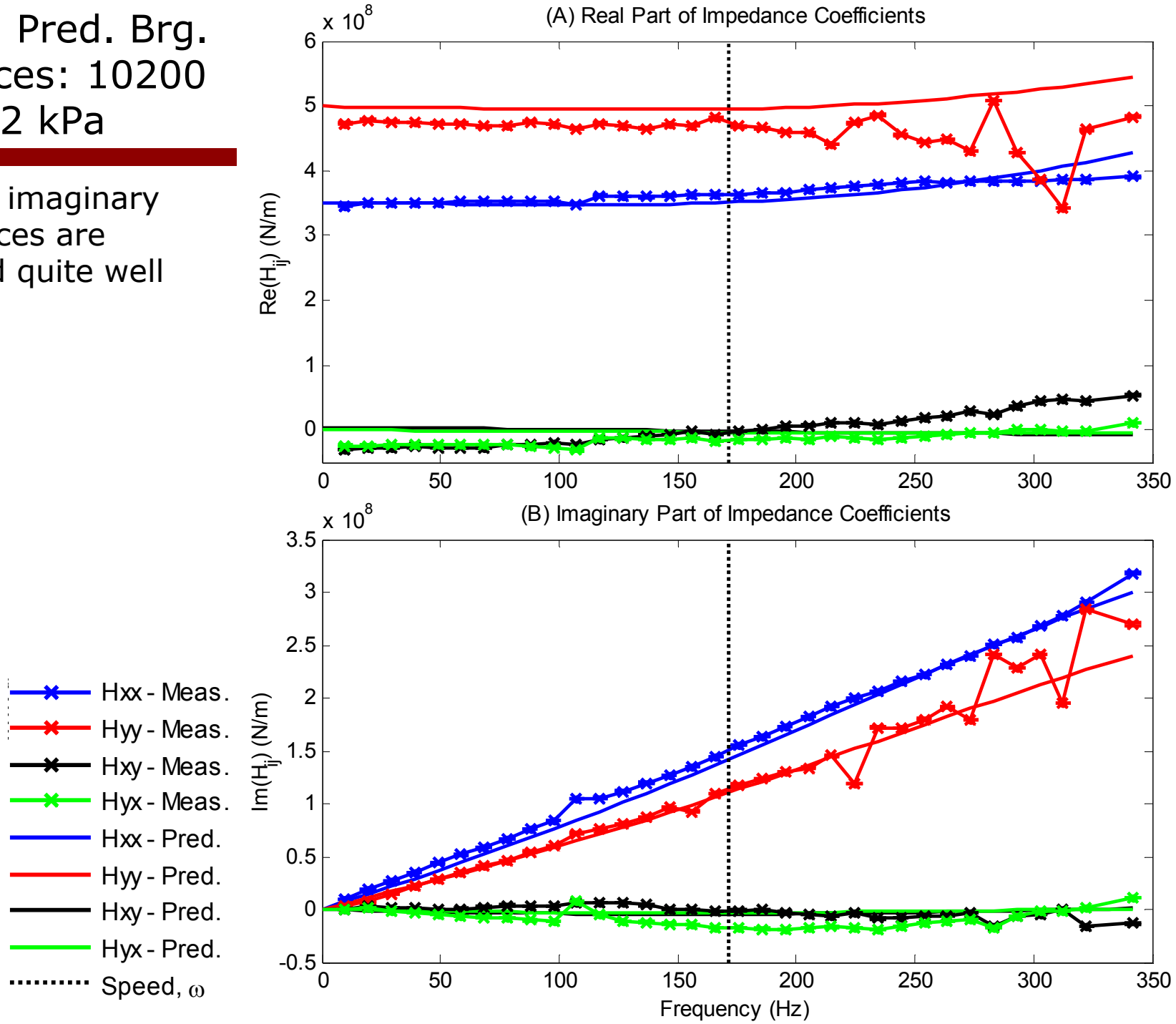

Impact of Pad and Pivot Flexibility : 4400 rpm, 3132 kPa

Relative error in prediction

Pad Model Type	k_{yy} (%)	c_{yy} (%)
$Flex_{pad,pivot}$	0.95	-14.10
$Rigid_{pad},Flex_{pivot}$	35.53	77.93
$Flex_{pad}$, $Rigid_{pivot}$	88.88	136.33
$Rigid_{pad,pivot}$	**201.61**	**810.78**

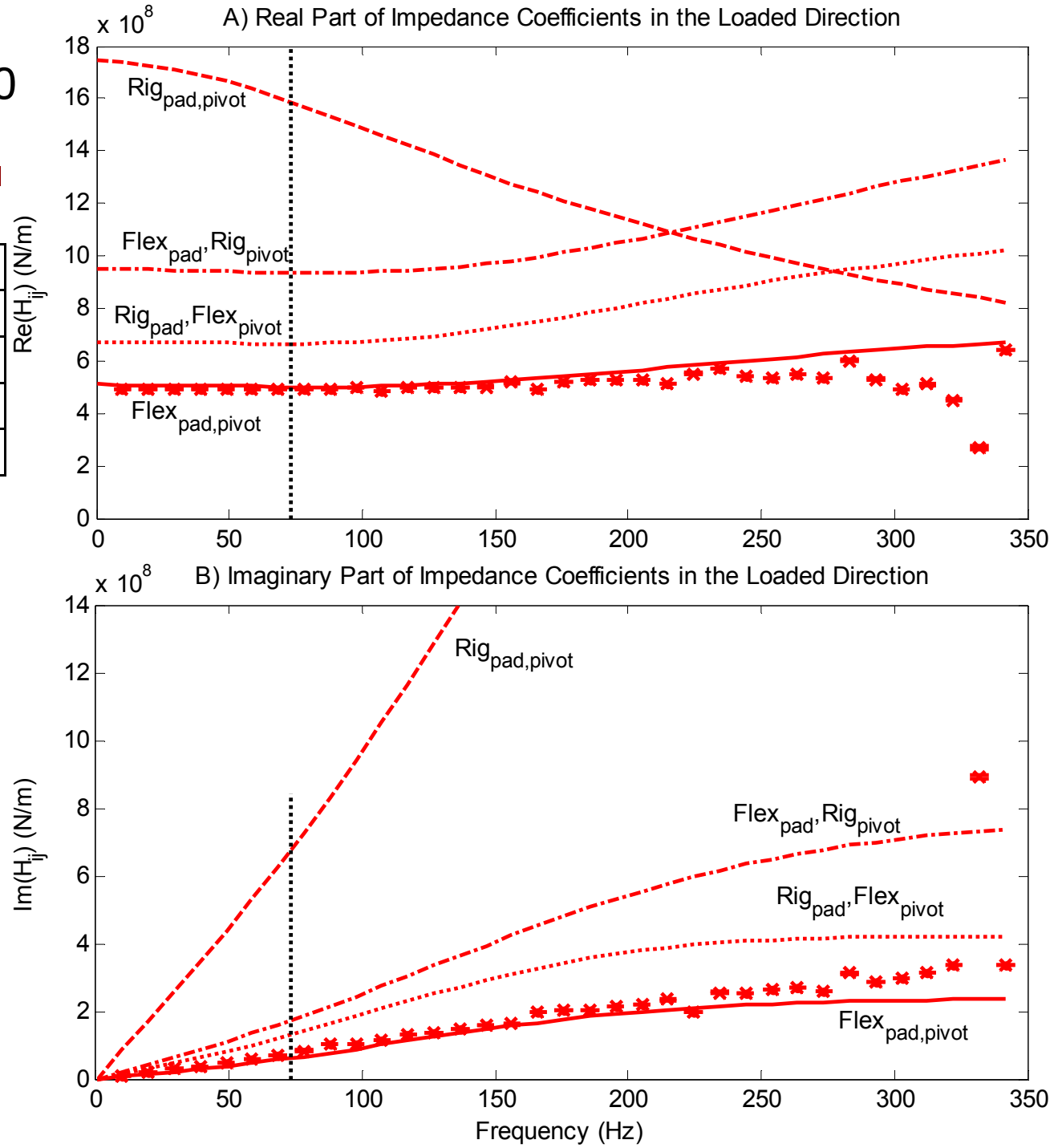

Impact of Pad and Pivot Flexibility : 10200 rpm, 3132 kPa

Relative error in prediction

Pad Model Type	k_{yy} (%)	c_{yy} (%)
$Flex_{pad,pivot}$	10.63	-2.15
$Rigid_{pad},Flex_{pivot}$	41.77	56.90
$Flex_{pad}$, $Rigid_{pivot}$	99.84	140.29
$Rigid_{pad,pivot}$	**176.65**	**512.99**

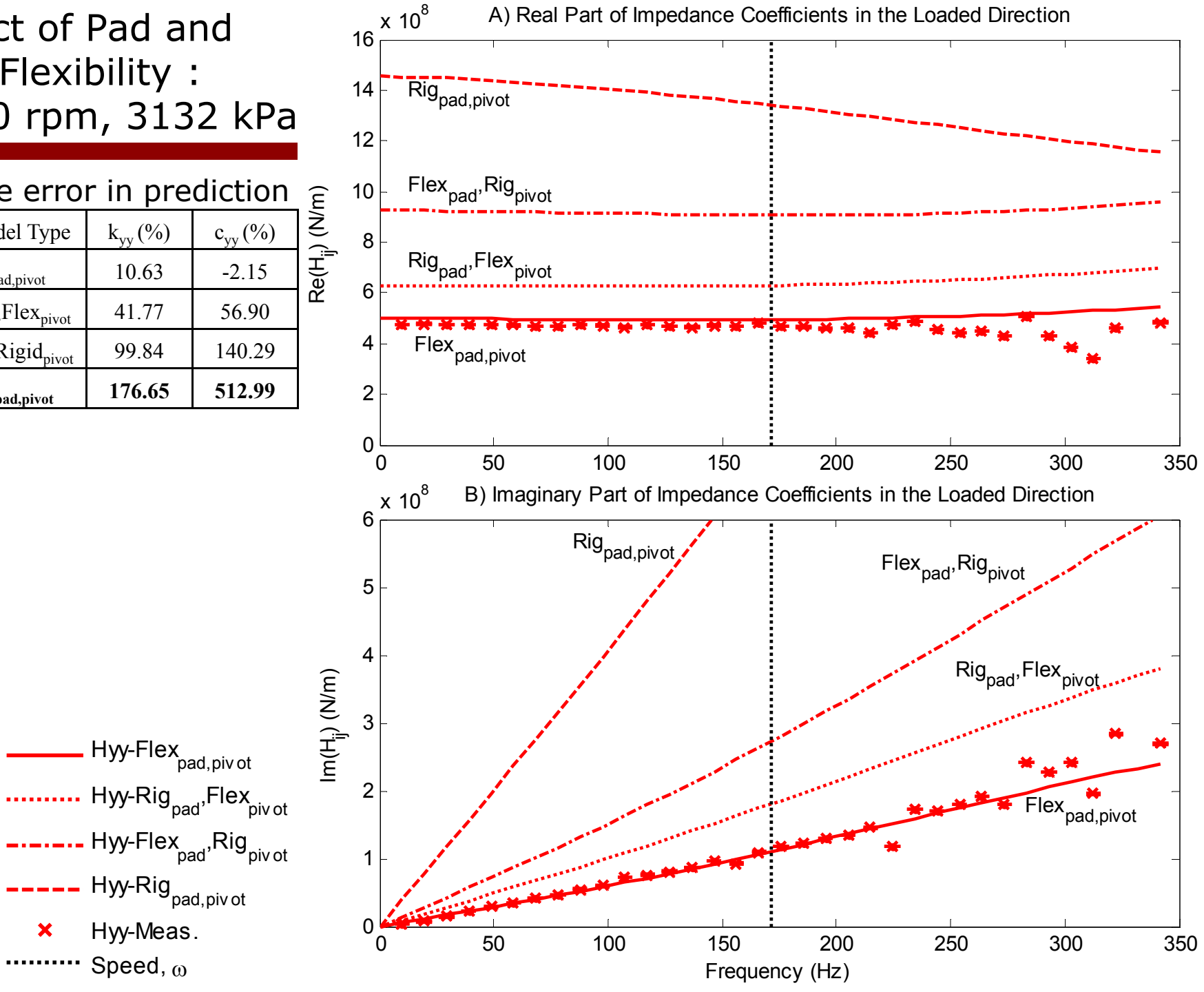

Impact of Pad and Pivot Flexibility: 10200 rpm, 783 kPa

Relative error in prediction

Pad Model Type	k_{yy} (%)	c_{yy} (%)
$Flex_{pad,pivot}$	4.59	5.41
$Rigid_{pad},Flex_{pivot}$	8.49	42.27
$Flex_{pad}$, $Rigid_{pivot}$	64.34	88.09
$Rigid_{pad,pivot}$	**51.16**	**181.93**

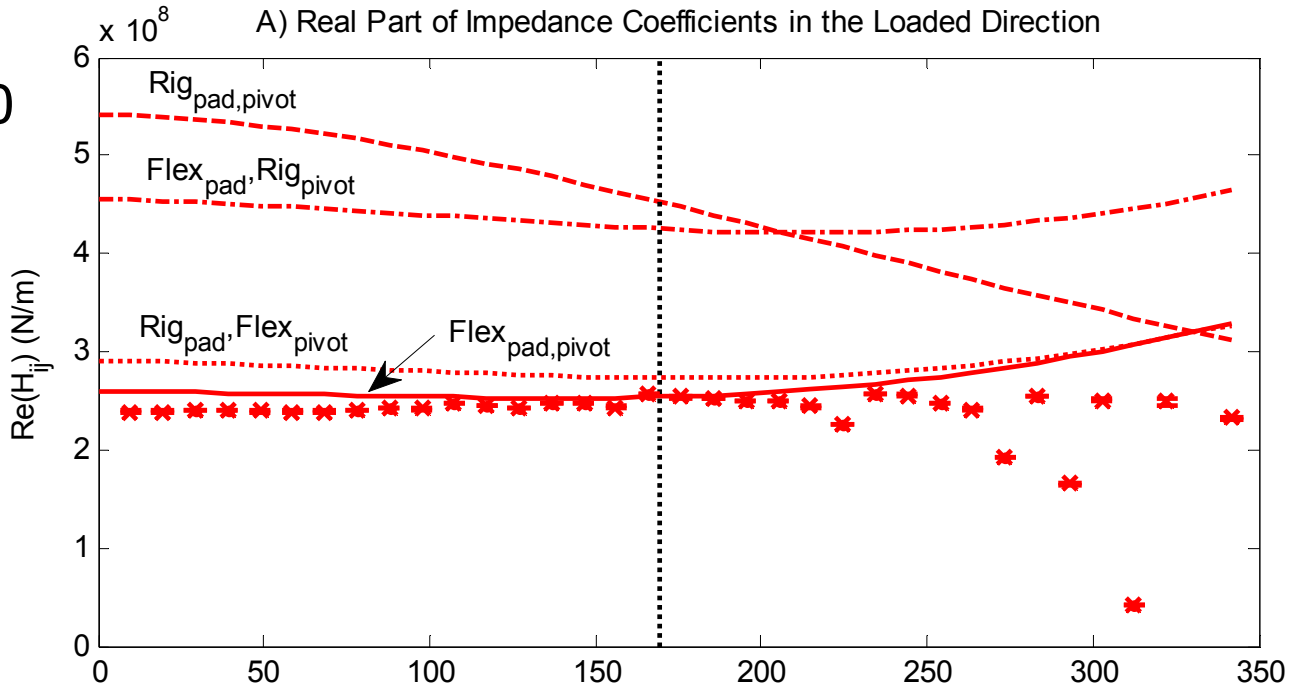

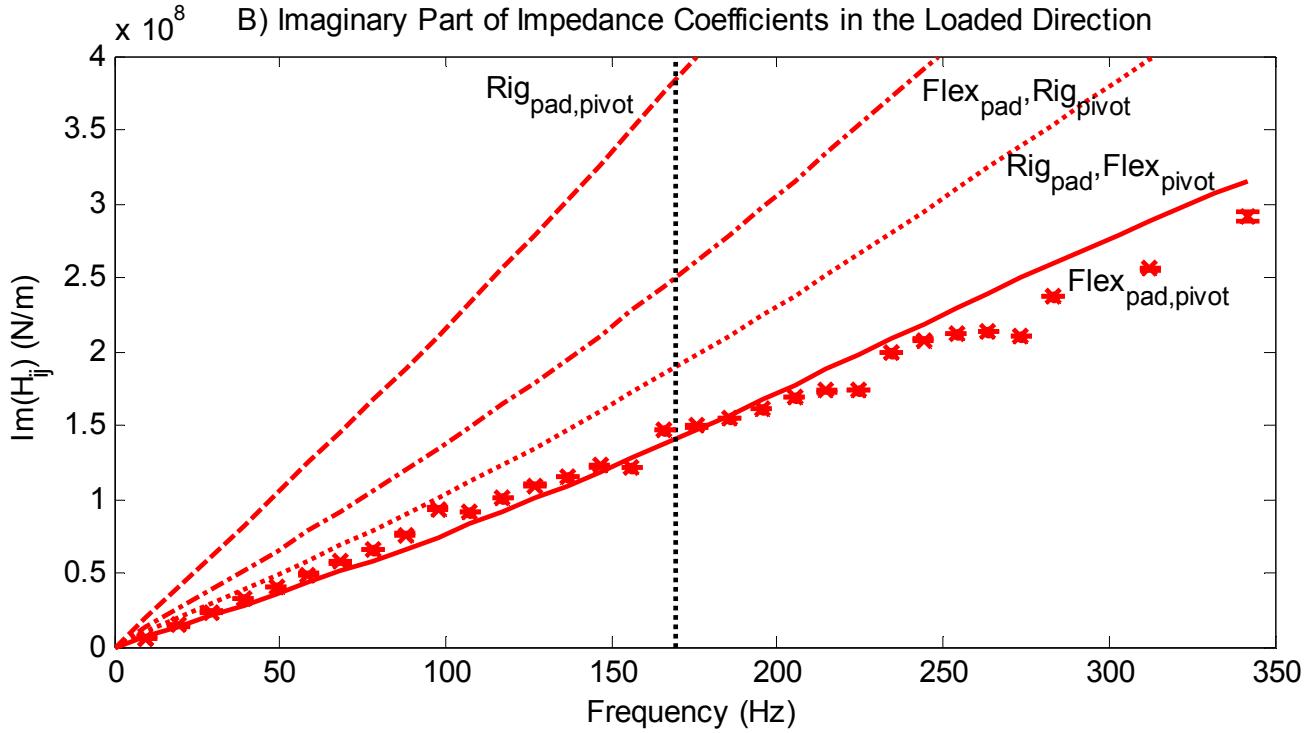

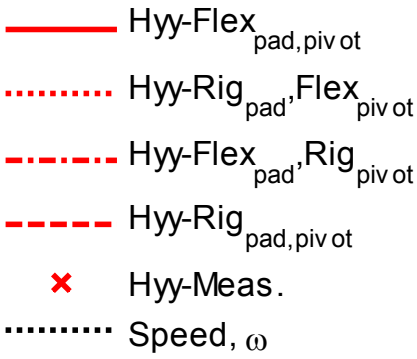

Bearing model for Stability Calculation?

- Subsynchronously reduced model results in 1% error
- Synchronously reduced model results in 25% error.
- Error is worse at low loads.

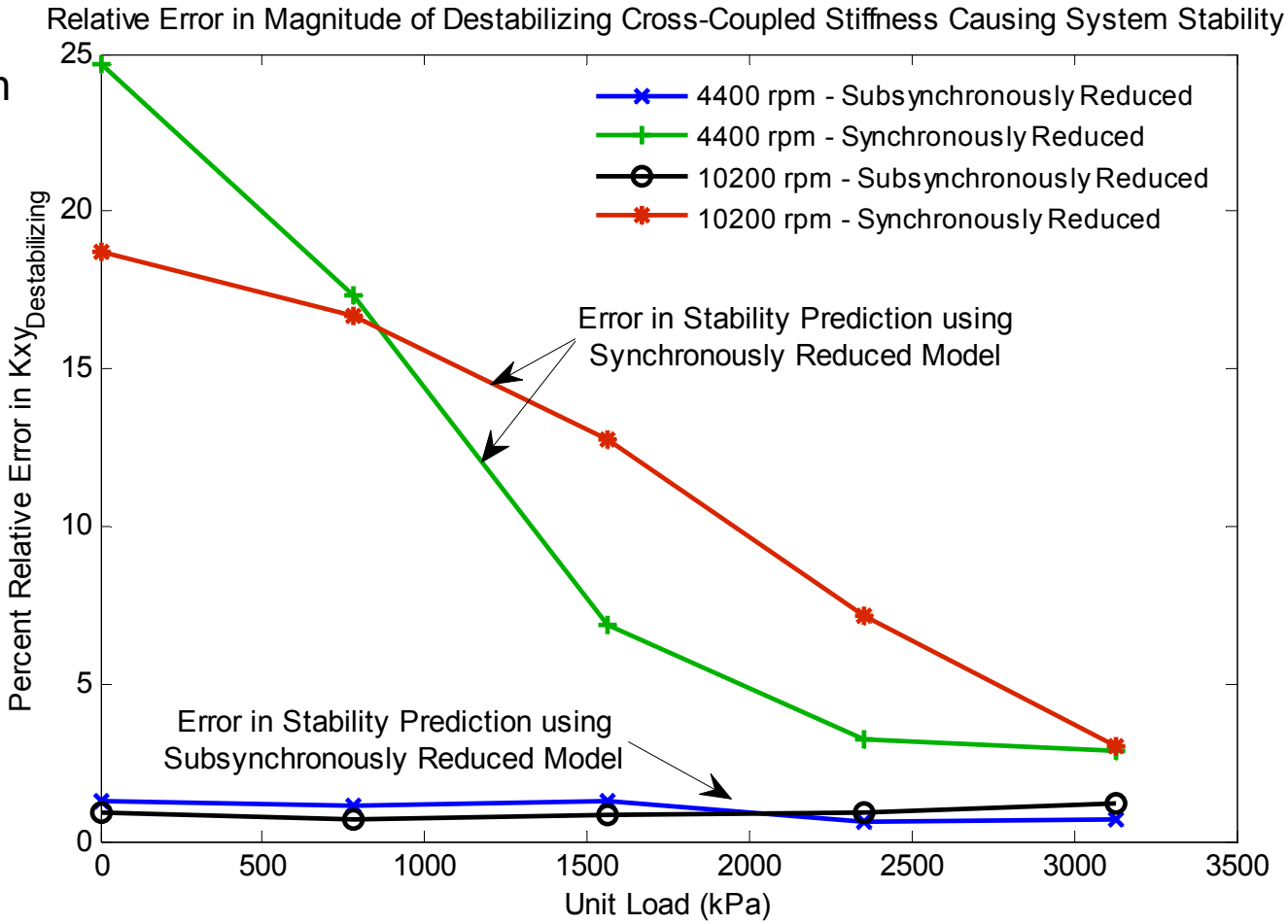

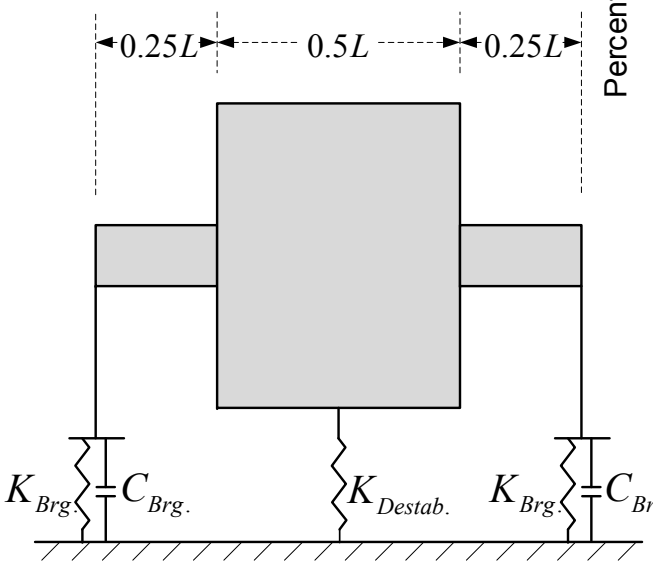

Speed (rpm)	4400	10200
L (m)	1.61	1.15
R_{mid} (m)	0.3	0.25

Frequency Dependent Damping is Predicted

- Synchronously reduced **stiffness** is **1%-6% lower**
- Synchronously reduced **damping** is **10%-15% higher**

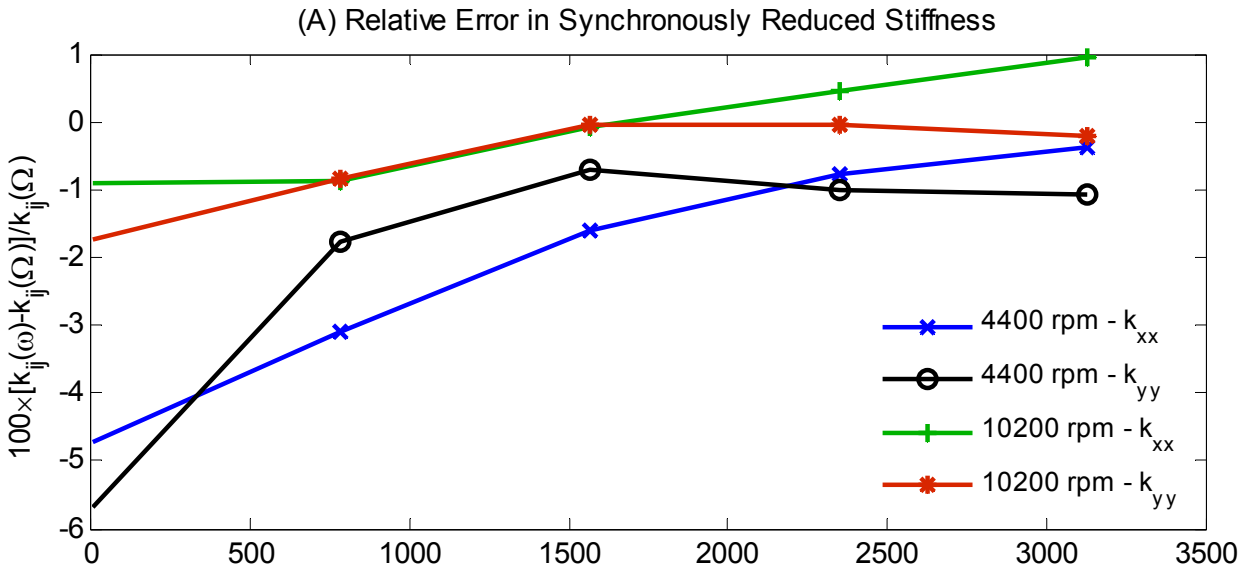

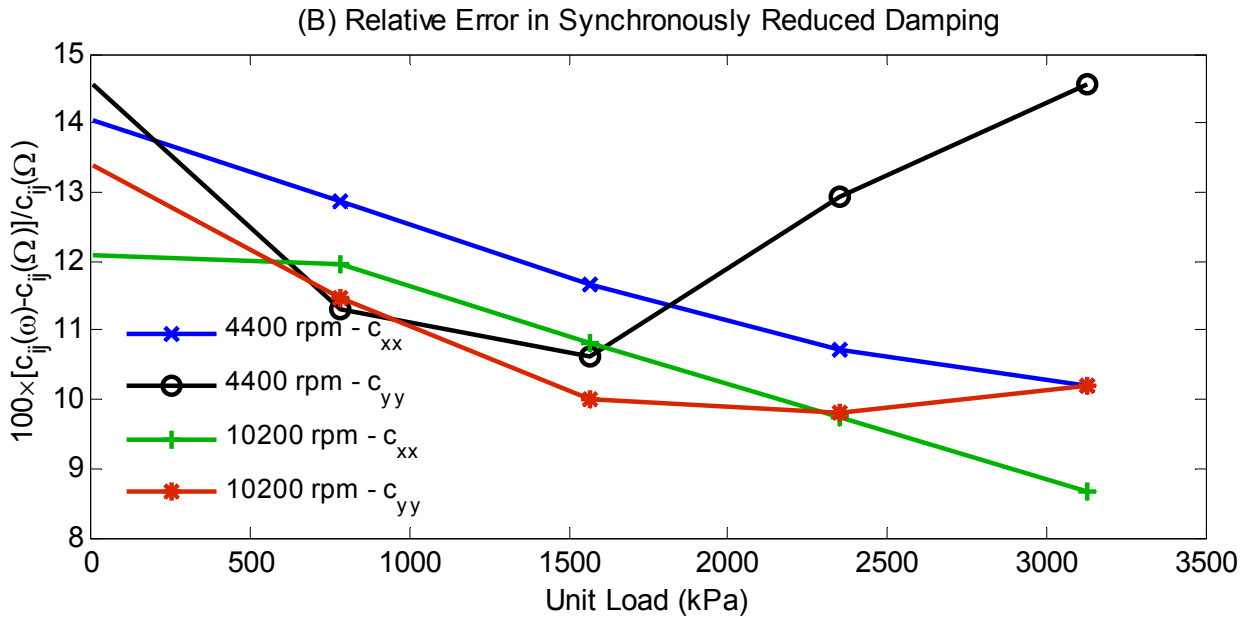

Was frequency dependent damping measured?

- At high loads, yes!

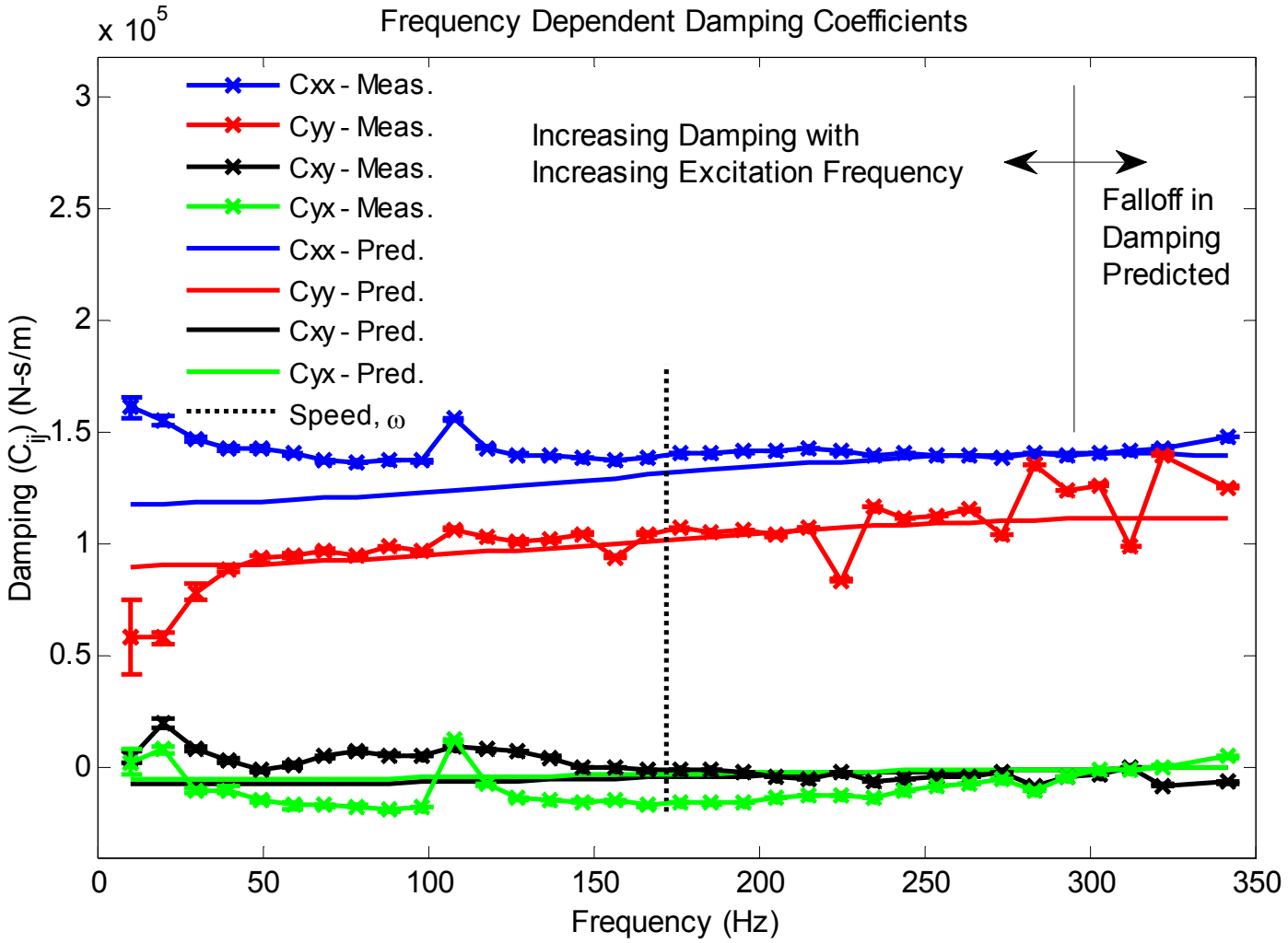

Frequency dependent damping at 10200 rpm, 3132 kPa unit load

Was frequency dependent damping measured?

- At lower loads, No!

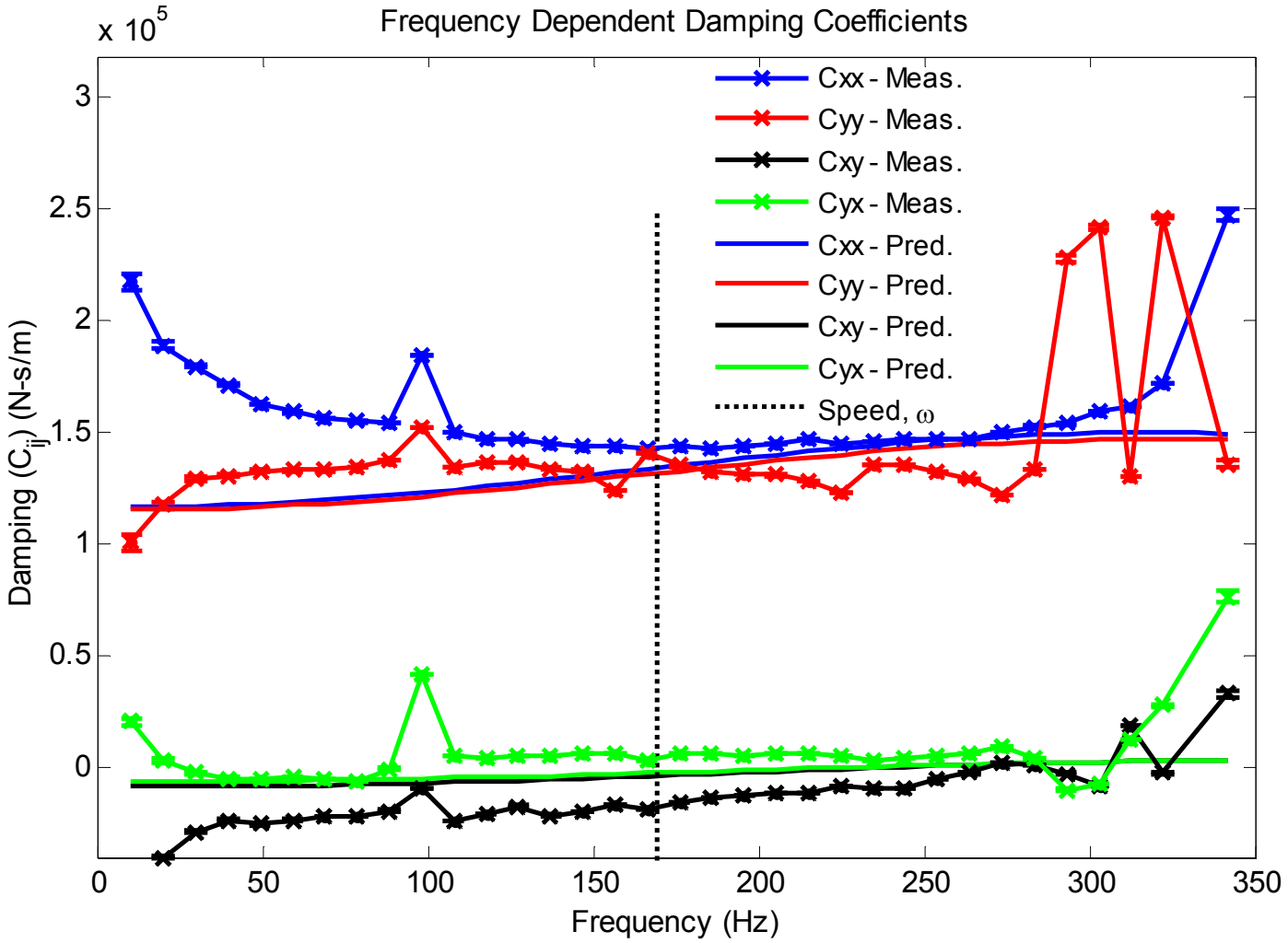

Frequency dependent damping at 10200 rpm, 783 kPa unit load

Predicted system stability with measured KC?

- Both the full bearing predictions and synchronously measured impedances underestimate system stability.

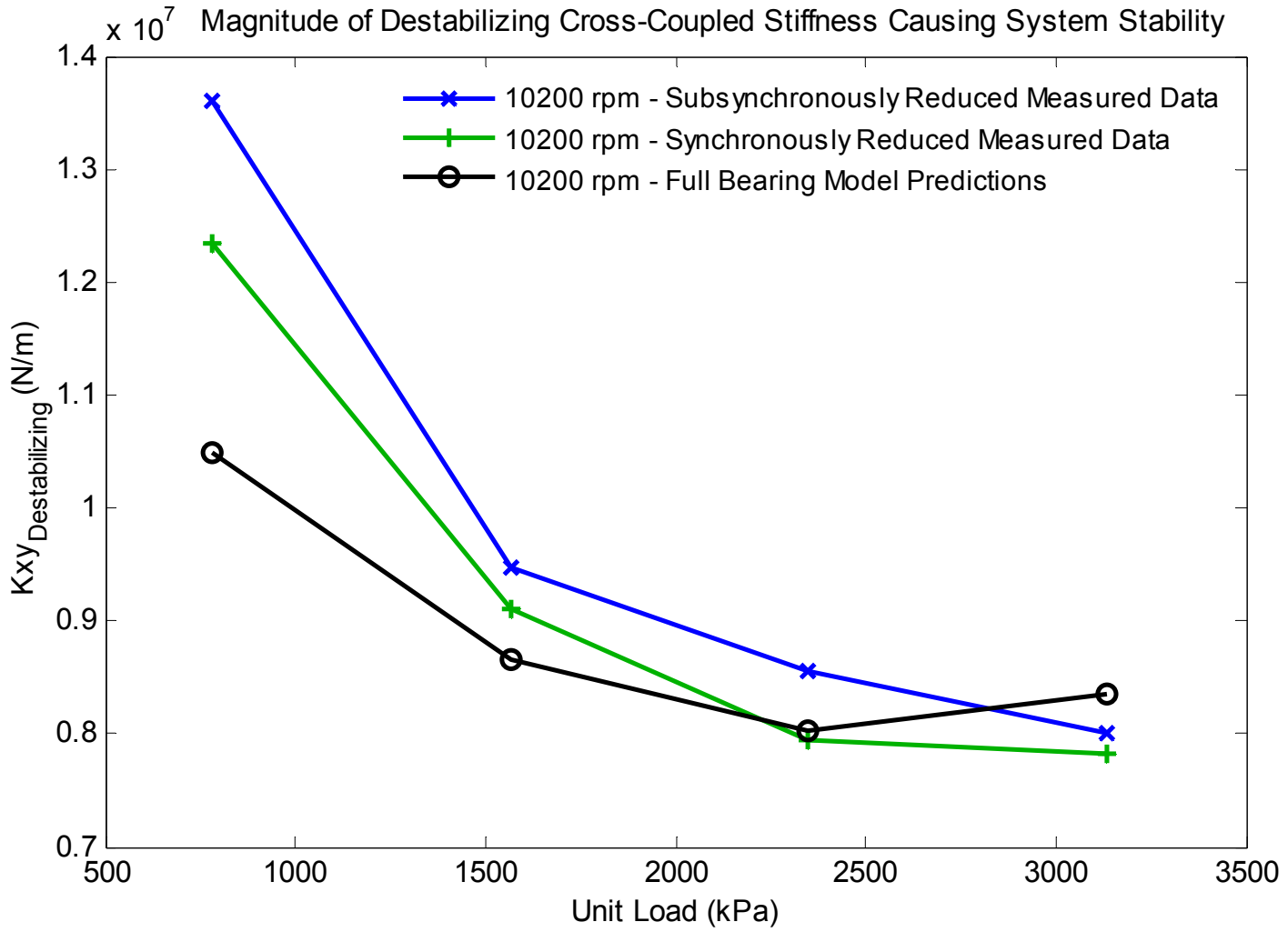

Summary and Conclusions

- Original Contributions:
  - Including perturbations of both the journal and bearing in TPJB analysis
  - Perturbing pad tilt, radial and transverse pad motion, and changes in pad clearance (all previously perturbed in literature, but not in the same analysis).
  - Though allowing for an arbitrary pad center of gravity was included in the analysis, this feature was insignificant for the bearing tested.
  - Though previous researchers solved for pad motion as a function of rotor motion while reducing bearing impedances, this is the first work to define the rotor-pad transfer functions, and to suggest that comparisons between measured and predicted rotor-pad transfer functions may be used to rectify modeling deficiencies.
  - Measuring static and dynamic pad rotations (tilt, pitch, yaw), pad translations (radial and transverse pivot motion), and changes in pad clearance.
  - Converting measured pad motions into rotor-pad transfer functions, and comparing them to predicted rotor-pad transfer functions.
  - Measuring bearing clearances using slow frequency circular excitation, and correlating these measured clearances to changes to pad surface temperatures.

Summary and Conclusions

- Static Measurements
  - Measured hot bearing clearances after shutdown are up to 30% smaller than the cold bearing clearance.
  - Measured hot bearing clearance is inversely proportional to average surface temperature at each pad's pivot location.
  - Approximating reductions in clearance based on the expansion of a pad at elevated temperatures accounts for only ½ of the reduction in measured bearing clearance (note that this observation pertains to bearing clearances measured on a floating bearing test rig)
  - Measured operating pad clearances were 60% larger than the installed pad clearance (this effect will tend to reduce the frequency dependence of measured bearing impedances)
- Journal vs. bearing perturbations
  - For the test bearing, journal perturbed impedances were nearly the same as bearing perturbed impedances (slight differences between the two were only noted at higher frequencies).
  - For the test bearing having 10× heavier pads, differences in journal and bearing perturbed impedances were significant at high frequencies.
  - Comparing journal perturbed impedance predictions to impedances measured on a floating bearing test rig appears to be valid for bearings similar to the test bearing, but this may not necessarily be the case for larger bearings having heavier pads, or possibly gas bearings with significantly smaller impedances.

Summary and Conclusions

- Rotor-pad transfer functions
  - The rotor and pad have the same frequencies of motion. These motions occur at 1x, 2x, etc. in which the harmonics have an amplitude of 5-10% of the fundamental frequency.
  - Pad tilt due to transverse rotor motion showed that the pad tracked the rotor, thus the pivot allowed the pad to rotate freely.
  - The current work shows that pivot compliance allows for significant radial pad motion. Neglecting this degree of freedom produces large errors in predicted bearing impedances.
  - A similar result was shown for pad flexibility; however, for the test bearing, pad flexibility appears to be less significant than radial pivot flexibility

- Rotor-pad transfer functions
  - Transverse pad pivot motion was predicted and observed; however, this motion appears to be lightly damped, which suggests that it is caused by transverse compliance of the pivot, not slipping.
  - In general, the rotor-pad transfer functions were predicted well; however, pad tilt due to radial rotor motion had a tendency to be underpredicted.
- Bearing Impedances
  - The current work shows that when the rotor-pad transfer functions are predicted well, this resulted in a decent prediction of bearing impedances.
  - The accuracy of the predicted bearing impedances was moderately good at 4400 rpm, and very good at 10200 rpm.

Summary and Conclusions

- Full versus Reduced bearing models
  - Stability predictions using a subsynchronously reduced bearing model were within 1% of a full bearing model (explicitly containing all pad degrees of freedom).
  - Stability predictions using a synchronously reduced model overestimated stability by as much as 25% compared to the full bearing model.
  - This error in stability calculation resulted from an increase in predicted damping at synchronous frequencies relative to subsynchronously reduced damping (frequency dependent damping).
- Frequency Dependent Damping
  - An increase in direct damping in the loaded direction was measured only for highly loaded operation, while this trend was predicted for all loads.
  - Calculating stability using the full bearing model and synchronously measured coefficients were more conservative than stability calculations using subsynchronously measured bearing impedances
- Unresolved Issues
  - Why does predicted damping increase with frequency while measurements show the opposite?

Acknowledgements

- To my family for supporting me throughout my tenure as a student.
- To the Turbomachinery Research Consortium (TRC) for sponsoring this research.
- To my committee for their advice on this subject and the manner in which it is presented.
- To Chris Kulhanek and Gustavo Vignolo, for helping me to get the test rig in its current condition
- To Eddie Denk and all of the A&M Turbomachinery Laboratory staff.

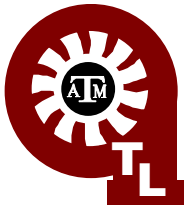

Thank You

Questions?

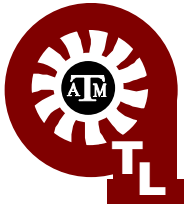

Jason Wilkes (PhD?)

Static Eccentricity Prediction

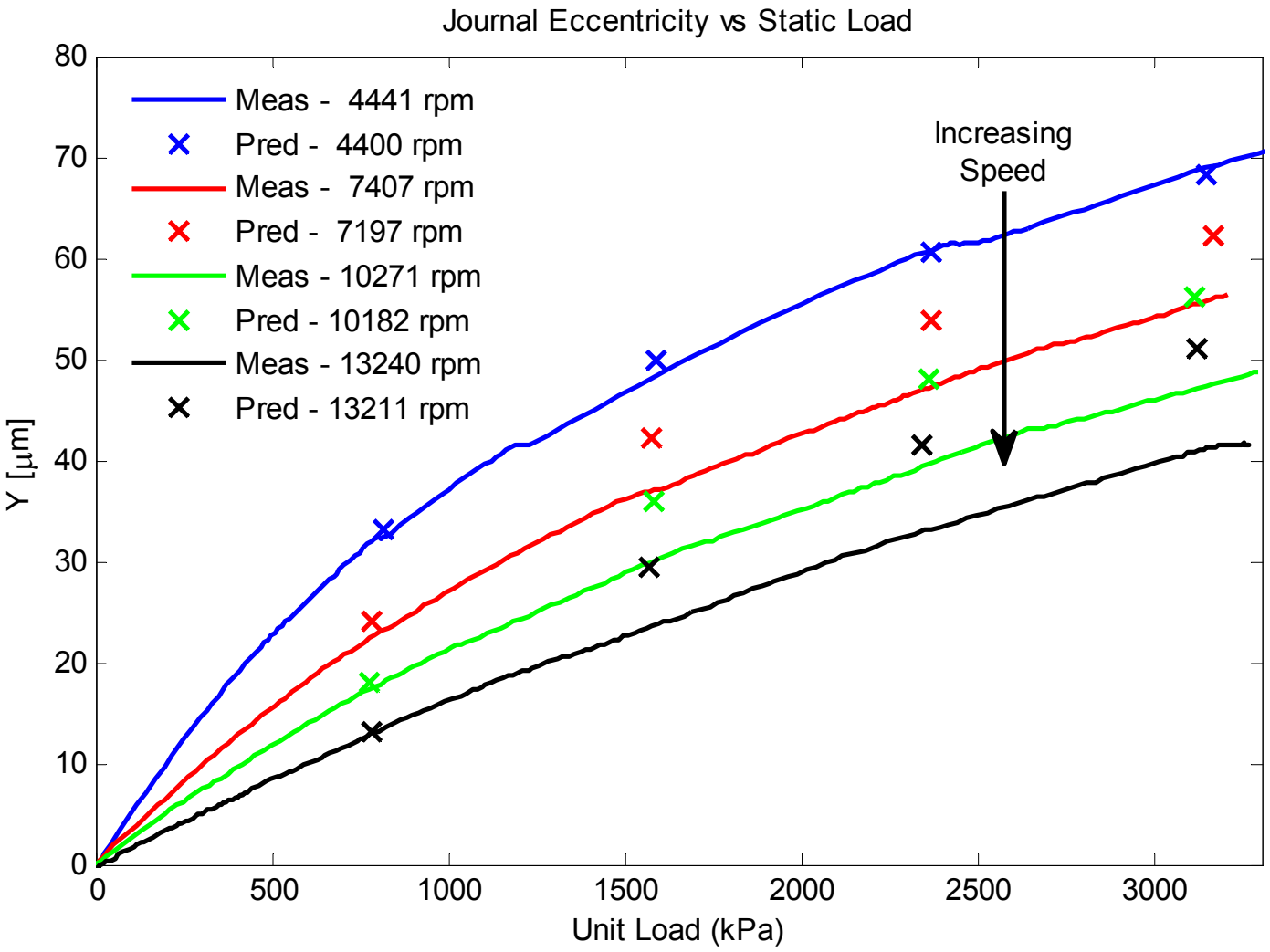

Power Loss

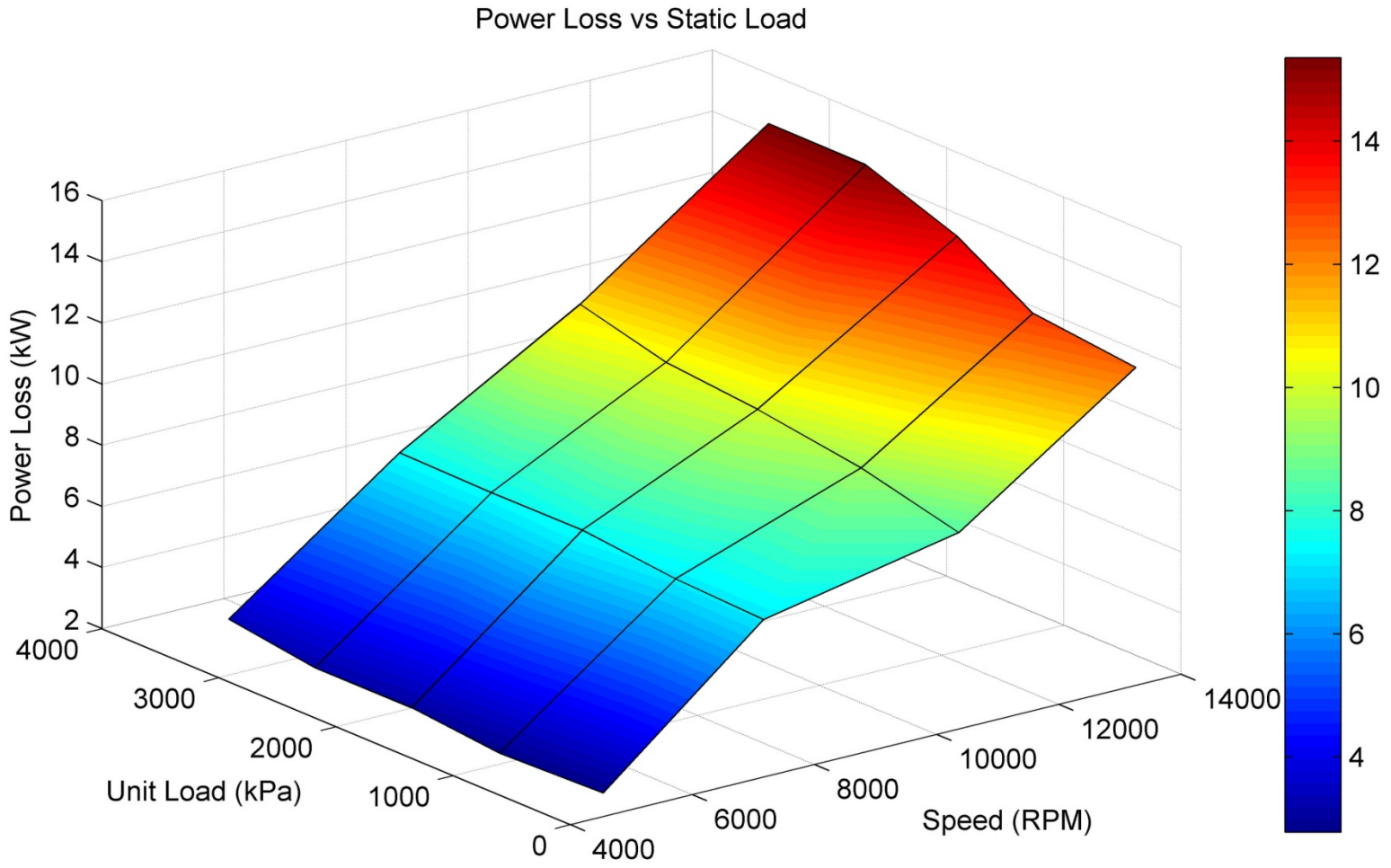
Power Loss vs Static Load
Power Loss (kW)
16
14
12
10
8
6
4
2
Unit Load (kPa)
4000
3000
2000
1000
0
Speed (RPM)
4000
6000
8000
10000
12000
14000
14
12
10
8
6
4

Pad Tilt Angle

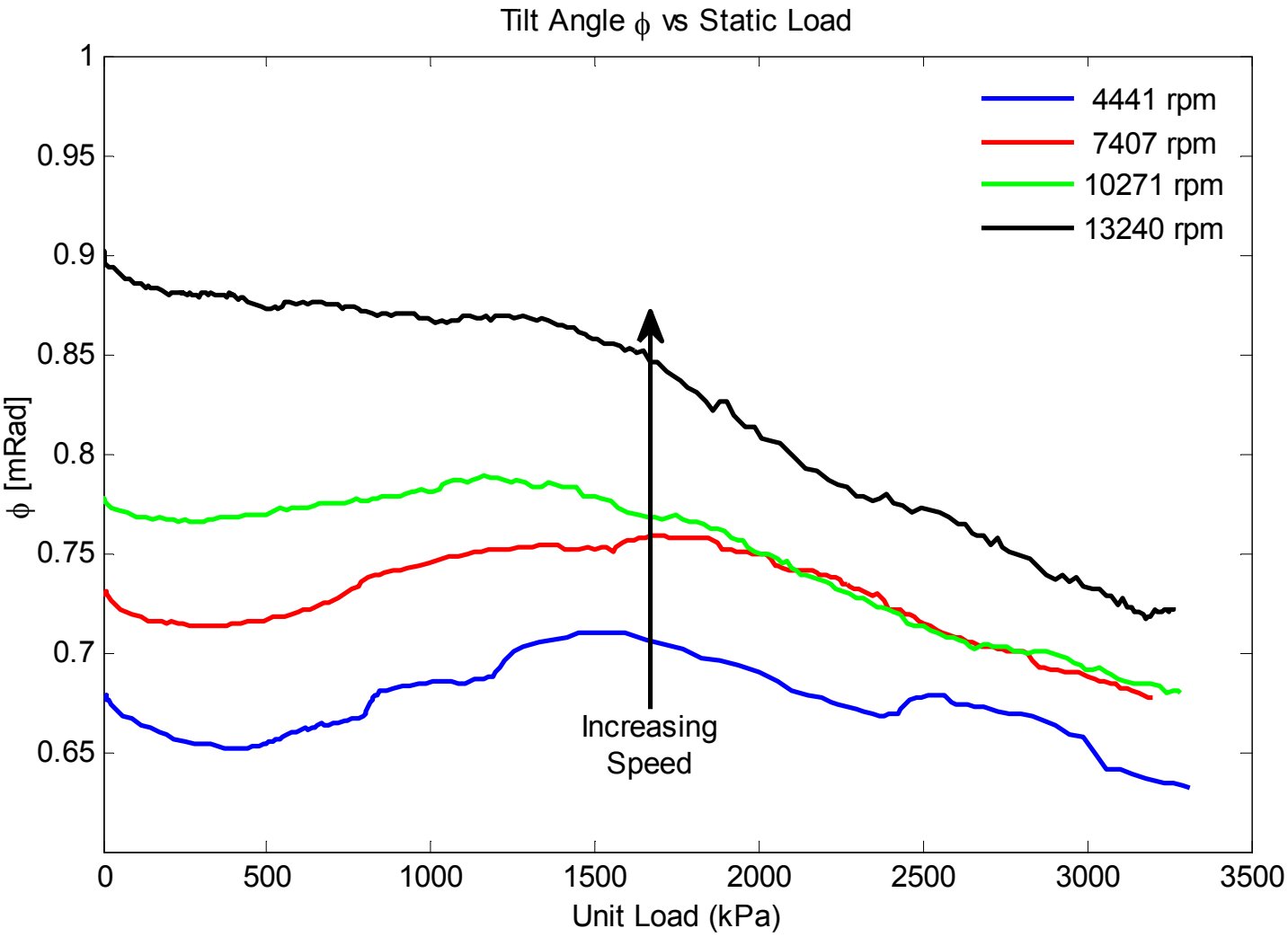

Determination of Offset for Pad Tilt

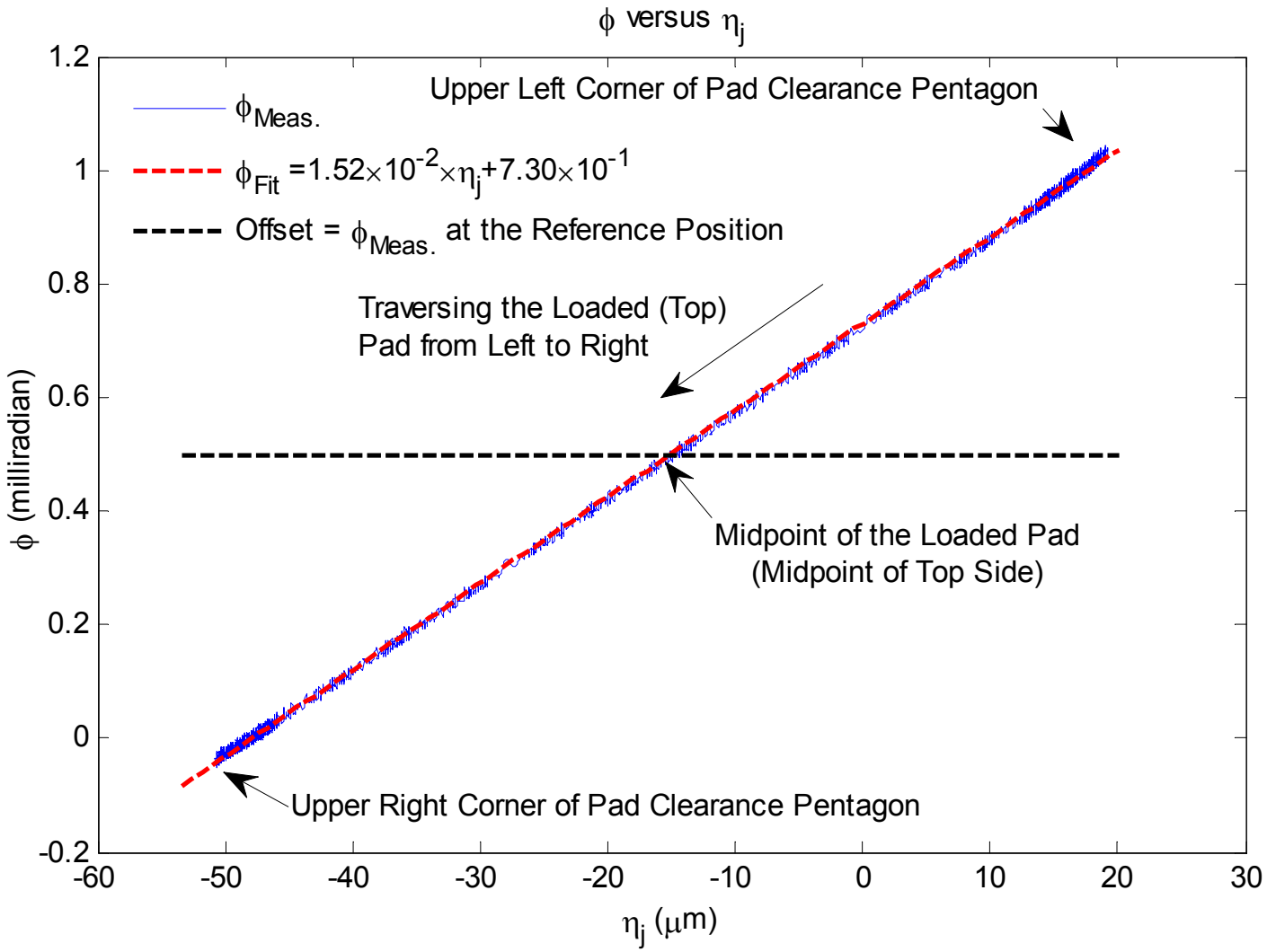

Tilt Waterfall Plot

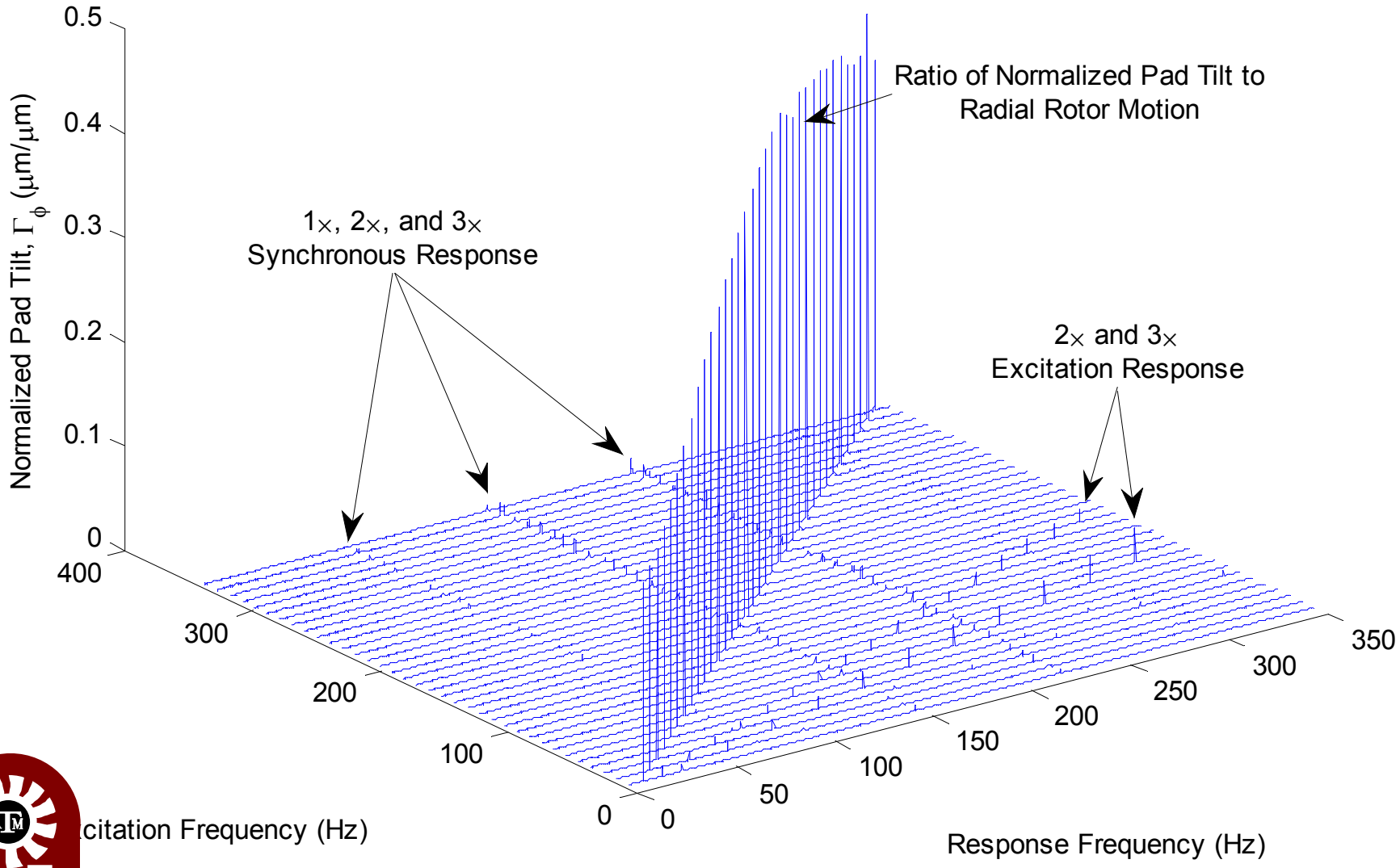

Additional Moment term due to Rolling Without Slipping

- Change in offset creates a moment

$$M_{\eta f_c,k} = -f_{c\xi 0,k}\eta_{f_c,k}$$

- where the moment arm

$$\eta_{f_c,k} = r_{rh}\sin\left(\theta_{f_c,k}\right) = r_{rh}\sin\left(\frac{r_r}{r_{rh}-r_r}\phi_k\right)$$

- Additional reaction moment

$$M_{\eta f1_c,k} = -f_{c\xi 0,k}\frac{r_r r_{rh}}{r_{rh}-r_r}\cos\left(\theta_{f_c,k}\right)\phi_{1,k}$$